

The Journal of THE BRITISH INSTITUTION OF RADIO ENGINEERS

FOUNDED 1925

INCORPORATED 1932

*"To promote the advancement of radio, electronics and kindred subjects
by the exchange of information in these branches of engineering."*

VOLUME 20

MAY 1960

NUMBER 5

THE IMPORTANCE OF A NAME

MEMBERS know from annual reports of the Council's intention to strengthen the Institution by appointing Specialized Group Committees. Their main responsibility is the arrangement of meetings related to various branches of the science of radio and electronic engineering.

During the last session the first three Group Committees to be set up—Medical Electronics, Computers, and Radar and Navigational Aids—completed their first full programmes of meetings. The Council has now established a further Committee which will arrange meetings under the broad theme of Electro-Acoustics and next session this Group will make significant contributions to the Institution's proceedings.

One of the first tasks of the Group Committee, and one which led to much discussion, was to decide on the recommendations to be made to Council regarding title and terms of reference. The Committee was indeed originally convened as an "Audio Frequency Engineering" Group Committee, but it was soon agreed that this was unduly limiting. The plain title of "Acoustics Group" would also not reflect adequately the Institution's interests. The title of "Electro-Acoustics Group Committee" was therefore put forward to Council for approval.

The Group Committee then gave consideration to the equally important question of its terms of reference. These were finally approved by the Council as follows:—

"The Electro-Acoustics Group specializes in those aspects of radio and electronic engineering which are associated with the propagation, conduction, generation, perception, measurement, reproduction and control of all kinds of material

vibrations. The objects of the Group are:

(a) to promote Institution activity in those techniques and to disseminate knowledge by arranging meetings in collaboration with the Programme and Papers Committee;

(b) to advance knowledge in this field by collaboration with other bodies and to work towards the preparation and acceptance of standards in this field of engineering."

Planning for the programme of meetings is now well advanced and full details will be announced in due course. The Committee is, however, pleased to give this early advice to all members that Wednesday, 12th October, has been provisionally allocated for its Inaugural Meeting and that Professor Colin Cherry of Imperial College of Science and Technology has accepted an invitation to give an Address. Other meetings will deal with loudspeakers, stereophonic broadcasting, noise measurement and audiometry.

The Institution's programme of meetings in London next winter will therefore be further increased over the record number of meetings held during the session which has just ended. To ensure that all members benefit, consideration is being given to means of circulating the fullest notice of these meetings, and in addition Local Section Committees are to be advised of Group papers likely to be of interest to members in their areas. The Council is confident that the extension of the Institution's work through the establishment of the Specialized Groups will prove to be one of the most valuable steps ever taken in the pursuit of the aim of "promoting the exchange of information."

G. D. C.

INSTITUTION NOTICES

Electro-Acoustics Group Committee

As announced on page 321 of this issue of the *Journal* the Council has established an Electro-Acoustics Group. A Group Committee has been appointed consisting of the following members:—

H. J. Leak (Member)—Chairman
C. T. Chapman (Associate Member)
J. W. R. Griffiths, Ph.D. (Associate Member)
S. Kelly (Member)
M. B. Martin (Associate Member)
K. R. McLachlan (Associate Member)
E. D. Parchment (Associate Member)
F. Poperwell (Associate)
A. I. F. Simpson (Member)

The new Committee will be principally concerned with the arrangement of meetings in collaboration with the Programme and Papers Committee; it will also assist in the procurement of papers for publication only.

“Collected Clerk Maxwell Memorial Lectures”

The above Institution publication, described on page 170 of the March *Journal*, is now available and members may order copies from 9, Bedford Square.

A 72 page volume, 10 in. × 6½ in., with a frontispiece and plates, bound in red cloth and gold blocked, the price of the book is 21s. post free.

Royal Society Tercentenary Celebrations

It has been announced that Her Majesty The Queen will open the Celebrations of the Royal Society's Tercentenary in the Royal Albert Hall, London, on 19th July. Her Majesty will be accompanied by H.R.H. The Duke of Edinburgh, a Fellow of the Society since 1951.

Immediately before Her Majesty's Address there will be a processional entry of Fellows and Foreign Members of The Royal Society, and of over 250 scientists from some 50 countries who have been invited to participate.

The Tercentenary Address at the Celebrations will be delivered by Sir Cyril Hinshelwood, the Society's President, who was recently honoured by appointment to the Order of Merit. Members will recall that at the Institution Dinner in London in May 1958, Sir Cyril proposed the toast of “The Institution.”

The History of the Institution

Reference was made in the editorial of last month's *Journal* to the preparation of a History of the Institution. This has now been completed and copies of the First Edition are shortly expected from the printers.

The contents trace the history of the Institution against the pattern of the development of radio science and industry. It is, therefore, a valuable reference work.

This First Edition is a crown quarto volume bound in cloth and gold blocked. It extends to 120 pages with a frontispiece in full colour and half-tone plates. The price to members is 30s. post free.

Members wishing to secure a copy are advised to place orders now.

Back Copies of the Journal

The Institution has received requests for the following issues of the *Journal* which are now out of print:—

June and November 1959.

Members who have copies of these issues, in good condition, for disposal, are invited to send them to the Brit.I.R.E. Publications Department, 9, Bedford Square, W.C.1; a payment of 5s. per copy will be made.

Correction

The following amendment should be made to the paper “A Timing Pulse Generator” by C. S. Fowler published in the February 1960 *Journal*.

Page 125, Section 1, second paragraph, lines 5 and 6, the sentence “. . . whereas G.M.T. is taken from mid-day to mid-day” should read “. . . whereas G.M.T. was, prior to 1st January, 1925, taken from mid-day to mid-day.”

A fuller explanation is that before 1st January, 1925, Greenwich Mean Time was reckoned in 24 hours commencing at noon; since that date it has been reckoned from midnight. In view of the risk of confusion in the use of the designation G.M.T. before and after 1925, the International Astronomical Union recommended in 1928 that astronomers should, for the present, employ the term Universal Time, U.T. (or Weltzeit, W.Z.) to denote G.M.T. measured from Greenwich mean midnight.

Some Aspects of Vidicon Performance†

by

H. G. LUBSZYNSKI, DR.ING.‡, S. TAYLOR, B.A.‡ and J. WARDLEY, A.R.C.S., B.SC.‡

A paper presented on 3rd July 1959 during the Institution's Convention in Cambridge.

Summary: The performance of the 1-in. vidicon is discussed, particularly the effect of various operating conditions on transfer characteristics, lag, resolution and geometry. When target voltage and dark current are high, maximum sensitivity is obtained, but this is at the expense of the other parameters. In the E.M.I. vidicon, the optimum performance as regards γ and lag is obtained for signal currents of 0.2 to 0.3 μA and dark currents of 0.01 to 0.03 μA . Methods of measuring sensitivity, γ and lag are described and possible sources of error indicated. The effect of bias illumination on γ , lag and resolution is analysed. Improvements in geometry are described together with a method of improving resolution. Infra-red and ultra-violet sensitive tubes are mentioned.

1. Introduction

The vidicon photoconductive camera tube is so well known¹ that only the briefest mention will be made of its operating principles. A tubular glass envelope (Fig. 1) of about 1 inch diameter and 6 inches length has a flat window sealed to it. The window carries on the inside a transparent conductive coating, acting as the signal plate. A layer of photo-conductive

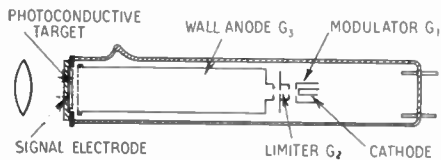


Fig. 1. Diagram of vidicon.

material is applied to the signal plate and this constitutes the sensitive target. At the other end of the tube is an electron gun which generates the scanning beam. An ion trap mesh is mounted on top of the last gun electrode called the wall anode. This mesh also serves to produce a strong, uniform decelerating field in front of the target. The beam of slow electrons stabilizes the surface of the target at the

potential of the cathode of the gun. Thus, by applying a positive voltage to the signal plate, a potential difference is set up across the target. Where light falls on the target a more conductive path is established; a current flows across the target and the potential of the illuminated target elements rises towards the signal plate potential. When the beam scans over the target surface, it restores the elements in turn to cathode potential, and thereby a train of current pulses is generated in the signal resistor which constitutes the video signal.

2. Factors Affecting Performance

Breaking down the functions of the various components, it may be seen that mainly four processes are involved in signal generation in a vidicon.

- (1) Generation of charges by photoconduction in the target.
- (2) Restoration of charges by scanning beam.
- (3) Generation of the scanning beam.
- (4) Focusing, deflection and alignment of the beam.

The performance characteristics required from the tube can be listed under a number of headings.

- (a) Sensitivity and transfer characteristic.
- (b) Response time or lag.
- (c) Picture resolution.
- (d) Geometry.
- (e) Spectral response.
- (f) Other effects.

† Manuscript received 3rd June 1959. (Paper No. 554.)

‡ Research Laboratories of Electric & Musical Industries, Ltd., Hayes, Middlesex.

U.D.C. No. 621.397.331.222

Starting from the assumption that low velocity scanning is to be employed, the target surface will be stabilized at cathode potential. If an element, on illumination, would leak to a more negative potential the scanning beam could not reach it. Therefore, the signal plate must be made positive with respect to the cathode. For a target material which is an *n*-type photo-conductor, the maximum thickness is limited by the depth of penetration of the incident light. If the target is too thick, there will be a residual layer of high insulation in series with the photo-conducting path, and the sensitivity will be reduced. Conversely, if the material is a *p*-type photo-conductor the maximum target thickness is not so much limited by the depth of penetration of the light as by the range of holes generated in the neighbourhood of the signal plate. Thus in either case the target capacitance cannot be easily reduced below a limiting figure.

conductor. The maximum usable thickness was found to be approximately 10 microns when using visible light. Such layers are practically opaque. Beyond this thickness, sensitivity is lost due to recombination of holes on their way through the layer. Amorphous antimony trisulphide which is in general use now, is an *n*-type material and, therefore, its thickness is limited by the penetration of the light. A solid layer of this material absorbs light very strongly and a target 1 micron thick is practically opaque to all visible light except red.

In order to reduce the target capacitance, a target layer of the so-called "spongy" type² was introduced. Such a target absorbs much less light than an equal thickness of the solid material due to its open structure and it has a considerably greater resistivity. It is made by evaporating the antimony trisulphide in a residual gas atmosphere. Thereby the evaporating molecules are cooled by collisions with the gas molecules so that, when the slowed-down antimony trisulphide molecules collide with each other, they do not bounce off again but stick together. Thus larger and larger particles are formed on the way from the evaporator to the target. The structure of such a layer is shown in the electron micrograph of Fig. 2.

A further substantial improvement was obtained by evaporating, in a high vacuum, a solid layer of antimony trisulphide on top of the spongy layer³. Thereby sensitivity was doubled, accompanied by a substantial reduction in lag. The latter, we believe, is due to the solid layer sealing the pores in the surface of the spongy target. This prevents, to a certain extent, the beam electrons from filtering into the layer and thereby the effective target capacitance is decreased. This type of target is now in general use in vidicons.

The layer consists of long chains of particles. The size of the particles is of the order of 300 angstroms. This target structure was also observed by Russian workers⁴. From the point of view of capacitance, it is obvious that there will be an optimum particle size. If the particles are very small, they will pack more tightly in the layer and the capacitance will be large, approaching that of a solid layer. If the particles are so large that their size is a substantial fraction of the target thickness, the



Fig. 2. Electron micrograph of target layer of vidicon.

This has an effect on the capacitance- or discharge-lag as we shall see later. In the earliest vidicons, the target layer consisted of amorphous selenium² which is a *p*-type photo-

effect will be to approach the conditions of a solid layer again. The photo-conductive lag, too, is affected by the size of the particles in the layer. As is well known, the rate of recombination of photo-excited holes and electrons can be greatly modified by the presence of surface states.

3. Sensitivity and Transfer Characteristic

The transfer characteristic of a vidicon is approximately a power law following the equation $S = kI^\gamma$, where S is the signal, k is a constant determined by the tube sensitivity, I is the illumination and γ is approximately constant. Over a large range of illumination γ does, in

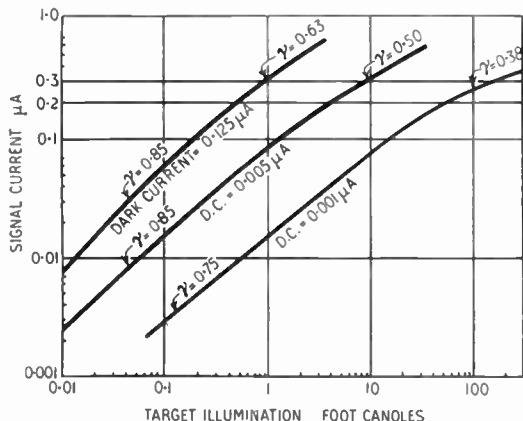


Fig. 3. Signal as a function of the illumination for Emitron 10667. (Chequer board test chart.)

fact, vary, from 0.4 - 0.85 (see Fig. 3), but over smaller ranges such as the operating range for any given application, it may be considered to be constant. Because γ is less than unity, sensitivity measured as signal divided by illumination varies with the light level and is higher for lower illuminations. The sensitivity is also a function of the voltage across the photoconductive target, and curves showing the dependence of signal on target voltage are given in Fig. 4.

3.1. Operating Voltages

From considerations of signal/noise ratio, lag, resolution, etc., it is found that the optimum peak white signal lies between 0.25 and 0.3 microamperes and, with this in mind, curves as shown in Fig. 4 enable one to choose a suitable

operating target voltage for the tube in any of its various applications.

In telecine use, the target illumination is from 50-100 ft.-candles and the target voltage lies between 10-20 volts. The chief problem associated with low voltage operation, namely shading due to the electron optics, can be minimized during the manufacture of the tube⁵ and by suitable design of scanning and focus coils⁶.

In studio use, the target illumination is of the order of 5 ft.-candles, derived from a scene brightness of 100 ft.-lamberts and a lens stop of T2.2. Here the normal operating voltage range is from 25 to 60 volts, and due to the decreased illumination lag begins to be important.

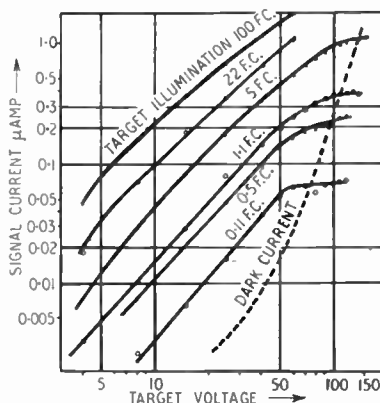


Fig. 4. Signal as a function of target voltage.

A third category may be defined for the use of vidicons, where the target illumination level is 0.5 ft.-candle or less. This condition arises in industrial or military applications where a certain amount of lag and noise may be tolerable. The target voltage can be anything up to 100 volts. At these high voltages two new features become of importance, the high dark current and the saturation of the photo-current.

3.2. Saturated Photo-currents

It can be seen from Fig. 4 that when the dark current is of the same order as the photo-current, the latter saturates. Obviously for higher illuminations the onset of saturation occurs at higher voltages. From simple considerations one might expect that when a photo-current is saturated, all the photo-electrons

would be collected at the signal electrode, and the γ would be unity. Values of γ approaching unity have in fact been observed for saturated photo-currents, with the value for the tube shown being 0.85. Such a high γ does not, however, produce pictures with good gradation. Thus one of the virtues of the vidicon in its normal operating range, i.e. its transfer characteristic with a γ between 0.5 and 0.65 allowing one to use a camera channel without a γ -correction circuit, is then lost.

A further disadvantage of high voltage operation is that in some tubes there is danger of a low level negative image remaining for some time after removal of the light, and it is prudent to keep the target voltage below 100 volts.

3.3. Variation of γ with Voltage

The fact that the curves of Fig. 4 are not parallel means that γ is changing with voltage. As the voltage increases, γ decreases, passes through a minimum, and then increases.

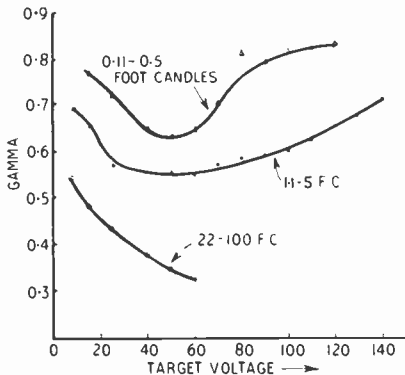


Fig. 5. γ as a function of target voltage.

The curves of Fig. 5 show this variation of γ at the three illumination levels already defined. The values of γ are calculated over a range of illumination of approximately 4:1, this range being marked on each curve. The minimum value of γ of the two upper curves occurs at a target voltage of about 50 volts corresponding to a dark current of 0.01 μ A. Over a number of tubes the minimum has usually been found to occur at dark currents between 0.01 and 0.03 μ A. It is advantageous to have a low γ , and one as low as 0.4 would be desirable in many respects. This can be achieved by suitable choice of operating target voltage.

3.4. Sensitivity Measurement

The authors measure signal current by the following null method. A negative-going variable amplitude current pulse is injected into the input of the head amplifier. This square wave pulse appears in the picture as a black vertical bar of width equal to 1/10th of the picture width. Its position can be varied so as to cover any white signal in the picture. The pulse amplitude is then adjusted, so as to balance the white signal against an adjacent black signal, and the signal current read off from a calibrated scale. The reading is thus unperturbed by any drift or non-linearity in the amplifiers or in the line monitor.

It follows from the previous Sections that any specification of sensitivity should also include a reference to the illumination level and to either the voltage or the dark current at which it is measured. At an illumination of 2 ft.-candles on the target and at a target voltage which gives 0.01 μ A of dark current, the signal from an average Emitron 10567 is 0.2 μ A. Under these conditions, the sensitivity is 77 μ A/lumen. As has been pointed out, this is subject to considerable variation with illumination and target voltage. For example, at 0.1 ft.-candles and a dark current of 0.15 μ A the sensitivity is 450 μ A/lumen.

3.5. Measurement of Gamma

In order to prevent confusion in the measurement of the transfer characteristic of the vidicon, close control of the measuring conditions should be maintained. This is so because in all optical systems a certain amount of scattered light is inevitably present, even apart from dust and the occasional fingerprint which may find its way onto the lens or window. The vidicon, with a γ of less than unity is relatively more sensitive at low light levels, and small amounts of scattered light may affect measurement appreciably. The following calculations will demonstrate this.

Suppose the test chart shown in Fig. 6(a) is used, which consists of a plain white rectangle, in the centre of which are two small areas, one black and the other variable from black to white by means of neutral density filters. If there were no scatter, the illumination on the target would be as shown in Fig. 6(b), where I_w and I_c are

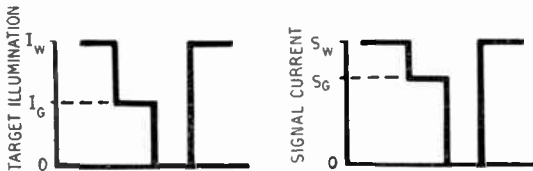
the target illuminations in the white and grey regions and there is no light in the black region. When scattering agents are present the situation is as shown in Fig. 6(c). Here, the illuminations in the white, grey and "black" areas are I'_w , I'_g and I'_b . The corresponding signals from these illuminations are also shown in the figure and are given by the following equations.

$$\left. \begin{aligned} S_w &= kI_w^\gamma \\ S_g &= kI_g^\gamma \\ S'_w &= kI'_w{}^\gamma \\ S'_g &= kI'_g{}^\gamma \\ S'_b &= kI'_b{}^\gamma \end{aligned} \right\} \dots\dots(1)$$

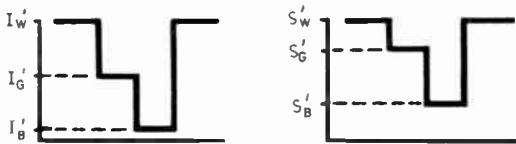
$$\left. \begin{aligned} S'_w &= kI'_w{}^\gamma \\ S'_g &= kI'_g{}^\gamma \\ S'_b &= kI'_b{}^\gamma \end{aligned} \right\} \dots\dots(2)$$



(a)



(b)



(c)

Fig. 6. Effect of scatter on the γ of the vidicon. (a) test chart; (b) signal output for illuminated target without scatter; (c) ditto with scatter.

In order to calculate values of I'_w , I'_g and I'_b we will at first consider a uniform white test chart of brightness $4T^2I_w$ where T is the transmission stop of the lens. In the absence of scatter, the illumination on the target is I_w . If a fraction m of the light is scattered, a further fraction h of this will still reach the target, and we will assume that this is uniformly distributed over the target. The new target illumination is therefore given by

$$I'_w = I_w - mI_w + hmI_w \dots\dots(3a)$$

We now return to the original test chart. Let the two small grey and black areas be of brightness $4T^2I_g$ and zero respectively. Since these areas are much less than the total test chart area, the scattered light reaching the target, hmI_w , is not appreciably changed. The illumination in the grey and "black" areas is therefore given by

$$I'_g = I_g - mI_g + hmI_w \dots\dots(3b)$$

$$I'_b = hmI_w \dots\dots(3c)$$

Also, since S'_b is the new black level, the measured signals S_w'' and S_g'' are given by

$$\begin{aligned} S_w'' &= S'_w - S'_b \\ \text{and } S_g'' &= S'_g - S'_b \end{aligned} \dots\dots(4)$$

From eqns. (2), (3) and (4) the values of S_w'' and S_g'' may be derived.

$$\begin{aligned} S_w'' &= kI'_w{}^\gamma - kI'_b{}^\gamma \\ &= k \{ I_w^\gamma (1 - m + hm)^\gamma - (hmI_w)^\gamma \} \\ S_g'' &= kI'_g{}^\gamma - kI'_b{}^\gamma \\ &= k \left\{ I_g^\gamma \left(1 - m + hm \frac{I_w}{I_g} \right)^\gamma - (hmI_w)^\gamma \right\} \end{aligned} \dots\dots(5)$$

From eqns. (1) the correct value of γ is given by

$$\gamma = \frac{\log S_w/S_g}{\log I_w/I_g}$$

and similarly the measured γ would be assumed to be

$$\gamma'' = \frac{\log S_w''/S_g''}{\log I_w/I_g}$$

Using eqns. (5) the ratio

$$\frac{S_w''}{S_g''} = \frac{I_w^\gamma}{I_g^\gamma} \times \frac{(1 - m + hm)^\gamma - (hm)^\gamma}{\left(1 - m + hm \frac{I_w}{I_g} \right)^\gamma - \left(hm \frac{I_w}{I_g} \right)^\gamma}$$

Therefore $\gamma'' = \gamma + \frac{\log A}{\log B}$

where $A = \frac{(1 - m + hm)^\gamma - (hm)^\gamma}{(1 - m + hmB)^\gamma - (hmB)^\gamma}$

and $B = I_w/I_g$.

It can be shown that the expression $\log A / \log B$ is always positive when γ lies between 0 and 1. Therefore, the measured γ is always greater than the true γ of the tube. The simplest way to minimize the effect of light scatter is to alter the test chart so that it is all black except for a small area, the brightness of which can be varied. The amount of scattered light is thus greatly reduced, so that the change in black level will usually be negligible, and any residual light scatter will be proportional to the brightness of the illuminated area. In this case the eqns. (3) become

$$\begin{aligned} I_{W'} &= I_W (1 - m) \\ I_{G'} &= I_G (1 - m) \\ I_{B'} &= 0 \end{aligned}$$

and it easily follows that the measured γ is not increased by the scatter. Two curves of signal against illumination measured with the original and the modified test charts are shown in Fig. 7.

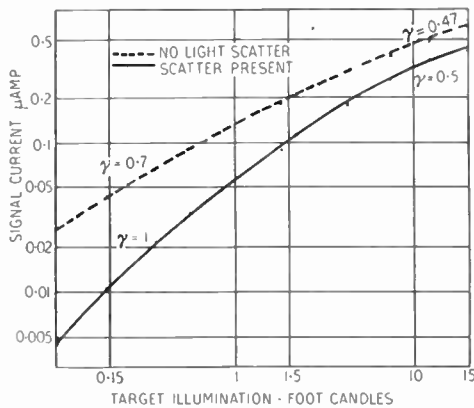


Fig. 7. Signal as function of illumination with and without scatter.

The correct procedure to adopt when measuring γ depends, of course, on the subject under investigation. If we are interested in the properties of the photo-conductor itself non-scattering conditions would always be used, whereas to obtain the operating γ of the vidicon in normal broadcast use, a certain amount of scattered light should be present. This could be done by surrounding the black, grey and white squares by a transparency of a typical scene, so that the whole of the vidicon target is illuminated. The

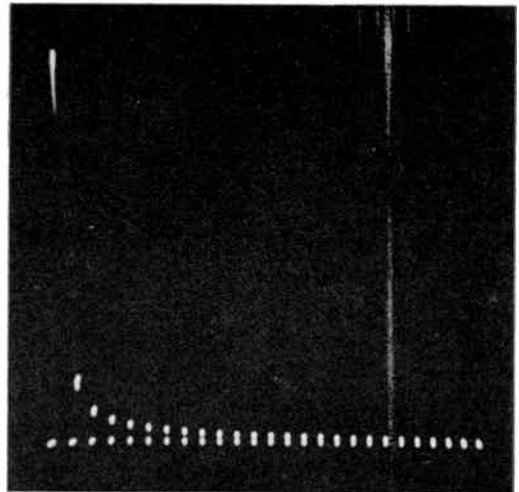


Fig. 8. Oscillogram of typical lag curve (total lag).

signal vs. illumination curves of Fig. 3 were in fact measured using a chequer board test chart.

4. Lag

One of the most important aspects of photo-conductive tube performance is the problem of lag. Lag is due to two effects; first, there is the lag inherent in the discharge mechanism of the electron beam; secondly, there is the inertia of the photo-conductive process itself.

4.1. Measurement of Lag

At this point it is perhaps appropriate to describe the method used to measure lag. A uniform, stationary patch of light is produced on the screen of a cathode-ray tube by means of a special gun. The screen material has a decay constant of only a few microseconds. This patch is imaged on the vidicon target for a few seconds. Then a line selector pulse is used to switch off the illumination immediately prior to the scanning beam reaching the image of the patch. Simultaneously, an oscilloscope with a slow time-base is triggered off, the Y-plates of which are fed with the signal. Each time the vidicon beam passes over the previously illuminated patch a signal is generated, due to the lag of the tube, and thus the whole lag curve is plotted. It must be borne in mind, of course, that at the moment the light is switched off, the interlaced field has only had half the exposure

of the field being scanned at the time and, hence the interlace signals are proportionally smaller. A typical lag curve is shown in Fig. 8. For measuring build-up lag the illuminating cycle is reversed, i.e., the cathode-ray "lamp" is pulsed on, instead of being cut off, by the line selector pulse.

The discharge lag can be measured in a similar manner by pulsing the cathode negatively in the dark, at the right moment and observing the decay curve of the resulting signal which we call the capacitance signal. In order to be independent of any shading, the signal to the oscilloscope is gated so as to take in only the small area under consideration. The method has the further advantage that, in this way, the variation of lag over the whole of the target area can be measured point by point.

4.2. Discharge Lag

To deal with the discharge lag first, it has been shown elsewhere⁷ that the speed of discharge depends on the slope of the beam acceptance curve and the target capacitance. The slope of the curve is limited theoretically by the spread of thermal energies of the beam electrons. In practice, it is found that the theoretically possible slope is never reached. Meltzer and Holmes⁸ have measured tempera-

tures in electron beams of C.P.S. Emitrons and found values of the order of 2,500°K, whereas the actual cathode temperature is only round about 1,050°K. The beam temperature was in part dependent on beam intensity and, therefore, closely connected with the electron optics of the tube and gun. It is obvious that there is scope here for further improvement.

For signals greater than 0.1 μA the discharge lag component is usually less than 3 per cent. after 1/25th sec. It becomes, however, more important in the case of small signals of the order of less than 0.05 μA .

When interpreting lag measurements of this kind, it is necessary to take into account the fact that the scanning pattern is interlaced. Furthermore the size of the scanning spot is certainly larger than one line width. Thus, when scanning the odd lines 1, 3, 5, etc., the beam will lap off a certain amount of charge from lines 2, 4, 6, etc. Thus the signal of the odd field will be somewhat higher than it should be, while that for the even field is reduced in amplitude. By overscanning the target in the vertical direction, the scanning lines can be spaced wide enough so that no overlapping occurs. It is found that when overscanning 2:1, the signals from the two fields are almost paired as shown in Fig. 9(a). The overlapping effect may be restored

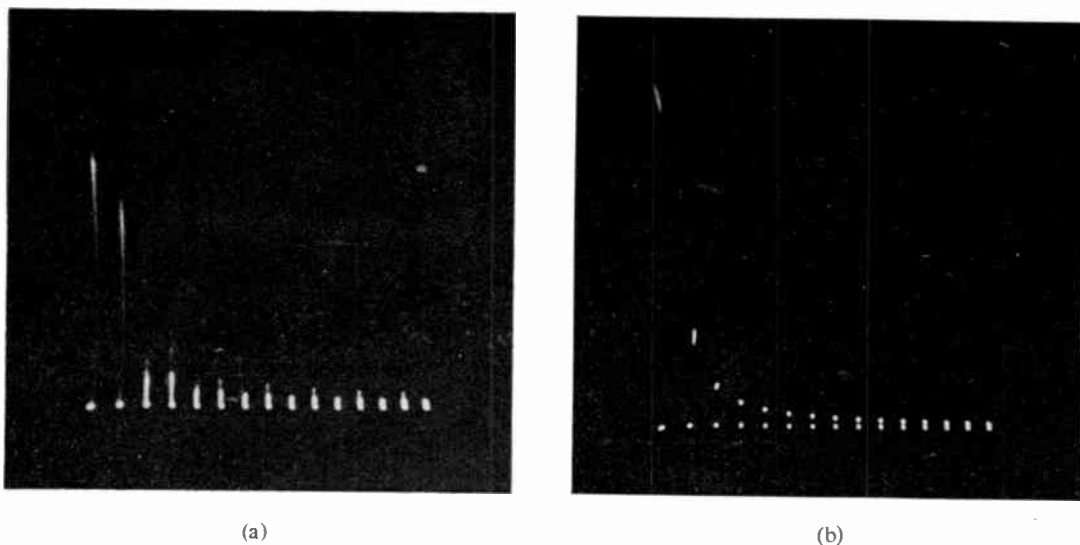


Fig. 9. Discharge lag curve. (a) overscanned 2:1 in the vertical direction. (b) the same, slightly defocused to simulate normal scanning conditions.

without altering the target capacitance by slightly defocusing the beam, as is shown in Fig. 9(b). This permits a conclusion to be drawn about the actual spot size. It appears, that the size of the spot is just over two lines wide. This is also borne out by experiments described in the section on resolution.

4.3. Photo-conductive Lag

After cessation of illumination, the photo-conductor does not return immediately to its highly insulating state but the conductivity decays over a period of time. We have measured lag curves on a very large number of tubes and have obtained certain reproducible results. It is well known that the lag decreases with increasing illumination. By measuring the first

till it is so small that it becomes negligible compared with the photo-conductive lag. The surprising fact is the subsequent maximum. One might expect the lag to rise for signal currents so high that the beam is insufficient to discharge the target. However, the observed rise is certainly not due to this effect, because the lag actually decreases again for still larger signals. Also, the signal amplitudes in the rising parts of the curves are quite moderate and the target should be easily discharged by the beam. The minimum lag occurs for signal currents between 0.25 and 0.3 μA over a range of target illuminations from 30 ft.-candles down to about 2 ft.-candles. At lower illuminations the minimum tends to shift to lower signal currents and is less pronounced. For example, for the tube shown in the figure, it occurs at about 0.08 μA of signal current for a target illumination as low as 0.4 ft.-candles. The authors are still unable to explain the occurrence of the minimum or of the following maximum, but from the point of view of the user it appears preferable to operate the tubes with signal currents between 0.25 and 0.3 μA when aiming at minimum lag. It has been proposed⁹ to operate tubes at rather high dark currents of the order of 0.2 μA . This is possible without excessive shading for very uniform target layers in tubes of the so called "pip-less" type. As has been seen earlier, this is certainly the condition for obtaining high sensitivity. A limit is set, however, by the fact that the photo-currents saturate. These saturation points coincide with the maxima of the lag curves in Fig. 10 where also the γ of the tube rises steeply towards unity. If the overall γ is then reduced by means of a correction circuit, the effect is to raise the low signal amplitudes in relation to the high ones and thus the low amplitude lag signals can sometimes become more visible.

When measuring the photo-conductive lag, it is found that the signal amplitude drops very rapidly at first, followed by a long, low-level tail. This tail may extend over many frames. At first it was thought to be most essential to reduce the first lag signal as much as possible. Soon it became clear, that the tail can be at least as troublesome, depending on the picture content. If an object of some shade of grey moves across a background of fixed scenery such

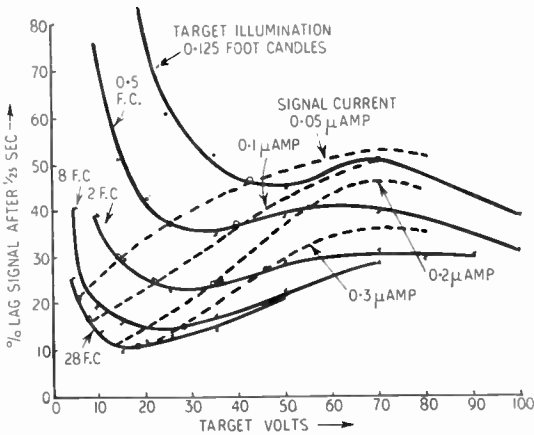


Fig. 10. Lag as function of target voltage for different illumination.

lag signal after 1/25th sec as a function of target volts, illumination and output signal, it is possible to draw families of curves such as shown for a typical tube in Fig. 10. It can be seen, when plotting the first lag signal after 1/25th sec against target voltage, that the curves have a minimum, followed by a maximum.

Each of these curves applies to a different, constant illumination which we have chosen to represent typical applications such as film scanning, studio and low brightness subjects. The first decrease in lag for increasing target volts is, of course, to be expected, because the signal increases and, with it, the voltage swing on the target. Hence the discharge lag decreases

as furniture, windows, etc., the long-term lag makes the stationary signal appear superimposed on the moving one. A moving person, for example, becomes semi-transparent. This effect has been called "print-through." The visibility of this kind of lag is enhanced by an increase in gamma because the contrast with the surrounding field is increased, and these signals are compared with their surroundings by the eye of the observer. Here, one must be on one's guard again, however. The lag was measured with an oscilloscope. A number of observers were then asked to assess the visibility of this lag when viewing a test scene consisting of a fixed geometric white and grey pattern, covered up by a moving black square. It was found that the visibility varied at random between observers and from one test to the next. The cause of this was traced to the way in which the lag was observed. When the eye of the observer was fixed on the stationary pattern, the lag was much less visible than when the eye followed the leading edge of the moving black square covering up that pattern.

Another way of reducing lag is the application of bias light⁷. If a uniform bias illumination is superimposed upon the picture illumination the surface potential on the target is increased and the discharge lag is thereby reduced. Moreover, the increased total illumination causes a reduction in photo-conductive lag. At a target illumination of 5 ft.-candles and for a bias illumination which causes a signal of about $0.05 \mu\text{A}$, the first lag signal was found to be reduced by one third and the amplitudes of the signals in the tail of the lag curve by nearly half. No substantial further improvement was found for light bias values causing signal currents of more than $0.05 \mu\text{A}$. These figures were measured objectively and are certainly correct, but subjectively the difference in a studio picture with and without bias light was hardly noticeable. The main reason was found to be that most scenes carry their own bias light, because the general scene illumination produces, in most cases, a signal of the order of $0.05 \mu\text{A}$ or more, beyond which further bias light has little effect.

Under special circumstances, such as white figures against a black background, bias lighting can give a substantial improvement. We may

say therefore, that an increase in γ will improve the subjective lag of a white object moving across a black background while it will increase the visibility of lag from an object moving across a patterned grey background. No completely satisfactory solution of the problem of lag has yet been found.

5. Resolution

The resolution of a vidicon is limited mainly by the finite size of the focused scanning beam. In considering lag it was shown that the beam is just over two lines wide. It is known that the beam electrons are not homogeneous in velocity, but have varying lateral components due to their thermal emission energies and the imperfections in the electron optics of the tube.

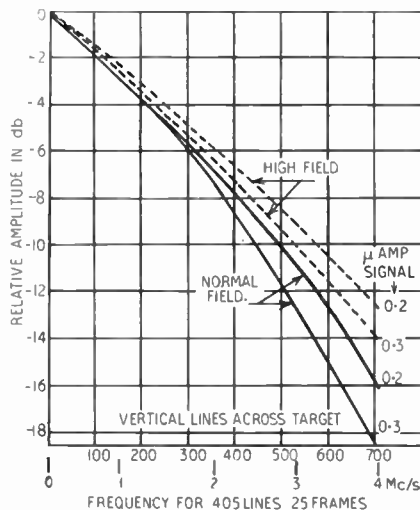


Fig. 11. Frequency response curve of E.M.I. vidicon 10667.

The part of the beam actually used in discharging a picture element will depend on the instantaneous potential of that element. For small signals and, therefore, small potential changes on the target, only the fine tip of the beam is effective, whilst larger signals will require the whole of the beam for discharge. Hence one expects, and finds, that the modulation decreases with increasing signal current. The discharge of an element as the beam moves in the line direction will be by the leading edge

of the beam, and the subsequent frequency response will be a complex function of the above-mentioned factors. The frequency response for a typical tube under varying operating conditions is given in Fig. 11.

The resolution can be improved by increasing the field between the mesh and the target. This could be achieved by reducing the mesh-to-target spacing but the mesh would come into focus and be seen in the picture. Instead, the first anode voltage can be raised from 300 to 500 V, the wall anode voltage to about 490 V, and the axial magnetic field increased sufficiently to focus the beam. Then at 3 Mc/s or 530 lines across the target, there is an improvement of 2.5 db in modulation at a signal current of 0.2 μ A.

As the beam is wider than one line, there is an added complication due to interlaced scanning. While the beam scans one field it will also discharge some of the signal on the interlaced field that it overlaps. By sampling the signals along a vertical line in the picture¹⁰ one can measure the width of a horizontal black-to-white transition. Using this method, it has been confirmed that the focused spot is between two and three lines wide as deduced from measurements of capacitance lag. Under normal operating conditions two to three lines are necessary for such a transition, whilst under high field condition it takes only two lines. Of course, such high field operation requires about 70 per cent. more scan power and about 30 per cent. more focus current. At present, tubes are operated at maximum voltages of 300 V, mainly from circuit considerations.

The γ of the pick-up tube has a considerable influence on the measured modulation. Consider a pattern of vertical black and white bars projected optically on to the tube face. Let the peak white illumination for a large area be I_0 , and the intensity for a white bar be I_2 . There will be some illumination in the black bars due to optical aberrations and scatter and the intensity there may be equal to I_1 . The transfer characteristic is $S = kI^\gamma$, therefore, the modulation

$$M = \frac{S_2 - S_1}{S_0} = \frac{I_2^\gamma - I_1^\gamma}{I_0^\gamma}$$

Taking a practical example of $I_0 = 100$ units, $I_2 = 90$ units and $I_1 = 10$ units of illumination, the modulation can be seen to vary with γ as given in Table 1.

Table 1

γ	% Modulation	Amplitude Loss db
1.0	80	-1.9
0.85	68	-3.4
0.65	64	-3.9
0.50	58	-4.8
0.35	48	-6.4

6. Geometry

The picture geometry produced by a vidicon is governed by the electron optics of the tube itself, and the action of the scanning and focus fields on the electron beam. Correct geometry can be attained by mutually matching tube and scanning and focus coils. It can happen that a tube may give a geometrically accurate picture in one set of coils, but be quite unsatisfactory in those of a different design.

It has been shown¹¹ that the optimum dimensions for a low-velocity scanning system are achieved when the length of the deflecting field is made equal to an integral number of focus loops of the electron beam in the axial magnetic field.

In these circumstances, deflection of the beam does not introduce any further lateral components into the beam. Unfortunately, the vidicon has only one loop between gun and target. The scanning field must, therefore, be shorter than this in order to leave sufficient room for alignment coils. Thereby some errors are introduced. The most common geometrical error is that of pin-cushion distortion in the displayed picture; this corresponds to barrel distortion of the scanned raster on the target of the pick-up tube. Another error is the difference in focusing voltage between the centre of the target and the corners. The deflection of the beam causes an inevitable increase in path length and this causes the corner focus to be in front of the

target whilst in the centre of the picture the electrons are in focus at the target.

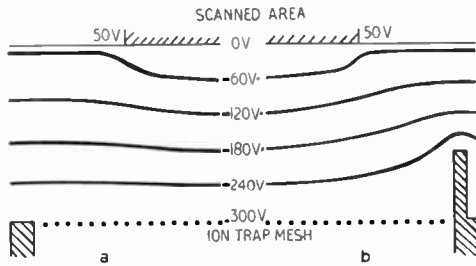


Fig. 12. Electrostatic field in front of target without and with "geometry" ring.

Some correction of the pin-cushion error and the differential focus can be made by modifying the planar electrostatic field between the ion trap mesh and the target. By keeping the average velocity of the deflected beam higher than that of the undeflected beam after passing through the mesh it will then be in focus nearer the target. The potential and therefore the velocity of the deflected beam can be kept higher by means of a ring electrode extending forward from the ion trap mesh and at the same potential. The change in equipotentials can be seen in the two halves of Fig. 12. It is found that, with a suitable depth of this "geometry" ring, substantial correction can be made both for differential focus and the pin-cushion distortion. A considerable improvement in geometry and overall focus can be made by increasing the diameter of the scanning coils themselves. This is due to the electron beam in its extreme deflected position not being too close to the distorted magnetic field associated with the end turns of the scanning coils. By making the two sets of deflection coils separate and mutually adjustable for both relative angle and longitudinal position, it is possible to realize an accuracy in picture geometry better than three picture points. This has been achieved in the E.M.I. three-vidicon colour camera¹² where it is necessary to register accurately three such vidicon assemblies.

It has been found that tubes made with completely non-magnetic electrodes and signal plate rings are no better in performance than those of normal construction employing magnetic materials.

7. Spectral Response

The response of the antimony trisulphide layer is substantially panchromatic and quite adequate for normal broadcast applications. In the ultra-violet, the glass window limits the response and by replacing it with a quartz window, the tube is still quite sensitive at 2350 angstroms.

For the infra-red region a different photoconductive layer is necessary. Unfortunately, infra-red sensitive photo-conductors have low resistivity, and the choice of a material used for such a target is necessarily a compromise between sensitivity and adequate resistivity for full storage. It has been possible to develop layers¹³, giving a response out to 1 micron.

8. Other Effects

The target of the vidicon can be permanently damaged by passing grossly excessive currents. It appears to be inevitable that a faint burnt-in image of the scanned raster will appear after several hundred hours' use. However, if the tube is always scanned with the correct size raster, properly orientated, no trouble arises.

Scanning failures do not burn the target, unless the dark current is excessive. In fact, it has been found with E.M.I. tubes that burning only occurs when the dark current exceeds 0.8 μA , which is far above the normal operating value. Burning does not occur when the total signal exceeds 0.8 μA , providing that the dark current component itself does not exceed 0.8 μA . Of course, a focused image of the sun or any other intense source will cause permanent damage due to its heating effect alone.

Vidicon tubes also exhibit fatigue effects initially, i.e. the sensitivity is lower temporarily after exposure to light. The tendency to fatigue is not persistent and disappears after 10 or 20 hours' normal use of the tube.

9. Conclusion

We may say, therefore, that vidicons are still not able to perform all the functions fulfilled by the ideal pick-up tube. On the other hand, by choosing the optimum operating conditions suited to a particular application, very good performance can be achieved.

10. Acknowledgments

We wish to thank our colleagues and staff for their help in this work, especially Mr. H. Jepson who made many of the measurements, Mr. J. N. Perren who took the electron micrographs, and Messrs. F. W. Jackson and R. D. K. Gilden.

Thanks are due to the directors of Electric & Musical Industries Ltd., for permission to publish this work.

11. References

1. P. K. Weimer, S. V. Fergie and R. Goodrich, "Vidicon—photo-conductive camera tube," *Electronics*, **23**, May 1950, pp. 70-73.
2. B. H. Vine, R. B. Janes and F. S. Veith, "Performance of the vidicon, a small developmental television camera tube," *R.C.A. Review*, **13**, pp. 3-10, March 1952.
3. H. G. Lubszynski, British Patent No. 827058 (15th February 1955).
4. A. M. Reshetnikov, "The structure of thin films of antimony trisulphide obtained by subliming in an atmosphere of nitrogen at pressures below 4 nm of mercury," *Soviet Physics, Doklady*, **3**, p. 382, 1958.
5. R. G. Neuhauser and L. D. Miller, "Beam-landing errors and signal output uniformity of vidicons," *J. Soc. Motion Pict. Telev. Engrs*, **67**, pp. 149-153, March 1958.
6. J. Castleberry and B. H. Vine, "An improved vidicon focusing-deflecting unit," *J. Soc. Motion Pict. Telev. Engrs*, **68**, pp. 226-229, April 1959.
7. R. S. Webley, H. G. Lubszynski and J. A. Lodge, "Some half-tone charge storage tubes," *Proc. Instn Elect. Engrs*, **102B**, pp. 401-410, July 1955.
8. B. Meltzer and P. L. Holmes, "Beam temperature, discharge lag and target biasing in some television pick-up tubes," *Brit. J. Appl. Physics*, **9**, pp. 139-143, April 1958.
9. L. D. Miller and B. H. Vine, "Improved developmental one-inch vidicon for television cameras," *J. Soc. Motion Pict. Telev. Engrs*, **67**, pp. 154-156, March 1958.
10. R. Theile and F. Pilz, "Transmission defects of the super-orthicon television camera tube," *Arch. Elekt. Ubertragung*, **11**, pp. 17-32, January 1957.
11. A. Rose and H. Iams, "Television pick-up tubes using low velocity electron beam scanning," *Proc. Inst. Radio Engrs*, **27**, pp. 547-555, September 1939.
12. I. J. P. James, "A vidicon camera for industrial colour television," *J. Brit.I.R.E.*, **19**, pp. 165-180, March 1959.
13. S. Taylor, "An infra-red-sensitive television camera tube," Proceedings of Symposium on Photo-electronic Devices, held at Imperial College, London, in September 1958. Published in "Photo-electronic Image Devices," Volume 12 of "Advances in Electronics and Electron Physics" (Academic Press, New York and London, 1960).

MEDICAL ELECTRONICS GROUP ACTIVITIES

The Medical Electronics Group of the Institution has made valuable contributions to the Institution's proceeding since it was officially formed in February 1959. Many members of the Institution who are not professionally engaged in medical electronics have found that meetings of this Group offer a wide range of interests in the application of electronics. Techniques employed in practice are often unconventional from the engineer's viewpoint, a situation which has been created by slender budgets and the unusual requirements of medical practitioners.

The meetings of the Group have always attracted enthusiastic attendance. A very diverse series of subjects has been covered, as extracts from the Group's proceedings show.

"Aviation in Medicine and Electronics"—G. H. Byford. This paper reviewed the work of the R.A.F. Institute of Aviation Medicine, making particular reference to electronic techniques employed. It will shortly be published in the *Journal*.

"Physiological and Acoustical Aspects of Hearing"—Dr. R. P. Gannon of the Charing Cross Hospital Medical School. The especial interest of this paper was the way in which it showed the part played by electronics in discovering the mechanism of hearing.

"Measurement of Signals in the Presence of Noise"—D. A. Bell, Ph.D. and Dr. G. D. Dawson. At this very well attended meeting a number of new techniques of cross correlation were described, including storage tubes.

"The Unification of Electronic Clinical Instruments"—Dr. F. D. Stott. This paper emphasized the need for drawing up accepted technical specifications on instruments in common use so that they were interchangeable and the results obtained were comparable. During the discussion the importance of laying down safety requirements was raised, and the Group Committee is considering a programme of work on this subject.

"Continuous Recording of Heart Activity"—Dr. I. Boyd and W. R. Eadie (Associate Member). The problems dealt with in this lecture were the recording of cardiac output, rate and volume, involving the development of a sensitive venous pressure meter and a servo assisted pen recorder.

"Nerve Impulses from Stretch Receptors in Muscle"—Dr. J. G. Nicholls of University College, London. The paper discussed the highly sensitive biological transducers associated with nerves in which a stretch gives rise to potentials in the nerve endings.

Bibliography on Medical Electronics.—The Institution has, in co-operation with the Rockefeller Institute for Medical Research, provided data for the compilation of the second edition of the Bibliography on Medical Electronics. This is being published by the Professional Group on Medical Electronics of the Institute of Radio Engineers of America. Arrangements are being made for the Brit.I.R.E. to distribute the Bibliography to members of the International Federation for Medical Electronics.

International Health Study by the United States Senate.—A Sub-Committee of the United States Senate on international organizations has been set up as part of an international research review. The Institution has co-operated in the completion of a survey on the use of medical electronics in the United Kingdom, and the Committee was congratulated by Senator H. H. Humphrey for its assistance and other important work in this field.

A Descriptive Title.—In view of this month's editorial on the naming of a Specialized Group, it is worthy of note that the Council has asked the Medical Electronics Group Committee to consider the suggestion made by Professor A. V. Hill in his Inaugural Address. Professor Hill pointed out that "Biological Electronics Group" was a more appropriate name, and the Group Committee is considering the incorporation of this phrase in its title.

The J. Langham Thompson Premium.—The Group Committee has been much encouraged by the endowment by a Vice-President of the Institution of a Premium for outstanding papers published in the *Journal* on medical electronics. It should be emphasized, that all papers on medical electronics may also be eligible for consideration for other Institution awards, for example, the Clerk Maxwell or Heinrich Hertz Premiums or the Rutherford Award.

CHAIRMEN OF LOCAL SECTIONS



The present Chairman of the North Eastern Section, **Jack Bilbrough**, has held office since 1958. Before that he had served the Committee for a number of years as Programme Secretary, and he continued to look after this important aspect of the Committee's work until the end of the 1959-60 session.

Born near Sheffield in 1915, Mr. Bilbrough received his technical education at Barnsley Technical College and at the beginning of the war he joined the Ministry of Aircraft Production as Technical Officer. He worked for seven years at the Telecommunications Research Establishment in Swanage and Malvern on airborne centimetric radar and air transportable equipment.

In 1946 he joined Scanners Limited of Pelaw-on-Tyne as engineer in charge of the development of the Company's products; in 1950 he left to form Microwave Instruments Limited of North Shields, and became director and general manager. He was initially responsible for all technical aspects of the Company's work, particularly in the design of microwave test equipment and since 1956 he has been managing director. He continues to take a leading part in the Company's technical developments.

Mr. Bilbrough was elected an Associate of the Institution in 1952 and in 1958 he was transferred to Associate Member.

Frank Christopher Potts was elected Chairman of the Merseyside Section in 1958 having previously served the Section in the offices of Vice-Chairman and of Treasurer.

Born in Wallasey, Cheshire, in 1914, Mr. Potts was educated at Birkenhead School and Liverpool University, where in 1935 he received a B.Sc. degree with honours in physical chemistry; in 1937 he was awarded an M.Sc. for a thesis on spectroscopic determination of copper.

With the exception of war service, first with the Air Ministry and later as a serving officer with the R.A.F., Mr. Potts has been exclusively engaged in the patent profession. He joined the Liverpool firm of W. P. Thompson & Co. as a Technical Assistant in 1938 and in 1946 became a Chartered Patent Agent; he was a partner in this firm from 1946 until 1957, when he became sole proprietor of the practice of A. J. Davies in which he had been a partner since 1952. He now divides his time between his practices in London and on Merseyside.

Mr. Potts was elected an Associate Member of the Institution in 1943.



Joseph Cotterell, Chairman of the South Wales Section since 1958, is Principal of Llandaff Technical College, Cardiff. He has served on the Committee since the Section was formed in 1954.

Mr. Cotterell was born in Wednesbury, Staffordshire, in 1914 and received his technical education at the Wednesbury County Technical College, obtaining the Higher National Certificate in 1937. Before becoming a lecturer in radio engineering at Birmingham Central Technical College in 1940, he held engineering appointments with the Midland Electric Corporation. From 1942 to 1946 Mr. Cotterell lectured in radio and electrical engineering subjects at Walsall Technical College, latterly as senior lecturer, and in 1946 he was appointed to take charge of the Engineering Department at Burton-on-Trent Technical College. He

became Principal of Llandaff Technical College in 1954.

Mr. Cotterell was elected an Associate of the Institution in 1943 and in 1948 he was transferred to Associate Membership.



A Proposed Space-Charge-Limited Dielectric Triode†

by

G. T. WRIGHT, PH.D.‡

A paper read before a meeting of the Institution in London on 13th January 1960

In the Chair : Dr. T. B. Tomlinson (Associate Member)

Summary : Recent experiments have shown that large, controllable, space-charge-limited (s.c.l.) current can be obtained in insulating crystals of cadmium sulphide if these are grown sufficiently free from lattice defects and provided with a suitable cathode contact. A dielectric diode made in this way is analogous to the thermionic vacuum diode; in particular there is the possibility of adding a control electrode to form the dielectric triode which, together with the vacuum triode and the semi-conductor transistor will complete the basic trio of charge-control devices. This paper anticipates the construction of this triode and deduces the characteristics which it should possess.

The basic equations of the triode are derived and it is shown that its d.c. characteristics should be very similar in form to those of the vacuum triode. Frequency characteristics are determined by electron trapping effects and equations are derived describing the response of the triode to time-varying signals. These equations are solved for the case of a sinusoidal signal voltage and the frequency dependence of mutual conductance and anode resistance calculated. It is shown that a triode relatively free from electron traps should have quite uniform characteristics up to frequencies at which transit times of the order of $1\mu\text{sec}$ become significant and should therefore be useful as a wide-band video amplifier. However, if the triode possesses a high density of shallow traps its parameters are markedly dependent on frequency. It is shown that in this case the mutual conductance should rise and the anode resistance should fall, possibly by very many times, as the operating frequency increases. The high frequency values should be maintained up to frequencies at which transit times of the order of $0.1\mu\text{sec}$ become significant; the device should thus be a useful v.h.f. amplifier.

Because of its necessarily small size there are many technological problems involved in the construction of a practical triode. The development of the device is a worthwhile proposition, however, because it should possess a high input resistance, be relatively insensitive to temperature changes, and in its applications should be able to utilize the vast amount of circuit design accumulated for the vacuum triode.

1. Introduction

It has recently been shown that large and controllable space-charge-limited (s.c.l.) current can be obtained in insulating crystals of cadmium sulphide if these are grown sufficiently free from lattice defects and provided with a suitable cathode contact¹. A new class of s.c.l. dielectric devices is now being developed which is expected to complement semi-conductor

devices in applications at moderately high impedance or voltage levels, where insensitivity to temperature changes is required or where operation at very high frequencies is required.

One of the most attractive of the new devices which can be envisaged is an amplifying s.c.l. dielectric triode. This device would have the usual advantages of crystal valves as regards small physical size, mechanical robustness, and freedom from heater supplies, should have a gain-bandwidth product at least comparable with that of the vacuum triode or the transistor, and should possess the high input impedance which is characteristic of the vacuum triode.

† Manuscript received 9th October 1959. (Paper No. 555.)

‡ Materials Group, Electrical Engineering Department, University of Birmingham.

U.D.C. No. 621.315.61

This paper anticipates the development of this device and presents a simplified theory of its operation. It is shown that by using a crystal relatively free from electron trapping levels it should be possible to make a wide-band video amplifier. Alternatively, by using a crystal containing a high density of shallow electron trapping levels it should be possible to make an amplifier in which the mutual conductance rises many times as the operating frequency rises; such a device would be particularly suitable for high frequency applications.

Much of the theory of the dielectric triode and particularly any assessment of its potential value is based on the results of research with s.c.l. dielectric diodes^{2,3}. It is therefore appropriate to discuss briefly the mechanisms of diode operation and summarize experimental diode characteristics before considering the design and operative mechanisms of the triode.

2. Space-Charge-Limited Dielectric Diodes

The whole possibility of achieving current in insulators rests on the central fact that electrons can travel freely through an electric potential field which is periodic in space. The interior of a perfect crystal represents such a periodic potential field, consequently an electron should be able to travel through it without difficulty. The only condition to be met is that the energy of the electron must be within certain well-defined ranges; these allowed ranges are characteristic of the crystal and form the "allowed energy bands" of the crystal.

However, under normal circumstances current does not flow in insulating crystals; there are two main reasons for this. Firstly, the allowed bands of insulators seem to be above the energy levels occupied by electrons in metals. Thus at the contact between a metal and an insulator there is a step in electron potential which forms a contact potential barrier preventing the large scale introduction of electrons into the crystal from an external source. Secondly, all real crystals contain lattice defects some of which are able to act as electron traps. Thus even if small numbers of electrons do manage to enter the crystal most fall into electron traps and are unable to contribute to current.

2.1. Construction of Experimental Diodes

Experiments have shown that for the case of insulating crystals of cadmium sulphide at least, it is possible to eliminate these various obstacles to electron movement and obtain s.c.l. current. Thin, flat, transparent, yellow, crystal plates of this material can be grown quite readily by condensing the vapour in nitrogen at a temperature of about 900°C. Diodes are made by soldering the crystal plates with indium on to brass or nickel stubs which act as heat sinks. During this process, which forms the electron injecting cathode, temperature control is rather critical; a temperature of about 340°C maintained for a few seconds has been found most suitable. The anode is formed by any convenient means such as using colloidal graphite or silver paste cement or vacuum evaporated metal layers. Diodes made in this way have electrode areas typically of the order of 1mm². Reverse resistances in the dark are typically of the order of 10¹⁰ to 10¹² ohms; forward currents in the dark are typically in the range of a fraction of a microampere to hundreds of milliamperes depending on trap content and thickness of the crystal and the applied voltage.

2.2. Diode Operation and Characteristics

The basic equations which describe current flow in insulators are mathematically intractable and probably impossible to solve in their general form. However, approximate solutions⁴⁻⁸ have been found for various restricted ranges of interest and by combining these a fairly representative overall picture of theoretical characteristics can be obtained. These calculations are illustrated in Fig. 1 which shows on one diagram the various types of current characteristics to be expected. This overall picture is well supported by the experiments which have been made with cadmium sulphide diodes.

2.2.1. Deep-trap limited current

At small applied voltages the charge injected into the crystal is small. Most of this charge falls into deep-lying traps and does not contribute to current.⁸ Thus currents are very small and non-linear; this is region (a) in the diagram.

The density of conduction electrons is given by $n(x) = N_0 \exp(-W_1/kT)$ and the density of

trapped electrons is given by

$$n_t(x) = N_t / (1 + \exp [(W_t - W_f) / kT]).$$

In these expressions N_0 is the total effective integrated density of conduction levels ($N_0 = 2[2\pi m kT / h^2]^{3/2}$); N_t is the density of trapping levels; W_f is the position of the Fermi level measured downwards from the conduction band of the crystal, and W_t is the position of the trapping levels measured in the same way. Under practical conditions $n(x)$ will always be very much smaller than N_0 so that classical statistics can always be applied to the occupation of the conduction levels.

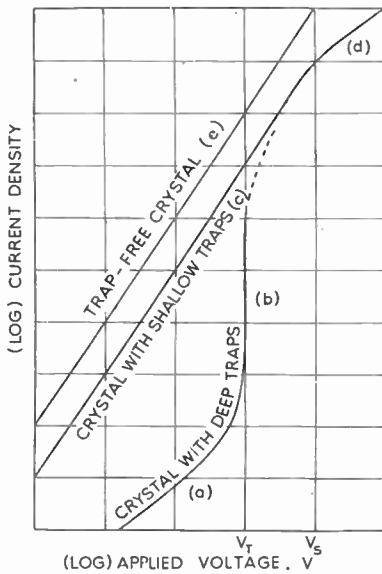


Fig. 1. Illustrating current/voltage relations for s.c.l. current in insulators.

- (a) deep-trap limited region,
- (b) trap-filled transition region: $V_T = eN_t d^2 / 2\epsilon$,
- (c) modified square-law region: $i = 9\epsilon_{11} \theta A V^2 / 8d^3$,
- (d) proportional current region: $V_S = 9eN_c d^2 / 8\epsilon$,
- (e) ideal square-law relation: $I = 9\epsilon_{11} A V^2 / 8d^3$.

To estimate the order of magnitudes involved we may evaluate the trapping factor

$$\theta = n(x) / [n(x) + n_t(x)]$$

for a crystal containing 10^{15} traps/cm³ at a depth of 0.8 eV; this is approximately one trap in every 10^6 lattice sites and is a typical figure. The quantity θ is a measure of the fraction of charge in the crystal which is free to contribute to current; in this case $\theta \cong 10^{-8}$ so that the current is very much smaller than if the traps were absent.

As the applied voltage rises more charge is injected into the crystal and eventually the traps-filled voltage limit V_T is reached at which all deep-lying traps are filled. At this point the current rises steeply towards its s.c.l. value for the deep-trap free crystal; this is region (b) in the diagram. The traps-filled voltage limit is given approximately by $V_T = eN_t d^2 / 2\epsilon$ where d is the thickness and ϵ is the absolute permittivity of the crystal. For a crystal 25 microns thick with a trap density of 10^{15} /cm³ the traps-filled voltage limit occurs at about 800 volts.

In order to obtain useful current at low voltages so that practical devices can be developed it is evident that traps as deep as this must be reduced in number. Using very careful crystal growing techniques diodes can be made with traps-filled transition voltages of the order of one volt and less^{2,3}. This shows that effective deep-trap densities in the crystals are of the order of $10^{12} - 10^{13}$ /cm³.

2.2.2. Square-law response

When the density of deep traps has been reduced to effectively negligible proportions the s.c.l. current follows a square-law dependence upon applied voltage^{4,6}; this is region (c) in the diagram. This square-law has been experimentally observed in a large number of diodes both for steady current conditions and for microsecond pulses; it is, of course, the solid state analogue of the three-halves law for vacuum.

Even though deep-traps may have been effectively eliminated the crystal may contain large numbers of shallow traps; these are traps which lie above the Fermi level while deep traps are those which lie below it. For shallow traps the trapping factor $\theta = n(x) / [n(x) + n_t(x)]$ becomes $\theta = N_0 / [N_0 + N_t \exp (W_t / kT)]$; it now has the same value at all points in the crystal and is independent of applied voltage. To illustrate the order of magnitude involved we may take once again the case of a crystal containing 10^{15} traps/cm³ but this time at a depth of 0.2 eV. For this case $\theta \cong 0.9$ and the current obeys a square-law dependence upon voltage but has only 0.9 of its value for the trap free crystal. More precisely $i = P(V - V_0)^2$ where P , the permeance of the crystal, is given by $P = 9\epsilon_{11} \theta A / 8d^3$. In this expression μ is the mobility of electrons in the crystal and A is the

area of the electrodes applied to the crystal. The voltage threshold V_0 is basically of work function origin and can, if desired, be absorbed into the definition of anode voltage V . Taking representative values of $\epsilon_r = 11$, $\mu = 0.05\text{m}^2/\text{volt sec}$, and $d = 25$ microns as before, gives $P/A = 0.032 \text{ amp/cm}^2 \text{ V}^2$. Thus for 10 volts applied the current density is 3.2 amp/cm^2 .

Diodes which operate under s.c.l. conditions should be relatively little affected by moderate temperature changes. Measurements made with cadmium sulphide diodes over the temperature range from $+120^\circ\text{C}$ to -190°C show that in general there is little variation in diode characteristics above room temperature but that the current at constant voltage increases slowly as the temperature falls and at -190°C may be about double its room temperature value. Most of this increase occurs below about -50°C and is attributed to mobility changes.³

In addition, the "switch-on" and "switch-off" response should be extremely rapid. Measurements have shown that after switching steady state conditions are reached in a time less than 3 millimicrosec, the response time of the sampling oscilloscope used, and that there is no detectable charge storage.³

2.2.3. Proportional current

If the applied voltage is high enough the whole cathode space-charge is moved across the crystal and the current is no longer space-charge-limited⁴. This occurs when the applied voltage is equal, approximately, to $V_s = 8e N_c d^2 / 9\epsilon$. In this expression N_c is the density of electrons in the crystal at the cathode contact; $N_c = N_0 \exp(-W_c/kT)$ where N_c is the effective height of the contact potential step at the cathode contact. If W_c could be made as small as 0.1 eV which is certainly possible in principle then V_s would be of the order of 1,000 volts and it could be assumed that the square-law would be obeyed under all practical voltages.

Above the voltage V_s the current is proportional to applied voltage because the electron velocity is proportional to the applied field; this is region (d) in the diagram. This region has not yet been observed experimentally because power dissipation in the crystal limits the voltage which can be applied.

From this very brief account of the mechanisms of s.c.l. current in insulators it is evident that if a practical triode is to be developed thin crystals must be used in which effective *deep-trap* densities are at least as low as about $10^{12} - 10^{13} \text{ traps/cm}^3$. Currents will then be of useful magnitudes at low applied voltages and will follow a square-law dependence upon applied voltage. Accordingly, in this paper we shall consider only the practical situation in which *deep-trap* densities have been reduced to effectively negligible numbers.

Under these conditions there is a marked resemblance between s.c.l. dielectric devices and s.c.l. vacuum devices^{4, 6}; this is demonstrated by a comparison of the dielectric diode and the vacuum diode.

2.3. Comparison of the Dielectric Diode and the Vacuum Diode

Like the thermionic vacuum diode the dielectric diode is basically a capacitor in which the negative plate can emit electrons into the normally insulating region between the plates. The charge stored on the capacitor is thus continuously in transit between the plates and current is obtained. The situation is illustrated in Fig. 2 which compares the vacuum diode and the dielectric diode on this basis. It should be

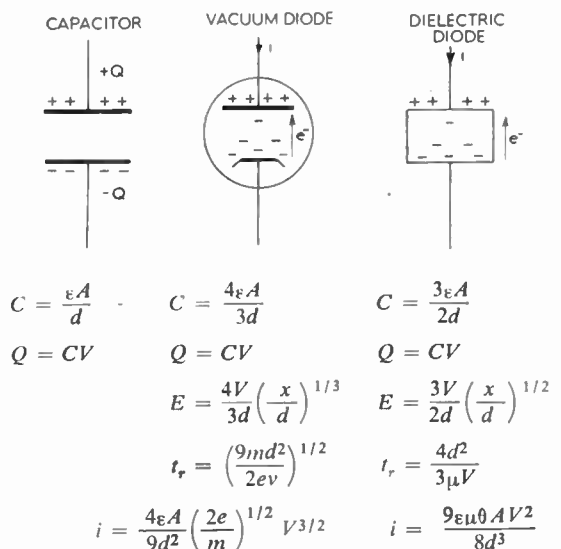


Fig. 2. Comparison of the thermionic vacuum diode and the dielectric diode.

remembered, however, that there are two fundamental differences between the two cases. Firstly, in the vacuum diode electrons move with an *acceleration* which is everywhere proportional to electric field strength; in the dielectric diode electrons move with a *velocity* which is everywhere proportional to electric field strength. This is basically the reason for the square-law dependence of current upon voltage for the solid compared with the three-halves law for s.c.l. current in vacuum. Secondly, in the dielectric diode some of the charge in the crystal is trapped. However, since the ratio of free to trapped charge is the same at all points in the crystal the electric field distribution and the total charge distribution in the crystal is not affected. Thus trapping only reduces the magnitude of the current and does not affect the form of the current/voltage relations. Bearing this in mind the current is given in each case by the ratio of free charge to transit time.

Most of the basic features of s.c.l. dielectric diodes have now been experimentally observed^{1, 2, 3} and it is therefore pertinent to enquire whether a s.c.l. dielectric triode can be developed. The possibility of such a device has, of course, been discussed previously but the absence of any practical demonstrations of s.c.l. current in insulators has precluded its consideration as a useful device. However, the development of s.c.l. dielectric devices now seems realizable and it therefore seems worthwhile to consider what sorts of properties a dielectric triode would have and to make some assessment of its potential value in complementing the transistor and the vacuum triode.

3. The Space-Charge-Limited Dielectric Triode: Static Characteristics

The dielectric triode is derived from the diode by inserting a third electrode between cathode and anode to act as a control "gate." Ideally, the gate should consist of a conducting layer parallel to the cathode, thin enough to be completely permeable to electrons in transit but thick enough to be sufficiently conducting that the charging time of the input capacitance of the device should not be greater than the transit time of electrons between cathode and gate. Such a device would have a high input resistance

and the very desirable pentode type characteristics. Unfortunately, even if a suitable compromise between the two basic and conflicting requirements for the gate could be achieved the insertion of a control electrode into the solid crystal would be a very difficult technological problem. Accordingly, for an initial practical device it seems more feasible to think in terms of a grid structure for the gate as in the vacuum triode. Such a control grid could possibly be made by etching slots in the cathode surface of the crystal to take the grid conductors deposited by some means such as vacuum evaporation. A further difficulty in this connection is that to make a useful device the spacing of the grid conductors would have to be very small, possibly of the order of a few microns. It will thus be necessary to develop micro-techniques for carrying out the rather intricate crystal shaping and precise electrode placing required. In this

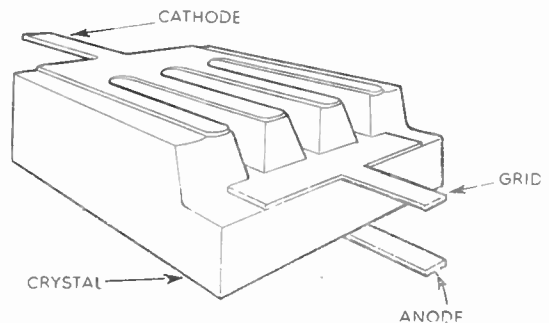


Fig. 3. Schematic illustration of a proposed design for a dielectric triode. The diagram shows a type of electrode arrangement which might be used.

connection it is relevant to note that techniques of fabrication of solid-state devices and their associated circuitry are already tending towards micro-miniaturization. Thus, although the construction of a practical dielectric triode at present is possible but difficult, there is little doubt that this tendency towards micro-miniaturization already existing will make the device a much more practical proposition within a relatively short time.

A possible form which a practical device might take is illustrated in Fig. 3. This diagram shows a rather idealized arrangement in which the grid conductors lie in narrow slots etched in the cathode surface of the crystal; this arrangement does have the advantage that the crystal itself provides support for the electrodes. This

design is not aesthetically pleasing and will probably not be simple to achieve in practice but it would seem that an electrode arrangement of this sort will be necessary if voltage amplification is to be achieved.

3.1. *Theoretical Steady-current / Voltage Relations*

The mechanisms of operation of the dielectric triode will be very similar to those of the thermionic vacuum triode. In both devices s.c.l. current flows through what is normally an insulating region and in both devices current is controlled by the electrostatic field produced by a grid placed between anode and cathode. Because of these basic similarities it is considered justified to apply to the dielectric triode the same type of semi-empirical analysis which has been used successfully for the vacuum triode; the theory developed in this and the next Section is based on this premise. There are differences between the two devices of course but these are essentially of degree and not of kind. Some of these differences are discussed in Section 5.1 and it is concluded that this theoretical approach is acceptable provided it is realized that it can only be regarded as approximate.

In the dielectric diode the current obeys a square-law dependence upon applied voltage. Thus:

$$i = PV^2 \dots\dots(1)$$

where the work function threshold voltage V_0 has now been absorbed into the definition of applied voltage.

For the triode the current will depend on grid voltage V_g as well as upon anode voltage V_a . In this case, by analogy with the vacuum triode we would expect the current/voltage relation to be of the form

$$i = PK \left(V_g + \frac{V_a}{G} \right)^2 \dots\dots(2)$$

The amplification factor, G , is calculated in the usual way from the relative contributions of grid and anode potentials to the electrostatic field at the cathode under space-charge free conditions. By referring to calculations of this sort for vacuum triodes⁹ it is found that in a dielectric triode in which the grid conductor spacing is roughly equal to the grid-cathode spacing,

amplification factors in the range from about 10 to about 50 should be realizable. The actual value would depend on the screening factor of the grid; for the numerical calculations given in this paper an amplification factor of $G = 20$ has been taken as representing what should be a typical value. For the purposes of these calculations an idealized triode is assumed in which the influence of the grid is uniform along the cathode surface. The constant K can be determined in the usual way by giving the grid the potential that would exist in the diode at the position occupied by the grid. In this way we find

$$i_a = P \left(\frac{d_a}{d_g} \right)^3 \left[1 + \frac{1}{G} \left(\frac{d_a - d_g}{d_g} \right)^{3/2} \right]^{-2} \times \left(V_g + \frac{V_a}{G} \right)^2 \dots\dots(3)$$

In this expression d_a denotes the cathode-anode spacing and d_g denotes the cathode-grid spacing.

If we write

$$d_c = d_g \left[1 + \frac{1}{G} \left(\frac{d_a - d_g}{d_g} \right)^{3/2} \right]^{2/3} \dots\dots(4)$$

$$V_c = V_g + V_a/G \dots\dots(5)$$

then

$$i = 9\epsilon_0 \mu_0 AV_c^2 / 8d_c^3 = P_c V_c^2 \dots\dots(6)$$

The mutual conductance, g_m , and anode resistance, r_a , of the triode are then given respectively by

$$g_m = \left(\frac{\partial i_a}{\partial V_g} \right) V_g = 2 P_c V_c \dots\dots(7)$$

$$r_a = \left(\frac{\partial V_a}{\partial i_a} \right) V_a = G / 2 P_c V_c \dots\dots(8)$$

Using these various expressions the expected steady-current/voltage characteristics of the ideal dielectric triode can be calculated. These are illustrated in Fig. 4 for two different triodes; Fig. 4(a) refers to a triode "A" constructed from a crystal 25 microns thick and Fig. 4(b) refers to a triode "B" constructed from a crystal 10 microns thick. The similarity of these characteristics to those of the vacuum triode is evident.

The working parameters of the triode, such as mutual conductance and anode resistance do of course depend on the operating point chosen; the characteristics illustrated are therefore best

Note.—A list of symbols is given in an Appendix.

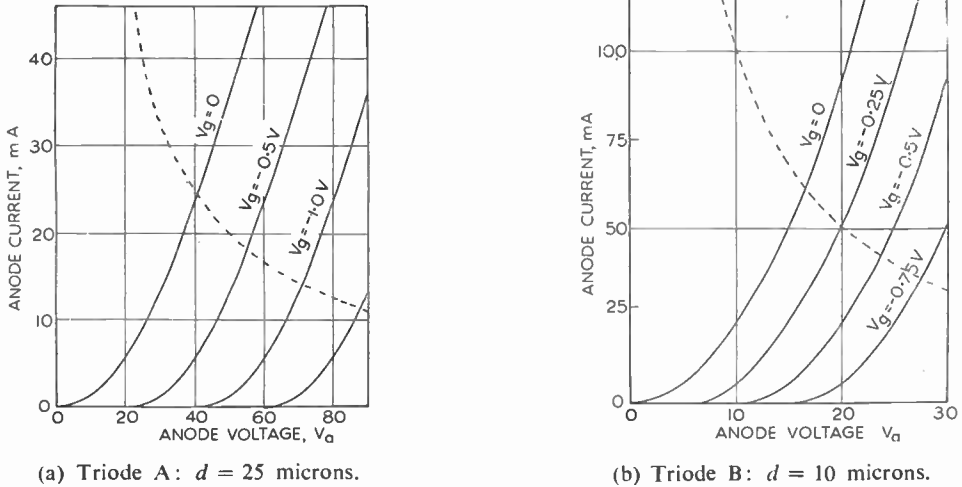


Fig. 4. Theoretical d.c. anode characteristics of idealized dielectric triodes having trapping factors near unity. The broken line indicates an operating power level of 1 watt. $A = 1\text{mm}^2$, $G = 20$, $\epsilon_r = 11$, $\mu = 0.05\text{m}^2/\text{volt. sec}$, $\theta = 0.9$.

compared by selecting an operating point in each case to give the same mean power dissipation. For triode "A" an operating point of $V_g = -1.0\text{V}$ and $V_a = 55\text{V}$ results in a mean anode current of 17.7mA and a mean power dissipation of about 1W . Under these conditions the mutual conductance is 20mA/V and the anode resistance is 1000Ω . For triode "B" an operating point of $V_g = -0.25\text{V}$ and $V_a = 20\text{V}$ results in a mean anode current of 51.3mA and a mean power dissipation of about 1W . Under these conditions the mutual conductance is 136mA/V and the anode resistance is 147Ω .

In each case the mutual conductance is proportional to the effective applied voltage and the anode resistance is inversely proportional to the effective applied voltage.

4. The Space-Charge-Limited Dielectric Triode: Frequency Characteristics

The dependence of the triode characteristics upon frequency of operation will be determined by the effects of electron transit times and the effects of electron trapping. The basic equations which describe the time and space dependence of the free electron density in the crystal upon both of these effects can be derived quite readily but unfortunately the general solution of these equations appears extremely difficult and probably impossible². However, transit times are extremely short and for a discussion of trapping

effects they may be neglected. Under these circumstances the general equations become much simpler. This Section, therefore, will be restricted to a discussion of frequency characteristics dependent only on electron trapping effects.

4.1. Derivation of Equations

The total number of conduction electrons in the crystal at time t will be denoted by n and variations in n can arise from three causes. Firstly, if the grid voltage increases by dV_g the charge held in the space between anode and cathode increases by $edn = CdV_g = CdV_e$. The capacitance $C = 3\epsilon A/2d_e$ and is equal to the space-charge capacitance of a diode with a cathode-anode spacing slightly greater than the cathode-grid spacing of the triode. Initially this charge is injected into the conduction band of the crystal; it then becomes distributed between conduction and trapping levels. Secondly, if n_t is the total number of trapped electrons in the crystal and if the mean lifetime of a filled trap is τ_e then in a time interval dt a number $n_t dt/\tau_e$ of electrons are ejected from traps into the conduction levels. Thirdly, if the mean lifetime of an electron in the conduction band is τ_c then in the same interval of time a number ndt/τ_c of electrons are captured by traps. The net rate of change of the number of conduction electrons with time is therefore

$$\frac{dn}{dt} = \frac{C}{e} \frac{dV_e}{dt} + \frac{n_t}{\tau_e} - \frac{n}{\tau_c} \dots\dots\dots(9)$$

Similarly the net rate of change of trapped electrons with time is

$$\frac{dn_t}{dt} = - \frac{n_t}{\tau_e} + \frac{n}{\tau_c} \dots\dots\dots(10)$$

Eliminating n_t and writing $1/\tau = 1/\tau_e + 1/\tau_c$ we have

$$\frac{d^2n}{dt^2} + \frac{1}{\tau} \frac{dn}{dt} = \frac{C}{e} \left(\frac{d^2V_e}{dt^2} + \frac{1}{\tau_e} \frac{dV_e}{dt} \right) \dots\dots\dots(11)$$

This equation can be integrated immediately and the constant of integration found to be zero by considering steady conditions. This gives

$$\frac{dn}{dt} + \frac{n}{\tau} = \frac{C}{e} \left(\frac{dV_e}{dt} + \frac{V_e}{\tau_e} \right) \dots\dots\dots(12)$$

Now the current at any instant is given by the ratio of free charge to transit time. Thus

$$i_a = 3e n_{\mu} V_e / 4d_e^2 \dots\dots\dots(13)$$

Eliminating n between eqns. (12) and (13) we have

$$\frac{d}{dt} \left(\frac{i_a}{V_e} \right) + \frac{1}{\tau} \left(\frac{i_a}{V_e} \right) = \frac{P_e}{\theta} \left(\frac{dV_e}{dt} + \frac{V_e}{\tau_e} \right) \dots\dots\dots(14)$$

From this equation the current/voltage characteristics of the dielectric triode can be derived for any time dependent voltage V_e . For our present purposes we shall consider the case of a sinusoidal signal voltage impressed on a steady voltage bias. Thus

$$V_e = V_0 + V_a/G + v \sin \omega t = \bar{V}_e + v \sin \omega t \dots\dots\dots(15)$$

Substituting this expression for V_e in eqn. (14) and integrating gives

$$i_a = P_e (\bar{V}_e + v \sin \omega t) [\theta \bar{V}_e + Zv \sin (\omega t + \varphi)] / \theta \dots\dots\dots(16)$$

The initial transient term of the form *constant* exp $(-t/\tau)$ has been dropped. In this equation

$$Z^2 = [(\omega^2 + 1/\tau \tau_e)^2 + (\omega/\tau_c)^2] / (\omega^2 + 1/\tau^2)^2$$

$$\tan \varphi = (\omega/\tau_c) / (\omega^2 + 1/\tau \tau_e)$$

$$\theta = \tau_c / (\tau_c + \tau_e) = n / (n + n_t)$$

4.2. Frequency Dependence of Triode Parameters

Under small signal conditions eqn. (16) reduces to

$$i_a = P_e \bar{V}_e + P_e v \bar{V}_e (1 + Z/\theta) \sin (\omega t + \varphi) \dots\dots\dots(17)$$

Linear operation is obtained and parameters of the triode such as mutual conductance and anode resistance may therefore be derived.

The mutual conductance of the triode is given by $g_m = (\partial i_a / \partial V_0) V_a$. Using this relation and neglecting phase differences between the current modulation and the applied signal voltage we have

$$g_m = P_e \bar{V}_e (1 + Z/\theta) \dots\dots\dots(18)$$

At low frequencies Z reduces to θ and we have $g_m = 2P_e \bar{V}_e$ as found in Section 3 for the steady-current/voltage case. At high frequencies, however, Z reduces to unity and we find

$$g_m = (1 + 1/\theta) P_e \bar{V}_e \dots\dots\dots(19)$$

Since θ is always less than unity the high-frequency mutual conductance is always greater than the low-frequency mutual conductance in a given triode. The physical reason for this is quite clear. At low frequencies ($\omega \ll 1/\tau$) the equilibrium distribution of electrons between conduction and trapping levels is always maintained; the signal voltage, therefore, modulates both the free and trapped charge content of the crystal. However, it is only the free charge which can contribute to current flow, consequently only part of the signal voltage is in fact used to modulate the current. At high frequencies on the other hand ($\omega \gg 1/\tau$), the population of the electron traps cannot respond to the variations of the signal voltage; this therefore modulates only the free charge and is consequently much more effective in modulating the current than at low frequencies. In fact, at high frequencies the triode would act almost as if constructed from a trap-free crystal.

The situation is illustrated in Fig. 5 which shows how a small-amplitude high-frequency signal voltage is reflected in the grid characteristic of the device to modulate the anode current. In an ideal trap-free triode the mean anode current would be $I_a = 9\epsilon_{\mu} A V_e^2 / 8d_e^3$ as shown in the diagram. A signal voltage on the grid would modulate this according to the relation $\Delta I_a = 2(9\epsilon_{\mu} A V_e / 8d_e^3) \Delta V_0$ as shown by eqn. (7). Half of this modulation is due to variation in electron transit time through the crystal and half is due to variation in the free charge content of the crystal.

Now if shallow electron traps are present a proportion $(1-\theta)$ of the total charge in the crystal is immobilized by trapping; if θ is small this effectively eliminates most of the steady component of the anode current as shown in the diagram and the mean anode current is now $i_a = \theta I_a$. If θ is small the signal voltage on the grid now causes variations in the free charge content of the crystal which are much greater proportionately than the variations caused in transit time; thus modulation of the anode current is now caused mostly by variations in the free charge content of the crystal rather than being due equally to this and transit time variations. We have, therefore, that

$$\Delta i_a = (9\epsilon\mu AV_e/8d_e^3) \Delta V_g$$

as indicated by eqn. (19). Thus $\Delta i_a = \Delta I_a/2$ and the mutual conductance of the device has been halved by the presence of traps.

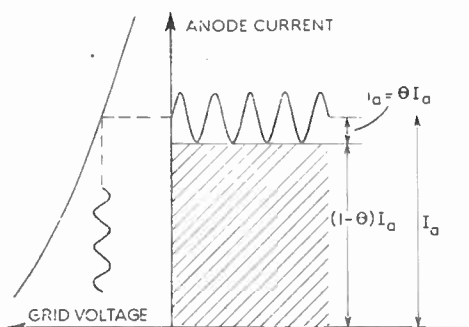


Fig. 5. Illustrating the high-frequency action of a dielectric triode containing a high density of shallow electron traps. $I_a = 9\epsilon\mu AV_e^2/8d_e^3$ and is the anode current for the idealized trap-free triode. $i_a = \theta I_a$ is the anode current for the practical triode with trapping. The component $(1-\theta) I_a$ of the anode current for the trap-free triode is eliminated by trapping in the practical triode. Thus unnecessary anode current and wasteful power dissipation is avoided yet high mutual conductance is retained.

However, this reduction is more than compensated by the increase which can be achieved by re-adjusting the operating point of the device. This re-adjustment is made possible by the fact that trapping has now eliminated most of the steady component of anode current which plays no useful part in the amplification process and only causes wasteful power dissipation in the device. Thus it is now possible to operate the device under conditions which would, without trapping, lead to excessive anode currents and

excessive power dissipation. Trapping reduces the current and power dissipation to tolerable values and yet allows the high mutual conductance pertaining to these conditions of operation to be mostly retained. In fact, to achieve the highest possible g_m for a given power dissipation it is necessary for trapping to be present.

From the diagram it is evident that these considerations only apply to small signal conditions. If the signal becomes large and negative all of the conduction electrons may be swept out of the crystal and the current would become zero. Under these conditions the relation $ed_n = CdV_e$ which is used in the derivation of the basic equation (9) is not true and the analysis given here is not valid. What this means in practice is that the analysis is applicable only to Class A operation of the triode.

If θ is nearly unity as for the triodes whose theoretical characteristics are shown in Fig. 4 the increase in g_m with frequency is not very much. Similarly the phase difference φ by which the current leads the voltage is never very considerable. For triode A the low frequency g_m rises from 20mA/V to a high frequency value of 21mA/V; the maximum value of $\tan \varphi$ is 0.05. For triode B the low frequency g_m rises from 136mA/V to a value of 143mA/V at high frequencies; as before the maximum value of $\tan \varphi$ is 0.05.

An estimate of the upper limit of operating frequency can be obtained from the magnitude of the ratio g_m/C . At high frequencies we have

$$\frac{g_m}{C} = \frac{3\mu(1+\theta)V_e}{4d_e^2} = \frac{1+\theta}{t_r}$$

where t_r is the electron transit time between approximately cathode and grid planes. For the cases considered so far θ is nearly unity so the gain-bandwidth product of the device may be taken approximately as $1/\pi t_r$. For triode A this has the value 300 Mc/s and for triode B it has the value 800 Mc/s. These triodes would be very suitable for use as wide-band video amplifiers.

The discussion of triodes A and B above and in Section 3 has considered the effects of trapping to be small. However, we have seen that if trapping is present the high frequency operation of the triode is more efficient and the high frequency mutual conductance attains its greatest value. Consequently it is of consider-

able practical interest to consider the case in which θ is much smaller than unity. If θ is small as in a crystal containing a large number of shallow traps the high-frequency g_m is $P_e \overline{V_e}/\theta$ and is a factor $1/2\theta$ greater than the low-frequency g_m . Thus by constructing a triode from a crystal containing a high density of shallow traps a many-fold increase in g_m should be obtained as the operating frequency rises. For example, a triode made from a crystal containing a trap density $N_t = 10^{16}/\text{cm}^3$ at a depth of 0.27eV has a trapping factor $\theta = 0.05$. Accordingly this device which we may term triode "C" should have a high-frequency g_m approximately ten times greater than its low-frequency g_m . The anode resistance would fall in the same ratio since the relation $g_m r_a = G$ is valid over the whole frequency range.

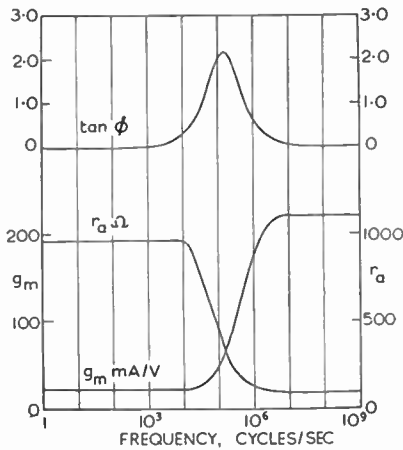


Fig. 6. Frequency dependence of the operating parameters of an idealized high-frequency dielectric triode: triode C.

The variation of mutual conductance, anode resistance, and phase angle with frequency for triode "C" should have a high frequency g_m calculations the same physical parameters have been taken as previously used for triode B. A value of $\tau = 0.24$ microsec has been used as the relaxation time for trap equilibrium to be reached. This has been calculated from the relation $1/\tau = 1/\tau_e + 1/\tau_c$ where the trap lifetime has been obtained from the relation $1/\tau_e = \nu \exp(-W_t/kT)$ with an assumed value of 10^{10} sec^{-1} for the escape frequency ν , and τ_c has been obtained from the relation $\tau_c/(\tau_c + \tau_e) = \theta = 0.05$. An operating point of

$V_a = 0$ and $V_a = 44\text{V}$ has been selected; this results in a mean anode current of 23mA and a mean power dissipation of about 1W .

Under these conditions at low frequencies the device should have a mutual conductance of 21mA/V and an anode resistance of 950Ω ; at high frequencies, however, it should have a mutual conductance of 220 mA/V and an anode resistance of 90Ω . As before, an estimate of the upper limit of operating frequency can be obtained from the magnitude of the ratio $g_m/C = (1+\theta)/t_r$. In this case θ is small and the gain-bandwidth product is given approximately by $1/2\tau t_r$; for this triode we have therefore a theoretical gain-bandwidth product of 1200 Mc/s .

As at low frequencies the actual values of mutual conductance and anode resistance depend on the operating point chosen. This is illustrated in Fig. 7 which shows the variation of these parameters with anode voltage.

5. Discussion and Remarks

5.1. Basic Theory

The theory outlined above for the dielectric triode can be criticized on a number of points.

In particular it is assumed that because of the qualitative similarity between the mechanisms of operation of the crystal triode and the vacuum triode the same type of quantitative analysis will be applicable in both cases. There would be no objection to this were it not for the fact that, in a crystal, electron trapping and electron scattering take place which do not occur in vacuum.

As regards electron trapping we have seen that the equilibrium ratio of free to trapped charge is the same at all points in the crystal. Further the charge and field distributions in the crystal respond to changes in applied voltages in a time of the order of the electron transit time whether traps are present or not. Thus, as for the diode, trapping affects only the scale of the current/voltage relations without affecting their form and therefore does not affect the type of analysis which may be applied.

Scattering of electrons by the lattice while these are in transit between anode and cathode does modify the form of the current characteristics from the vacuum case. As pointed out pre-

viously, it is because of electron scattering that the s.c.l. current obeys a square-law dependence on applied voltage instead of a three-halves law as for vacuum. As before, however, this does not affect the *type* of analysis which can be applied.

An additional minor difference between the two devices is that in the vacuum triode electrons move freely in space with high velocities; they do not therefore necessarily everywhere follow the lines of electric field intensity. This will cause the device to have characteristics slightly different from those predicted by the basic theory. The effect will be less for the dielectric triode than for the vacuum triode because of the smaller velocities in the crystal.

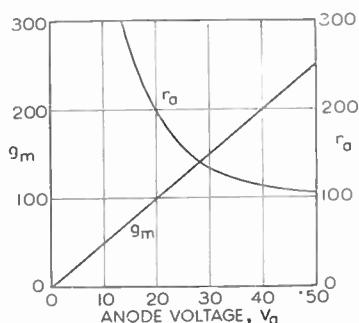


Fig. 7. Dependence of high frequency parameters of an idealized dielectric triode upon mean operating voltage: triode C.

In both cases it is true that the current is controlled by the joint electrostatic field of anode and grid; the concept of amplification factor is therefore valid in both cases. In the crystal, however, space-charge densities are much higher than in vacuum because of the lower electron velocities. This means that when current is flowing field distributions are further from their geometrical values, used for calculations of amplification factor, than in the vacuum triode. Nevertheless it is still permissible to describe the operation of the device in terms of an amplification factor even though this may in fact differ from the calculated value. A further point to notice in connection with the use of the amplification factor is that this has been considered to be a constant of the device. This is not strictly true even for the vacuum triode although for small signal operation as considered here it may be assumed constant. For

large signal operation on the other hand the possible variation of amplification factor with grid and anode voltage should be kept in mind.

In the analysis given it has been tacitly implied that the electron mobility is constant for all applied voltages. The electron velocity at any point in the crystal is given by μE . The average field in the cathode-grid space is given approximately by V_c/d_c and in the examples given has its highest value at 7×10^5 V/m for triode C. For field strengths of this order the electron mobility may differ from its low field value; it may fall because drift velocities are approaching the magnitude of the thermal velocities upon which they are superposed or it may possibly even become zero if a limiting carrier drift velocity is reached. For small-signal operation as considered here the mobility may be taken as constant although possibly different from its low field value; for large-signal operation on the other hand a possible dependence of electron mobility upon signal voltage should be kept in mind. The average field in the grid-anode space is several times larger than in the cathode-grid space. Electron mobilities in this region of the device may be significantly different from in the cathode-grid region. However, this will not affect the working of the device which is determined by the mechanisms operating in the cathode-grid space.

While discussing electron mobilities it may be noted that in cadmium sulphide these are relatively low. Electron mobilities are roughly an order of magnitude less than in the more common semiconductor materials so that although initial experimental success with s.c.l. current has been achieved with cadmium sulphide it is not necessarily the best material that may eventually be available. The use of materials with higher mobilities would enable operation at higher frequencies to be achieved or would enable thicker crystals to be used with a consequent easing of fabrication problems or would permit operation at lower applied voltages. To achieve a higher electron mobility will almost certainly require the use of a material with a smaller forbidden band gap and therefore unfortunately a lower intrinsic resistivity. However, it should be possible in principle to find a material in which electrons have a much

higher mobility than in cadmium sulphide yet possessing a band gap sufficiently large for the intrinsic resistivity to be great enough for it to be used in s.c.l. devices.

Changes in crystal permittivity may occur at the higher operating frequencies due to the ionic component of the dielectric polarization being unable to follow variations in the signal voltage. An effect of this sort will manifest itself in two ways. Firstly, it will effect the extent to which the signal voltage modulates the free charge content of the crystal and so affect the high-frequency mutual conductance of the device. Secondly, the dispersion which would accompany the changes in permittivity would introduce dielectric loss into the device. This loss would result in power absorption from the signal source. In practice these effects may not be important. However, permittivity changes due to ionic inertia may be expected at frequencies approaching 1000 Mc/s and may be significant before transit time effects set the working limit to the upper operating frequency.

As stated previously the differences between the dielectric triode and the vacuum triode are of degree rather than of kind; their electrical characteristics will certainly be of the same general form. Accordingly it is felt that the theory outlined can be accepted provided it is taken no more seriously than as a semi-quantitative account; this applies particularly to numerical values quoted.

5.2. Triode Operation

On the basis of the theory outlined in this paper it is expected that the dielectric triode will have anode and grid characteristics similar to those of the vacuum triode. In addition its input resistance will be very high. In its applications therefore the dielectric triode should be able to use circuit techniques similar to those already developed over many years for the vacuum triode; it will not be necessary to develop a new circuit philosophy for its use.

In this connection, however, it may be noted that it is possible in principle to construct a dielectric triode in which the current is carried by "holes" and not by electrons. In this case current would flow with a negative anode voltage and would be controlled by a positive grid voltage; in this sense the device would be an

inverse triode in the same way that an *n-p-n* transistor may be regarded as the inverse of the *p-n-p* transistor.

A point of notice in connection with the grid bias voltage V_g is that this contains in its definition a quantity V'_g which is equal to the difference between the work function of the grid conductors and the electron affinity of the crystal; this is analogous to the quantity V_0 which appears in the definition of anode voltage and has its origin in the same mechanisms. Thus if the applied external bias voltage is zero the grid has a "built-in" bias of V'_g . Measurements of the anode threshold voltage V_0 for cadmium sulphide diodes indicate that V'_g could be about 1.5 to 2V. Consequently in many applications an external arrangement for supplying negative grid bias would probably be unnecessary; the "built-in" bias should be sufficient.

When considering operation of the triode as a practical device it is necessary to enquire what limitations are placed on the applied voltages by the necessity to avoid breakdown of the crystal. Intrinsic electric strengths of insulators in single crystal form are of the order of a few hundred megavolts per metre. Allowing a safety factor of approximately ten times sets a rather arbitrary limit of about 2×10^7 V/m as a maximum safe working stress. The maximum average field in the cases treated occurs in triode C and is about 6×10^6 V/m which is several times below this limit. Thus the possibility of electric breakdown would probably not be a serious limitation on operating conditions. These figures refer, of course, to operation under conditions such that the mean power dissipation is 1 watt. At lower power levels working field strengths will be much smaller; it is quite possible, especially for very high frequency operation, that when working at similar power levels the dielectric triode will be electrically more robust than the transistor.

One most useful property which the device should have is insensitivity to moderate temperature changes. This is expected because under s.c.l. conditions the number of carriers available for current flow is independent of temperature. The experiments with diodes mentioned previously have shown that variations in current caused by temperature changes are relatively small so that under normal operat-

ing conditions it would probably be possible to ignore temperature variations.

Solid-state devices in general have noise figures considerably greater than those of s.c.l. vacuum devices. This is basically because of space-charge reduction of charge fluctuations in vacuum devices. Since this same mechanism should also operate in the dielectric triode it may be anticipated that this device will have a noise figure lower than those of semi-conductor devices. However, it is not possible to estimate readily the extent to which lattice scattering of electrons and trapping of electrons will increase the overall noise figure and, in addition, it may not be possible to make a noise-free contact to the crystal. Nevertheless it seems reasonable to expect that s.c.l. dielectric devices should have relatively low noise figures.

A very interesting feature anticipated for the dielectric triode is that by using a crystal containing a large number of shallow traps it should be possible to obtain a mutual conductance which rises with operating frequency. A large gain-bandwidth product is obtained in this way indicating particular usefulness at very high frequencies. However, the same gain-bandwidth product would be obtained by constructing a smaller area device from a trap-free crystal and it might be argued that there is therefore no advantage in using a crystal in which trapping takes place. Apart from the fact that in practice it might not be possible to obtain crystals free from trapping effects the advantage is that while trapping does not affect the gain-bandwidth product of the device it does allow this to be accompanied by a very high mutual conductance. This is extremely useful at high operating frequencies since the triode has to charge up circuit capacitances as well as its own shunt capacitances. For this reason the combination of high mutual conductance and high gain-bandwidth product is more attractive than high gain-bandwidth product alone.

The basic principle underlying the action of the dielectric triode is that s.c.l. current in insulating crystals can be controlled electrostatically just as in vacuum. There is no reason to suppose that this is not true but it is relevant to this discussion to note that direct experimental evidence of this control action is available¹⁰.

Using crystals of cadmium sulphide provided with a split-anode it has been shown that current to one half of the anode was modulated by a reverse voltage applied to the other half anode. This arrangement was extremely inefficient and no voltage gain was obtained. However, the essential feature of these experiments was that considerable current gain was obtained. There seems little reason to doubt that in some of the experiments made this was obtained through the negative field of the reverse biased half-anode repelling charge from the forward-biased half-anode thus verifying the principle of electrostatic charge control. Unfortunately it is not clear from the account given whether this interpretation was made at the time and these particular experiments do not seem to have been followed up.

6. Conclusions

The design calculations described in this paper indicate that the development of a dielectric triode is a worthwhile proposition. The device would have a high gain-bandwidth product, a high mutual conductance, a high input resistance, and the considerable advantage among solid state devices of being relatively insensitive to temperature changes. It should therefore complement semi-conductor devices particularly in applications where voltage amplification is required, where insensitivity to temperature changes is required, or where operation at high frequencies is required.

Now that the fundamental fact of steady space-charge-limited current in dielectric crystals has been experimentally demonstrated the remaining problems involved in the fabrication of a practical dielectric triode are mostly technological in nature. The main source of difficulties is that crystal thicknesses must necessarily be small in order to obtain usefully large current at a few volts applied. So far as can be estimated, however, the problems outstanding do not seem to be as difficult as those successfully overcome in the development of existing semi-conductor devices; if the resources of modern semi-conductor laboratories could be made available the dielectric triode should be a practical device. Together with the vacuum triode and the semi-conductor transistor the dielectric triode would then complete the basic trio of charge-control devices.

7. Acknowledgments

The author would like to thank Professor D. G. Tucker of the Department of Electrical Engineering for the provision of facilities for this work.

8. References

1. G. T. Wright, "Space-charge-limited currents in insulating materials," *Nature (Lond.)*, **182**, p. 1296, 1958.
2. G. T. Wright, "Some properties and applications of space-charge-limited current in insulating crystals," *Proc. Instn Elect. Engrs*, Paper No. 2928, 1959 (106B, Suppl. 17).
3. A. M. Conning, A. A. Kayali and G. T. Wright, "Space-charge-limited dielectric diodes," *J. Instn Elect. Engrs*, **5**, p. 595, 1959.
4. N. F. Mott and R. W. Gurney, "Electronic Processes in Ionic Crystals," Chap. 5 (Oxford University Press, 1948).
5. S. M. Skinner, "Diffusion, static charges, and the conduction of electricity in non-metallic solids by a single charge carrier: II. Solution of the rectifier equations for insulating layers," *Journal of Applied Physics*, **26**, p. 509, 1955.

6. A. Rose, "Space-charge-limited currents in solids," *Physical Review*, **97**, p. 1538, 1955.
7. G. H. Suits, "Exact current-voltage relation for the metal-insulator-metal junction with a simple model for trapping of charge carriers," *Journal of Applied Physics*, **28**, p. 454, 1957.
8. M. A. Lampert, "Simplified theory of space-charge-limited currents in an insulator with traps," *Physical Review*, **103**, p. 1648, 1956.
9. K. R. Spangenberg, "Vacuum Tubes," Chap. 7 (McGraw-Hill, New York, 1948).
10. I. Broser and R. Warminsky, "Von der Elektrodenanordnung abhängige elektrische Eigenschaften von Cadmiumsulphid Kristallen" *Z. Naturforschg.*, **5a**, p. 62, 1950.
11. R. H. Parmenter and W. Ruppel, "Two-carrier space-charge-limited current in a trap-free insulator," *Journal of Applied Physics*, **30**, p. 1548, 1959.
12. W. Ruppel and R. W. Smith, "A CdS analog diode and triode," *R.C.A. Review*, **20**, p. 702, 1959.

List of Symbols

A	electrode area	P_e	effective permeance of triode
C	capacitance	r_a	anode resistance
d	crystal thickness	t_r	electron transit time
d_a	cathode-anode spacing	T	absolute temperature
d_o	cathode-grid spacing	v	signal voltage
d_e	effective triode spacing	V	applied voltage
e	electron charge	V_0	anode threshold voltage
E	electric field intensity	V'_0	grid threshold voltage
G	amplification factor	V_a	anode voltage
g_m	mutual conductance	V_g	grid voltage
h	Planck's constant	V_e	effective voltage
i	current	$\overline{V_e}$	mean effective voltage
i_a	anode current in practical triode with traps	V_s	transition voltage between s.c.l. and proportional current
I_a	anode current in ideal trap-free triode	V_T	traps-filled limit voltage
k	Boltzmann's constant	W_f	Fermi energy level
m	electron mass	W_t	energy level of electron traps
$n(x)$	density of conduction electrons	x	distance
$n_t(x)$	density of trapped electrons	ϵ	crystal permittivity
n	total content of free electrons	θ	trapping factor
n_t	total content of trapped electrons	μ	electron mobility
N_c	density of electron space-charge at cathode	ν	trap escape frequency
N_0	effective integrated density of conduction levels	τ	time constant for trapping
N_t	density of electron traps	τ_c	mean lifetime of conduction electrons
P	permeance of diode	τ_e	mean lifetime of filled traps
		φ	phase angle
		ω	angular frequency

The term "ideal triode" used in this paper assumes that G is constant.

DISCUSSION

Dr. T. B. Tomlinson (Associate Member): Dr. Wright has stated that the input impedance of this device will be very high. I venture to suggest that a more correct statement would be that the input resistance *may* be high. The input capacitance is likely to be by no means negligible since the electrode spacing is to be very small and the permittivity of cadmium sulphide (which has been quoted as a suitable crystal) is in the region of 10.

The effects of such capacitance should be evident in the dielectric diodes which have already been constructed. Has the author carried out pulse tests on these diodes and estimated the capacitance? If so, I should also like to know if any carrier storage effects were discernible.

Dr. G. T. Wright (*in reply*): The input resistance should be high provided that surface leakage currents between the various electrodes can be kept small; internal electron current to the grid should be negligible.

The input capacitance will certainly be significant. A useful figure to remember in this connection is that a cadmium sulphide crystal 10 microns thick, fitted with electrodes 1 mm², forms a capacitor of very nearly 10 pF. However, the input capacitance of the transistor is also high; it is worth noting that for the same values of input capacitance and transit time of carriers across the active region the dielectric triode should have twice the mutual conductance of the transistor.

A small number of diodes have been tested using very fast voltage waveforms derived from a mercury-relay cable-discharge pulse generator. The resulting current waveforms were viewed with a travelling wave oscilloscope and for both switch-on and switch-off operation a transient current peak was observed lasting for rather less than one millimicrosecond. This peak was attributed to the charge or discharge current of the shunt electrode capacitance of the diode and was compatible with the shunt capacitance of a few micromicrofarads measured with a low frequency bridge on the reverse biased diode. For both switch-on and switch-off operation, however, the steady state was reached within one millimicrosecond; there was no evidence of carrier storage effects.

L. W. D. Pittendrigh (Member): In considering the application of a dielectric diode or triode as a replacement for their thermionic equivalent, does Dr. Wright consider that, since the source of electron flow in the first case would not arise from a hot cathode but from some purer source in the external circuit, a higher signal/noise ratio might be obtained?

Secondly, since the dielectric triode appears to give a stage gain which was a function of frequency, does he expect that in pulse operation some distortion of the pulse shape might occur additional to any imposed upon pulses by the external circuit?

Dr. Wright (*in reply*): It has not yet been possible to make any quantitative study of noise in the dielectric diode or the dielectric triode. However, one feels that owing mainly to space-charge reduction mechanisms these devices should have inherently low noise figures and should be better in this respect than semi-conductor diodes and transistors.

A triode containing appreciable numbers of shallow traps will certainly distort pulses which have a duration comparable with the time required for trap equilibrium to be reached. The distortion will take the form of a fall-off in the amplitude of the output pulse to a value equal at long times to θ times the initial amplitude. However, it is not suggested that a triode of this type would be useful as a wide-band device; for this one requires a triode effectively free from trapping effects. For operation at the very highest frequencies, however, it will be desirable to introduce shallow traps since this enables the highest possible mutual conductance to be obtained at very high frequencies.

K. Thaker (Associate Member): How are cadmium sulphide crystals grown? What is the effect of moisture on the crystals and what precautions, if any, are taken to gain stability against moisture?

As the crystals pass heavy current densities they must dissipate very heavy power. Taking into account the cooling arrangements, is there any reduction in size compared to transistors giving corresponding performance?

It might be possible to construct space-charge-controlled dielectric triodes much smaller than transistors; the cooling system might be meagre if such a triode can be used in Class D condition in which case the voltage waveform on the anode is of very small amplitude and consequently the valve dissipation is very small.

Dr. Wright (*in reply*): Cadmium sulphide crystals are grown by the standard technique of subliming the powder in a tubular furnace at about 1000°C and carrying the vapours to cooler condensing surfaces in a stream of inert gas. By suitably adjusting the temperatures, temperature gradients, and rate of gas flow thin plate-like crystals are obtained. Our experiments suggest that the necessary compensation of unfilled trapping levels is obtained by the introduction of

shallow donor levels.

Moisture does not seem to affect the storage of the crystals at least over a number of years. Diodes and presumably triodes can be quite well protected after construction by coating with an epoxy cement.

Any solid-state device working at a fairly high power dissipation will have similar physical dimensions to any other because the cooling arrangements such as heat sinks required to lead away the power dissipated in the crystal are so much larger than the basic device itself.

J. A. Sargrove (Member): As a suggestion to the production of the control electrode in the dielectric triode, does not Dr. Wright think that this is a similar problem to making the transparent top electrode to photo-voltaic cells. Here originally one sputtered gold onto the partially oxidized selenium layer. Later cells of this type have sputtered cadmium onto selenium. The makers state that these photocells are more infra-red sensitive than the purely gold sputtered ones. Have we not here a phenomenon in the cadmium selenide barrier-layer similar in some respects to the cadmium sulphide layers of Dr. Wright's device?

Does he not think that one might make a control electrode in a triode by sputtering cadmium onto a cadmium sulphide crystal and then burying it in a further crystal and thus create a triode as a sandwich?

Dr. Wright (*in reply*): The basic problem in forming the control electrode is how to insert it in such a way that it is more effective than the anode in controlling the electrostatic field at the cathode. One possible way, although admittedly inelegant, has been suggested in this paper. An alternative would be, as suggested here, to attempt to bury the grid in the crystal by growing more crystal over an evaporated grid structure. This method should certainly be tried but will probably run into difficulties caused by diffusion of the grid structure into the crystal at the high temperatures used for crystal growing. Another technique† worth trying is to form conducting threads, possibly by metallic diffusion, from one side of the crystal down the centre of the crystal along the crystallographic axis which lies parallel to the crystal surfaces (the *c*-axis for cadmium sulphide). These conducting threads would form a most effective grid but like the other two suggestions the method involves many problems. However, with the unsupported facilities of a university laboratory it

has not yet proved possible to make an experimental approach towards the construction of a practical device.

As indicated in this paper it is felt that interest in solid state s.c.l. devices should be revived following recent experimental demonstrations that s.c.l. current of theoretical magnitude can be achieved in insulators. This paper is an attempt to discuss quantitatively the electrical characteristics of a solid state s.c.l. triode and in particular to show that trapping levels, which on first thoughts would appear to be detrimental, are in fact advantageous for operation at very high frequencies.

Professor M. H. N. Potok (Associate Member): The g_m of the proposed triode is inversely proportional to the cube of grid to emitter separation. This separation is very small (10 microns or less). This would appear to lead to a great variation in characteristics from one triode to another quite apart from such variations as will be due to materials and contacts. Can Dr. Wright comment on this?

Have any measurements been made with the anode split into narrow strips, the alternate strips being kept at positive and negative potential and the negative strips being used as grid?

Dr. Wright (*in reply*): The electrical characteristics of the device will be very sensitive to the dimensions of the device, particularly the grid to cathode separation. This may make it difficult to produce accurately reproducible devices although some control of characteristics may be achieved by adjusting crystal thickness by etching and by controlling electrode areas.

Measurements of the type suggested using strip electrodes connected alternately positive and negative have been considered. Such an arrangement would demonstrate current gain but owing to the unfavourable geometry would not demonstrate voltage gain. In this connection the experiments of Broser and Warminsky¹⁰ using geometries of this sort show that current gain is indeed obtained. In view of the limited facilities available for this research it was decided not to repeat these experiments but to focus attention, experimentally at least, on the more fundamental aspects such as mechanisms of crystal growth, mechanisms of s.c.l. current in solids, and fabrication, performance and applications of diodes which are more suited to university type research.

However, I would like to refer to the recent work of Ruppel and Smith¹² who have followed up the preliminary experiments of Broser and Warminsky and have shown very clearly that current gain is obtained in a triode structure hav-

† I am pleased to acknowledge this suggestion by Professor G. F. J. Garlick.

ing essentially the geometry of a diode with a split anode. If an appropriate geometry can be achieved in a structure of appropriate dimensions as discussed in this paper there seems little doubt that a useful voltage amplification will be obtained.

D. D. Jones : Dr. Wright has said that he would like to have the facilities of a semi-conductor laboratory to develop his triode. Such facilities are very expensive and before an industrial organization can be expected to provide them it is likely that it will have to be convinced that the new device offers some advantages over the thermionic valve and the transistor.

When the transistor appeared it was clear that here was a significant development in electronics. At the time that it appeared people were contemplating extensions of electronics to communications and computing. Its efficiency, coupled with the feeling that being a solid-state device it should have a high degree of reliability, indicated that it might play an important part in these developments and these were sufficient incentives to bring about its intensive development and exploitation.

Although Dr. Wright has not actually constructed a triode I should like to hear him state, in the most optimistic way, the real advantages that this device might have (e.g. frequency range, cost) over the other two alternatives which are now well-established.

Transistors to cover the frequency range up to and including the v.h.f. f.m. broadcast band are in production and one can see the possibility of fairly cheap transistors to cover the requirements of television receivers appearing with the next three years or so. These devices will have their counterparts for the communications and data-handling industries. If the proposed triode is going to make an impact on these mass markets it must offer some advantages over the transistor. At frequencies beyond 300 Mc/s, say, the future is not as clear and I wonder whether Dr. Wright thinks that his proposed triode would be attractive here. At the same time we must not lose sight of the fact that the semi-conductor industry, through such devices as variable-capacitance diodes, for parametric amplification and harmonic generation, and tunnel (Esaki) diodes for negative-resistance amplification, is already forging ahead to provide new solutions in the higher frequency ranges. Superficially at any rate it appears that these new devices can be made cheaply.

The semi-conductor industry has also made devices having fairly high values of input resistance, the main example being the field-effect transistor. Unfortunately they usually have a sub-

stantial input capacitance and it would be interesting to know what Dr. Wright thinks about the relative input impedances of his proposed triode and these devices at high frequencies.

Dr. Wright states that the circuit engineer using the proposed triode would be able to look to thermionic valve circuits for his design information. Although it is true that a very large part of our university teaching still revolves around the thermionic valve, in industry transistor circuits are now a matter of routine; indeed a very large proportion of electronics engineers are far more familiar with transistor circuits than with valve circuits and I have come across few people who experience real difficulty in adapting themselves to transistors. We should not lose sight either of the fact that the circuits that they design are well able to cater for the variations with temperature of the characteristic of transistors.

Turning now to the proposed triode itself, the real difficulty is with the insertion of the grid. Although this is a formidable proposition I do not think that we need be dejected about it; if the triode can be shown to have real advantages I have no doubt that grids can be placed where they are wanted. Five years ago the design of an alloy transistor for use in a.m. broadcast receivers appeared to be fraught with difficulties, many of them connected with the very small electrode and yet today those devices are made cheaply by mass-production techniques and the laboratory difficulties have shifted to transistors working at frequencies of the order of 1000 Mc/s. Given the right incentive solutions are usually found to most problems.

I should like to ask Dr. Wright whether he has considered using silicon for this triode. Silicon of very high resistivity is now available and if this were a possible material it would enable him to take some advantage of the facilities of the semi-conductor industry.

Finally, a word about the diode. Can it be switched on and off very quickly? If so, it is attractive in that it offers the possibility of very high switching speeds with high reverse resistance, and it may be that it is with exploring the possibilities here that we should first concern ourselves.

Dr. Wright (in reply) : On theoretical principles the dielectric triode is superior to the transistor in having greater stability against temperature changes, having greater power amplification, being able to operate at higher frequencies, and possessing a lower noise figure. One can add that for high frequency use the dielectric triode should be elec-

trically more robust than the high frequency transistor. Further, it should be able to operate at temperatures both higher and lower than can be attained with semi-conductor devices.

However, it is not anticipated that the dielectric triode could ever attain the high current and low resistance levels of the low-frequency power transistor.

The main advantages of the device over the thermionic vacuum triode are of course basically those of smaller dimensions, greater mechanical ruggedness, freedom from heater supplies and, one hopes, long life.

The field-effect transistor has a large input capacitance because the input electrode is a reverse biased $p-n$ junction. Further, although designed as a high frequency device, it does have a relatively long carrier transit time because the length of the conducting channel cannot be made too small; this results in relatively small values of mutual conductance. Because of its different geometry and operating principle the transit time of the carriers in the dielectric triode is extremely short and this device can therefore operate with an inherently much smaller input capacitance than the field effect transistor.

The point about looking to thermionic valve circuits for design data is that like the vacuum triode the dielectric triode is a voltage-operated and not a current-operated device and should not require stabilisation against temperature changes. The circuitry should therefore be inherently simpler than that of the transistor and this is a good thing.

In principle there would appear to be a large number of materials suitable for use in s.c.l. devices. As high a value of mobility as possible is required together with a high resistivity in order that the injected charge should not leak away by ohmic conduction while traversing the active regions of the device. This latter requirement means that the dielectric relaxation time of the material should be much larger than the electron transit time, i.e. $\rho\epsilon \gg t_r$. More stringent requirements on the resistivity may be needed, however, if for example high reverse resistances for diodes or high input resistances for triodes are needed. Intrinsic silicon just about satisfies the requirement that $\rho\epsilon \gg t_r$ but in a s.c.l. device would not satisfy the latter requirement.

The diode can be switched on and off very rapidly indeed because it relies for its action on the fast process of majority carrier drift and because it is free from minority carrier storage. A thin crystal diode would thus be very fast, have

a high reverse resistance and have a low forward resistance. In our laboratories attention has in fact been confined mostly to the diode so far because this device can be constructed with simple equipment.

Dr. J. R. Tillman : What basic properties determine the figure of merit of a semi-conductor (or dielectric) for use in these triodes, i.e. what determines the gain-bandwidth product? It seems that, if $\theta - 1$ is neglected, $g_m/C = (t_r)^{-1}$ which is proportional to μ , and ϵ is unimportant (cf. materials for unipolar transistor for which μ/ϵ is important).

Several times this evening we have heard that the transistor depends for its action on the comparatively slow process of carrier diffusion; but modern diffused-base transistors make use of drift, caused by built-in fields, to reduce transit times considerably.

Presumably μ for cadmium sulphide has been deduced from Hall and resistivity measurements. Is there any evidence for a dependence on field strength, up to those suggested here; if the electrons become sufficiently out-of-thermal-equilibrium with the lattice, can any effects detrimental to the triode be produced, e.g. secondary emission at the anode? If the anode is so made as to cause some hole injection, could the net result be beneficial (the neutralization of space charge would make current flow easier, but presumably would lower the impedances of the control and output electrodes)? Is, on the other hand, some different geometry or system of control required with two-carrier devices?

The author seems to hope that a more suitable semi-conductor (or dielectric) can be developed; what substances, if any and no matter how backward their preparation, combine a much higher mobility with energy gaps of say not less than 2 eV? Does zinc oxide hold out any hope?

Materials with high electron mobility and energy gaps of about 1 eV are potential materials for unipolar transistors, no matter what their hole mobilities may be. For the same key physical dimensions (or equal difficulty of manufacture) what advantages can be claimed for the space-charge-limited triode over the unipolar transistor?

I should not like to see a programme of work on space-charge-limited current flow in dielectric stand or fall by the ability to make triodes or by their worthwhileness when made. Perhaps some electronic device of novel purpose is more likely to emerge and for that reason alone further studies of the effect should be encouraged.

Dr. Wright (in reply): For all charge control devices the gain-bandwidth product is inversely proportional to the carrier transit time and therefore a high value of mobility is desirable; the dielectric triode is no exception. However, in general there are circuit capacitances which have to be charged up and for high frequency use therefore a high value of g_m is desirable as well as a high value of g_m/C . This implies that a suitable figure of merit for a material to be used for s.c.l. devices is the magnitude of the product $\mu\epsilon$.

Measurements have been made on diodes using field strengths up to a few times 10^4 V/cm and the square-law dependence of current has been followed over this range. This implies that the mobility remains proportional to field strength up to carrier velocities of $\sim 10^7$ cm/sec. At very high field strengths electron avalanching might occur and in a material with a reasonably high hole mobility this could lead to electrical breakdown. If hole injection at the anode took place space-charge neutralization could increase the current flow by several orders of magnitude.¹¹ However, a device using neutralized s.c.l. flow would require separate grids to control cathode and anode emission and would be considerably more complicated than the single carrier device described here.

In principle, the range of materials which could be used for s.c.l. devices is so vast that all one can say at present is that more suitable materials than cadmium sulphide will almost certainly be found. For example a number of the III—V compounds currently being studied for their semi-conducting properties in the impure state, such as gallium phosphide, combine wide band gaps with quite high mobilities. Unfortunately the achievement of high resistivity material is an exceedingly difficult technological problem. Alternatively a number of the II—VI compounds, of which cadmium sulphide is a member, offer higher mobilities with sufficiently wide band gaps.

The unipolar transistor is a generic term covering a number of devices but is normally used to refer to the field-effect transistor; this point has been discussed in the previous reply.

Major J. K. Lee (Associate): I would like to refer to Dr. Wright's statement that "the device should by comparison with other solid state devices be relatively insensitive to temperature changes." Bearing in mind the very wide temperature change requirements of equipment for the armed forces, can he give any figures of performance versus ambient temperature, so that comparisons can be made with germanium or silicon transistors?

Dr. Wright (in reply): Under s.c.l. conditions the number of carriers available for current flow is independent of temperature. In a semi-conductor, on the other hand, the number of carriers able to pass over a potential step such as a forward biased $p-n$ junction depends exponentially upon temperature. Compared with the transistor, therefore, the electrical characteristics of the dielectric triode will be insensitive to temperature changes.

J. A. Sargrove (Member): I feel that we have been privileged to hear a most significant paper as it deals in a rather prophetic manner with a device in advance of its existence, since only the diode exists at present. I believe we can find a historic parallel to this in the work of O. W. Richardson only a few years after Ambrose Fleming had demonstrated his thermionic diode. Richardson worked out from basic principles the laws of the thermionic triode, for two special theoretical cases: the case of a triode with infinitely large plane cathode, grid and anode; and the case of a triode with an infinitely long cylindrical system with a filamentary cathode having a very small diameter.

We know, and so did he, that one cannot make a practical triode in either of these theoretical forms. Nonetheless, the two Richardson formulae are the classic start for all thermionic valve engineers when they work out a new range of valves and the actual valves sit nicely in between Richardson's two extreme calculations. In any case he was, so far as I know, the first to recognize the existence of a space-charge-limited current in a vacuum. Construction of actual triodes by Lee de Forest, Wehnelt, and later by von Lieben and Reisz, followed. I think we have in Dr. Wright's paper such a historic first! I believe we have here the rules of the solid-state dielectric triode and the recognition that it is also a space-charge limited device.

If the future proof will be forthcoming, as I sincerely hope it will, we shall be able to use a device of significantly greater utility than the more conventional transistor. A lot of effort and money will have to be put into this development, however, and I hope that the N.R.D.C., or the Minister for Science, or perhaps better still private enterprise, will grasp this new device in its pre-embryonic state and turn it into reality. I think the rewards would be very great. As the Americans and no doubt the Russians are also working on it we must hope the United Kingdom will not be lagging behind in supporting Dr. Wright in his work.

APPLICANTS FOR ELECTION AND TRANSFER

As a result of its meetings on March 30th and April 26th the Membership Committee recommended to the Council the following elections and transfers.

In accordance with a resolution of Council, and in the absence of any objections, the election and transfer of the candidates to the class indicated will be confirmed fourteen days after the date of circulation of this list. Any objections or communications concerning these elections should be addressed to the General Secretary for submission to the Council.

Direct Election to Member

KRIEGER, Horst A. C. *Co'logne, Germany.*
RAMACHANDRA RAO, Professor Barre, M.Sc., D.Sc. *Waltair.*

Transfer from Associate Member to Member

CHAPMAN, Cecil Thomas. *Bourne End, Bucks.*
EVERETT, Kenneth Edward, M.Sc.(Eng.), B.Sc. *Southampton.*
HADDY, Arthur Charles. *Cuffley, Herts.*
LEVENTHALL, Philip Eric, B.Sc.(Hons.). *Welwyn Garden City.*
NICHOLSON, Philip Ian. *Hatfield, Herts.*
STREET, Group Captain Charles Keith, M.B.E., R.A.F. *Hadley Wood, Middlesex.*
TATE, Clifford Edward. *Emsworth, Hants.*

Direct Election to Associate Member

ADBY, George Colin. *Reading, Berkshire.*
ADHAMI, Mohammad Rizwan, M.Sc. *London, W.8.*
CHING Yuen Kai, Ph.D., B.Sc., D.I.C. *Hong Kong.*
COLLIS, Reginald Edward. *Dartford, Kent.*
GODWIN, Major Jack, R.A. *Bromley, Kent.*
WATERS, Roy Frederick George. *West Malvern, Worcs.*

Transfer from Associate to Associate Member

AHMAD, Capt. Saiyed Amin Uddin. *Pak. Signals, Rawalpindi.*
BONAGE, William Frederick. *Chelmsford, Essex.*
HAMILTON, James Richard. *Hitchin, Herts.*
van den HEUVEL, Flt. Lt. Teunis, R.N.Z.A.F. *Christchurch, New Zealand.*
MUSTAFA, Ali. *Kirkuk, Iraq.*

Transfer from Graduate to Associate Member

BROOK, Denis. *King's Langley, Herts.*
CONNELL, Andrew Wallace, B.Sc.(Eng.). *Glasgow.*
DORMER, Flt. Lt. Donald Edward, R.A.F. *Henlow, Bedfordshire.*
FAULKNER, Harold John. *Cheltenham, Glos.*
FERMOR, Sqdn. Ldr. Brian, D.F.C., R.A.F. *Esher, Surrey.*
GANAPATHY, Natarajan, B.E. *Montreal.*
GEALER, Brian John. *Evesham, Worcs.*
JAQUES, James Brian, B.Sc. *Evesham, Worcs.*
JUSTICE, James William H. *Barnet, Herts.*
MAINWARING, Peter. *Upper Hutt, New Zealand.*
NEWELL, Allen Frederick. *Totton, Hants.*
RIESEL, Zwi Herbert. *Rehovot, Israel.*
SAUNDERS, Flt. Lt. Donald, Dip.El., R.A.F. *Thetford, Norfolk.*
SIMMONDS, Derek James. *London, N.8.*
STICKLER, Gordon Alan. *Newport, Mon.*
WRIGHT, Flt. Lt. Hayward, R.A.F. *Barry, Glam.*

Direct Election to Associate

CLANCY, Elvyn Edmund. *Brampton, Cumberland.*
CRIMP, John. *Dartford, Kent.*
KAY, John Douglas. *Coulsdon, Surrey.*
MARTIN, Gordon William. *London, S.E.20.*
MITCHELL, Victor Leslie Charles. *Stoke-on-Trent, Staffs.*
PARNELL, Henry Roy. *Staines, Middlesex.*
PRICE, George Douglas. *Liverpool.*
SCOULDING, William George. *Hornchurch, Essex.*
SMITH, Roy Douglas. *Evesham, Worcs.*
VIRGON, Michael. *Bristol.*
WAKERLEY, Philip Albert. *Wolverhampton, Staffs.*
WALTON, Sidney. *Nairobi, Kenya.*

Transfer from Student to Associate Member

CHAPMAN, Derrick James Kenneth. *Kingsbridge, Devon.*
MATTHEWS, Donald Charles Mackenzie. *Henel Hempstead.*
WEBSTER, Arthur. *Wigan, Lancs.*

Transfer from Student to Associate

BAKER, Dennis. *London, S.W.11.*
BURNHAM, Charles Seaton. *Chelmsford, Essex.*
CLEGG, Richard Arthur. *Cambridge.*
PANIKKAR, R. Sukumara, M.Sc. *Trivandrum, India.*

Direct Election to Graduate

AVORY, Leslie Edward. *London, W.12.*
BROWN, Peter William. *Romford, Essex.*
*BRUSH, Valera Alberto, *Lima, Peru.*
CASTLE, Anthony George. *Bromley, Kent.*
DURRANT, Frank Peter. *Hasant, Hampshire.*
EGLEN, Ronald Frederick James. *Bognor Regis, Sussex.*
EGLINTON, Malcolm Oliver. *Sale, Cheshire.*
EKEOCHA, Samuel Lemeke. *London, S.E.11.*
ETHERINGTON, Malcolm Patrick. *Epsom, Surrey.*
FIDLER, David Morris, B.Sc. *Cambridge.*
HERON, Major Anthony Norton, R.A. *Leatherhead, Surrey.*
HOLLEY, Lieut. Ronald Victor, R.N. *Winchester, Hants.*
JEALOUS, Captain John Leonard, R.E. *London, W.1.*
JONES, David Kenton, B.Sc. *Evesham, Worcs.*
MOBBS, John Charles William. *Chelmsford, Essex.*
MORAGHAN, James Sylvester. *Dublin, Ireland.*
PATON, Captain James Otway, B.Sc. *Ipo, Malaya.*
POYNTER, Roy Alfred. *Stevenage, Herts.*
PULLINGER, Gordon Patrick. *Birmingham.*
RUDD, David Walter. *Lowestoft, Suffolk.*
SLANEY, Brian Michael Arthur, B.Sc.(Eng.). *Leigh-on-Sea, Essex.*
SNOW, Anthony Cyril. *Cheltenham.*
TUCKER, Ronald. *Brighton.*
WILKINS, Robert Peter William. *Bromley, Kent.*
WILLIAMSON, John Morrison. *Chelmsford, Essex.*
WILMAN, Hugh. *Barnet, Herts.*
WOODGER, Peter. *Worcester.*

Transfer from Associate to Graduate

DINGLEY, James Thomas. *Upper Belvedere, Kent.*

Transfer from Student to Graduate

ABERCROMBIE, Frank Leonard. *Weston-Super-Mare, Somerset.*
ABRAHAM, V. T., B.Sc. *Kerala State, India.*
BEN ARI, Moshe J. *Maoz-Aviv, Israel.*
CARPENTER, Dennis Arthur. *London, S.W.15.*
CAPNISTOS, Emman. *Athens, Greece.*
CHEUNG, Leung Fat. *Hong Kong.*
DUGGAL, Jagmohan Sarup. *Bombay.*
FISHER, John Alexander. *Nottingham.*
HAIGH, Fred Ellison. *Newcastle-upon-Tyne.*
HARDING, Robert Harold. *London, N.W.4.*
LAMBERT, Keith Walter. *Cardiff.*
PODLASKI, Jan. *Manchester.*
RIVLIN, David. *Schefferville, Canada.*
STEELE, Michael. *Wallington, Surrey.*
SUBRAMANIAM, Vasudeva Ayyar, B.Sc. *Trivandrum, India.*
TIMMS, Anthony Francis. *Knowle, Warwickshire.*

STUDENTSHP REGISTRATIONS

The names of 71 students registered at the above meetings will be published later.

* denotes a reinstatement.

Television Field Scan Linearization†

by

H. D. KITCHIN, ASSOCIATE MEMBER‡

A paper read on 2nd July 1959 during the Institution's Convention in Cambridge.

Summary: Although the design of a field timebase is based on well established principles and theory, there are many points at which there is considerable divergency between the theoretical and practical results. Foremost of these is that of calculating the parameters of linearizing networks, particularly of the feedback type. The present paper examines conventional linearizing methods and it is shown that the deflection current produced is S-shaped under certain conditions. The deflection current demanded by modern wide-angle cathode-ray tubes is of this form and it is shown that by the correct choice of operating conditions conventional linearizing methods can approximate sufficiently close to the desired shape for normal domestic receiver requirements.

1. Introduction

In recent years, the increase in scanning angles used in domestic television receivers has emphasized the well-known problems in timebase design. On account of the greater scanning angle in the horizontal direction with the present 4:3 aspect ratio, the line timebase has been the subject of intensive work which has somewhat eclipsed that on the field timebase. Nevertheless, there are many difficulties associated with wide-angle field scanning and foremost of these is that of producing a linear scan. The three factors which determine the linearity of the scan are (i) the shape of the deflection coil current, (ii) the deflector coil field distribution, and (iii) the geometry of the cathode-ray tube.

In a theoretical treatment of linearization methods it is customary to ignore the second two factors and assume that a deflection coil current of linear sawtooth waveform is required. On this basis, it can be shown that the use of transformer coupling between the valve and deflection coils (which is universal to-day) requires the primary current to be of parabolic form^{1, 2, 3}. This can be provided by the valve characteristic curvature and the first of the

linearizing methods considered deals with the conditions under which this is possible. The succeeding sections are concerned with linearization by means of shaping networks and negative feedback systems. The treatment is essentially analytic and differs from that generally known in the quantitative examination of the residual non-linearity of conventional linearizing networks. It is shown that by suitably proportioning the circuit elements the deflection coil current can be made S-shaped. Such a shape is required in practice to provide a linear scan on wide-angle tubes, and the present analysis shows that the feedback method for linearization produces the most symmetrical shape of deflection coil waveform.

The amount of non-linearity necessary to produce a linear scan on wide-angle tubes is considered in the final section and it is shown that satisfactory linearization is possible using existing methods for cathode-ray tubes having diagonal angles of 110 degrees.

2. The Measurement and Specification of Non-linearity

The measurement of non-linearity is usually carried out by displaying a bar or line pattern on the c.r.t. face and measuring the width or separation of the bars or lines. It is desirable for the distances to be measured along a line normal to the tube axis and in the direction of the scan, as shown in Fig. 1 where P represents

† Manuscript first received 20th February 1959 and in final form on 9th May 1959. (Paper No. 556)

‡ Mains Radio Gramophones Ltd., Research and Development Department, 359 Manchester Road, Bradford 5.

U.D.C. No. 621.397.331.2

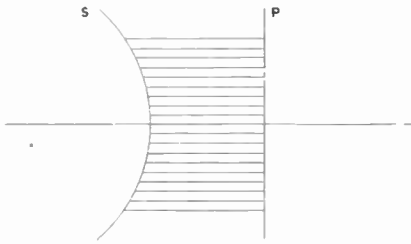


Fig. 1. Diagram showing the principle of measuring the linearity of a line pattern on a curved surface by projection onto the plane P.

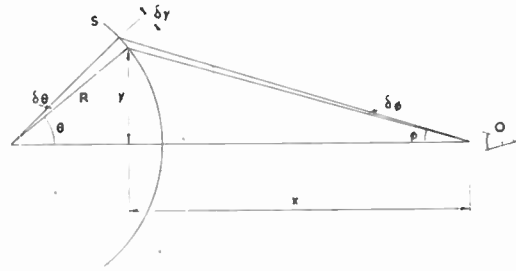


Fig. 2. Representing an observer situated at O viewing a spherical surface S upon which are equally spaced lines of spacing $\delta\gamma$.

the plane along which the distances are measured. This method is preferable to measurements made on the cathode-ray tube face itself because the convexity of the tube face introduces an apparent cramping at the top and bottom of the picture. This is an optical effect and should not be confused with the deflection distortion discussed in Section 4. The situation is represented in Fig. 2, from which the distortion can be shown to be a function of $\cos \phi$. For a typical 90 deg cathode-ray tube the non-linearity due to this effect is about $3\frac{1}{2}$ per cent. By measuring the non-linearity as suggested above this factor is included and the result more representative of the appearance to a viewer. A travelling microscope or telescope (depending on the distance away from the tube face) facilitates the measurements, and the bars should be sufficiently narrow to reveal any local region of cramping.

There are many ways in which the results of such measurements can be expressed of which the most commonly used is

$$\pm \frac{W_{\max} - W_{\min}}{W_{\max} + W_{\min}} \times 100\%$$

where W_{\max} is the width of the widest bar and W_{\min} is the width of the narrowest bar.

Some workers avoid the use of positive and negative deviations by using a figure twice the above.

In circuit analysis non-linearity is often of a simple exponential form, the maximum and minimum slopes occurring at the start and finish of the scan. It is then convenient mathematically to express the non-linearity as

$$\% \text{ non-linearity} = \left(1 - \frac{S_{\min}}{S_{\max}} \right) \times 100\%$$

where S_{\max} and S_{\min} are the maximum and minimum slopes. Non-linearity expressed by this method is hereafter termed the "slope" non-linearity.

Non-linearity of not more than ± 5 per cent is usually considered satisfactory in a mass-produced television receiver. For more exacting requirements, such as studio monitors, non-linearity not exceeding ± 1 per cent is desirable. The corresponding figures for the slope non-linearity are approximately 10 per cent and 2 per cent.

3. Linearization Methods

The widespread use of low impedance deflection coils has made the field output transformer mandatory and the practical and equivalent circuits of the anode circuit of the output stage are shown in Figs. 3(a) and (b). Analysis of the equivalent circuit of Fig. 3(b) reveals that the primary current necessary to produce a linear scanning current is of parabolic form, the degree of curvature being determined by the ratio $R_2T/(L_p + L_2)$, which will be denoted by m . The normal range of m is from 1 to 5. A commonly used design criterion is that giving an anode current with zero slope at the start of scan (often termed the "zero initial slope" or z.i.s. condition) and for which $m=2$. A more recent tendency is to employ transformers requiring rather more curvature than this, as it is then possible to improve the overall efficiency somewhat and reduce the transformer size. The anode current waveform in this case is characterized by a minimum value somewhere along the scan (often between 10 and 20 per cent).

The time at which the minimum value of the anode current occurs, expressed as a fraction of

the scan period T is given by

$$\left(\frac{t}{T}\right)_{\min} = \frac{1}{2} - \frac{1}{m}$$

The primary voltage developed across the transformer terminals also has a parabolic component caused by the flow of parabolic anode current through the primary resistance. The magnitude of this component is, however, appreciably less than the linear component developed across the reflected secondary circuit resistance R_2 , and the primary voltage waveform is, in consequence, much less curved than the primary current waveform. The waveform to be delivered during scan by the valve feeding the transformer is therefore dependent on the valve impedance; a low-impedance valve, approximating to a constant-voltage generator, must deliver an almost linear voltage sawtooth, whereas a high-impedance valve, approximating to a constant-current generator, must deliver a much more curved current sawtooth. These different output requirements are reflected in different grid input waveforms for the two types of valve, and this effect of the valve internal impedance on the grid input waveform is illustrated in Fig. 4. It will be seen that the

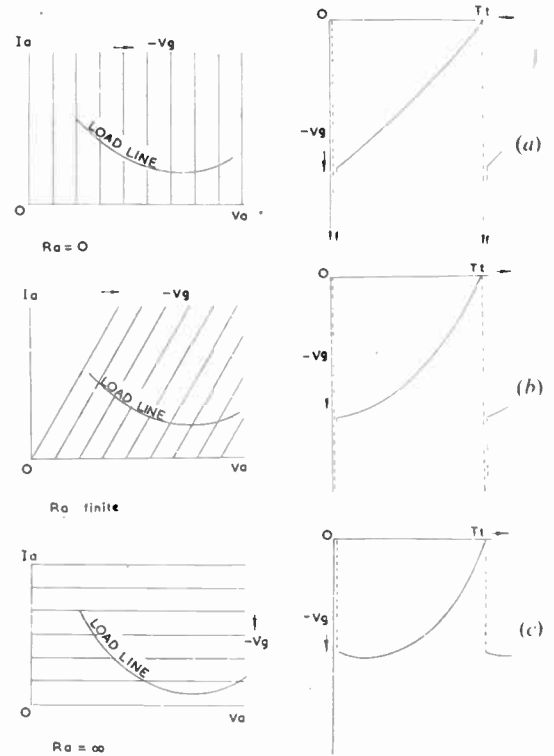


Fig. 4. The effect of the valve internal impedance on the required grid drive waveform. Conditions during fly-back shown dotted.

- (a) Ideal linear triode of zero impedance.
- (b) Ideal linear triode having finite anode impedance.
- (c) Ideal linear pentode having infinite anode impedance.

curvature of the grid input waveform during scan increases with valve internal impedance.

It should be noted that a positively-increasing sawtooth grid input to the valve is assumed, producing an anode current increasing during scan. This mode of operation is universal on account of the difficulties encountered during flyback with a negatively-increasing sawtooth input.⁴

The grid input is obtained from the sawtooth generator. This is nearly always of the R-C type, which develops a voltage sawtooth of exponential form. The curvature of such a waveform is opposite to that required by the anode circuit and the shaping of this sawtooth to produce the correct parabolic anode current is the object of linearization methods. These various methods will now be considered.

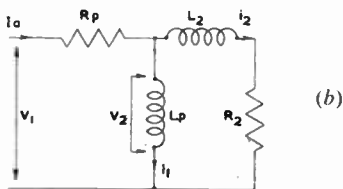
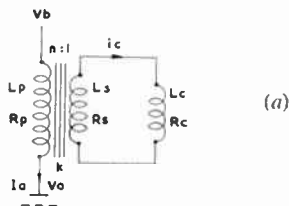


Fig. 3. (a) Anode load circuit of the field output valve when transformer coupling to the deflection coils is employed.

(b) Equivalent circuit of (a), where

$$L_2 = L_p(1 - k^2)/k^2 + n^2 L_s/k^2$$

$$R_2 = n^2(R_s + R_c)/k^2, \text{ and}$$

$$i_2 = (k/n) \cdot i_c$$

3.1. Linearization by Valve Curvature

To achieve good efficiency the frame output valve must be operated over a large part of its characteristics and it is essential to consider, in the treatment of linearization methods, the effect of valve characteristic curvature on the waveforms involved. It is fortunate that the curvature is in the correct sense to assist in the shaping of the exponential wave from the sawtooth generator to produce the correct anode current waveform, and it is possible by suitable design of the transformer and choice of valve to achieve a sufficiently good approximation to the correct anode current waveform with the valve grid input taken directly from the sawtooth generator. This mode of operation provides the simplest method for linearization, having been widely used in the past and still finding favour in some quarters. The performance possible by this method is considerably influenced by the choice of valve, particularly so concerning its impedance, and it is desirable to consider pentode and triode valves separately.

3.1.1. Pentode valves

If we assume the valve impedance to be infinite then the anode current will be a function of the grid voltage only, as given by the I_a-V_g curve for the particular valve and screen grid

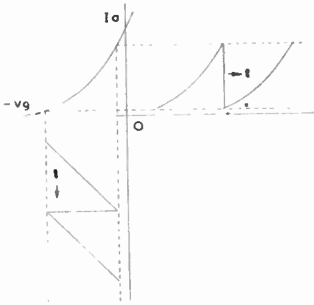


Fig. 5. The use of the I_a-V_g characteristic of a valve to provide the correct anode current waveform from a linear sawtooth grid voltage.

voltage used. A typical I_a-V_g curve is shown in Fig. 5, and upon this the anode current waveform produced by a given grid waveform can be easily constructed. The anode current waveform produced by a linear sawtooth grid voltage will obviously be a replica of that

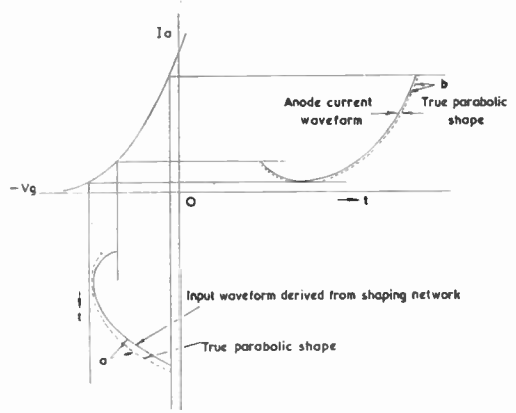


Fig. 6. Diagram showing how valve characteristic curvature assists in providing the correct parabolic shape of anode current from an exponential grid voltage when the waveforms exhibit minimum values along the scan.

section of the curve covered by the grid voltage excursion, as shown in Fig. 5. This case represents the maximum parabolic curvature that can be obtained by this method when using direct drive from the sawtooth generator, since any exponential curvature of the grid input waveform will subtract from the curvature of the anode current. The curvature of the anode current produced will also depend on the operating region on the curve and can be conveniently varied by the bias, thereby providing a method for the control of linearity. When this form of control is used, care should be taken to ensure that variations between valves do not necessitate bias settings for correct linearity such that valve limits are exceeded. Maximum curvature of the anode current waveform will be obtained when one limit of the voltage swing takes the valve to cut off, giving an anode current waveform with approximately zero initial slope.

It is not possible by valve curvature alone to produce an anode current having a minimum value along the scan, and transformers requiring greater curvature than the z.i.s. condition are inadmissible (i.e. $m > 2$). Nevertheless, the valve curvature still contributes towards providing the correct anode current waveform, even when the latter exceeds that of the z.i.s. condition, and the manner in which it operates to do this is illustrated in Fig. 6. At (a) is shown the correct parabolic shape of the anode current waveform along with the general shape of the waveform

produced by a typical R-C shaping network (such as that to be considered in Section 3.2). It will be noticed that the latter curve has a sharper minimum than the true parabolic shape. When this waveform is applied to the grid of a valve with a curved characteristic the effect of the curvature at low I_a is to flatten the minimum, thereby bringing it nearer to the true parabolic shape and reducing the non-linearity, as shown at (b).

3.1.2. Triode valves

The situation in this case is more complex than the preceding one because the anode current is dependent not only upon the grid voltage, but also upon the anode voltage. The relationship between the grid voltage, anode voltage and anode current is given approximately by the three halves power law:

$$I_a = K \left(V_g + \frac{V_a}{\mu} \right)^{3/2}$$

where K and μ are almost constant for a particular valve. The anode current and the anode voltage variations with time are fixed by the transformer and coil design, so that the required grid voltage can be calculated. However, it is difficult to arrive at general results of much assistance in design by this method, and recourse to plotting the loadline on the valve characteristic is invariably more revealing.

The potentialities of using the curved characteristic of a triode valve for linearization can be roughly assessed graphically by reference to Fig. 7. In this figure are drawn idealized triode I_a-V_a curves along with loadlines having different degrees of primary current curvature, and it will be seen that it is possible to generate an anode current having a minimum value during the scan period without a corresponding minimum being necessary for the sawtooth grid waveform. In this respect it differs from the pentode, as the latter can only provide an anode current waveform having a minimum value during scan if this is also present in the grid input.

Consideration of Figs. 7(b) and (c) suggests the limiting condition for the maximum curvature of the anode current that is possible to generate without requiring the grid waveform to have a minimum value during scan. This will be when the loadline at the start of scan has a common

tangent with one of the grid voltage lines. Such a limiting case is shown in Fig. 7(b). It is shown in Appendix 1 that the limiting condition is

$$L_p = T(R_a + R_p) \left(\frac{1}{2} - \frac{L_s + L_c}{T(R_s + R_c)} \right)$$

where R_a is the valve's V_a/I_a slope at the point $t/T=0$ on the loadline, the other parameters being as defined in Fig. 3(b),

On account of the exponential nature of the input sawtooth and the variability of valve characteristics it will normally be necessary to make L_p considerably greater than this limiting value if complete linearization by valve curvature alone is desired. The inherent superiority of the triode over the pentode valve in delivering the necessary curved anode current has led to linearization by valve curvature being nearly always associated with a triode output valve.

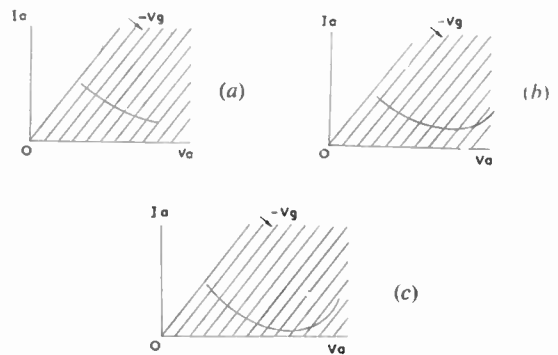


Fig. 7. Illustrating the possibility of generating anode current having a minimum value along the scan by use of triode characteristic curvature. (a), (b) and (c) show load lines having successively greater curvature of the anode current waveform.

When complete valve curvature linearization is undesirable or impracticable it is necessary to employ alternative means, and the methods available can be divided into two categories; those using passive shaping networks only and those employing the negative feedback principle.

To keep the mathematical expressions simple and thereby permit easy application of the theory to design work, it is assumed that the valve and transformer characteristics are linear, and that the sawtooth available from the sawtooth generator is linear. Of these assumptions, that of a linear transformer characteristic is reasonably realistic as transformer distortion is usually

low. The other two are, however, more questionable and it is considered later how they may best be taken into account.

Furthermore, the analysis will be restricted to the case of a single pentode stage as this is by far the most common and as shown above, requires the greatest amount of linearity correction.

3.2. Linearization by Shaping Networks

The networks employed can be, theoretically, either RC or RL combinations, but the practical difficulties associated with inductors (exaggerated in the field timebase because of the long time-constants necessary) have led to the exclusive use of the RC type. A network often employed (and from which many other networks can be derived⁵) is that shown in Fig. 8. The waveform

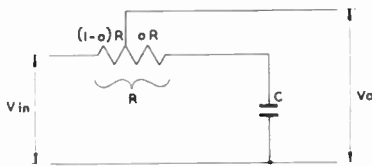


Fig. 8. Circuit of a commonly used passive shaping network used to provide an approximately parabolic output voltage from a linear input sawtooth voltage.

developed across the capacitor is approximately the integral of the input waveform and the tapping on the resistor serves to combine these together in any desired proportions. The integrating action obtained from this RC section can differ considerably from ideal mathematical integration and it is desirable to employ actual circuit analysis to assess its performance.

The voltage waveform across the capacitor depends upon its initial charge at the commencement of each scan, and two modes of operation can be distinguished.

The first is that in which the capacitor is discharged before the commencement of each successive scan period. This mode suffers from two basic defects: its inability to generate a parabolic wave having a minimum during scan, and the practical difficulty of discharging the integrating capacitor before the commencement of the scan period (which would be in addition to the normal discharge of the sawtooth generating capacitor).

The second mode of operation avoids the latter defect by not discharging the capacitor before the commencement of each scan period, in which case its charge can only change by current flow through the resistor. The expression for the output voltage V_o , produced by a linear sawtooth input, $\dot{V} \cdot t/T$, can be shown to be given by

$$\frac{V_o}{\dot{V}} = (1-a) \frac{\exp\left[-\frac{T}{CR}\left(\frac{t}{T}\right)\right]}{1 - \exp\left[-\frac{T}{CR}\right]} + \frac{t}{T} + (1-a) \frac{CR}{T} \dots\dots\dots(1)$$

where a is the fraction of the total resistance between the integrating capacitor and the tap.

The shape of the waveform defined by this equation, varies from a linear sawtooth identical with the input sawtooth, when $a=1$, to that shown in Fig. 9, when $a=0$. The latter waveform has a minimum value which occurs at a point along the scan determined by the ratio of the network time-constant, RC , to the repetition period, T , of the input sawtooth.

When T/RC is sufficiently small this minimum value tends to occur halfway along the scan period. Thus, by varying the position of the resistor tapping point a the minimum value of the output waveform can be chosen to occur anywhere up to halfway along the scan. The point at which the minimum of the output wave occurs can be shown to be given by

$$(t/T)_{min} = \frac{CR}{T} \log_e \frac{(1-a)T/CR}{1 - e^{-T/CR}}$$

The peak-to-peak value of the wave is given by

$$\frac{V_{o(p-p)}}{\dot{V}} = \frac{(1-a)e^{-T/CR}}{1 - e^{-T/CR}} + 1 - \frac{CR}{T} \times \left[1 + \log_e \frac{(1-a)T/CR}{1 - e^{-T/CR}} \right]$$

when $(t/T)_{min} \geq 0$, or

$$\frac{V_{o(p-p)}}{\dot{V}} = a,$$

when $(t/T)_{min} \leq 0$. The relationship between a and T/CR necessary to give $(t/T)_{min}=0$ (i.e. zero initial slope) is

$$a = 1 - \frac{CR}{T} (1 - e^{-T/CR}).$$

Now these results are well known, the usual treatment from this point being to assume that the exponent T/CR is sufficiently small to allow the first few terms of the series expansion for the exponentials to be substituted in the equations. The necessary relationships between the component values of the shaping network and the parameters of the output anode circuit are then easily derived. However, this procedure implies considerable attenuation in the shaping network which is rarely permissible in practice, and calculations based on these premises invariably require considerable modification during circuit development.

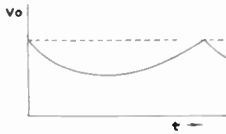


Fig. 9. General shape of the voltage developed across the capacitor of Fig. 8 when the input is a linear repetitive sawtooth and the charge on the capacitor is determined solely by current flow through the resistor.

This approximation can be avoided by starting from the expression for the output voltage of the shaping network (eqn. (1)) and deriving the resulting deflection current.

It is shown in Appendix 2 that the output waveform from the shaping network of Fig. 8 and given by eqn. (1), applied to the grid of a linear pentode results in a deflection current given by

$$i_2 = g_m \hat{V} \cdot \eta \left\{ \frac{1}{m} \left[1 - \frac{me^{-mx}}{1-e^{-m}} \right] + \frac{1-a}{m-p} \left[\frac{me^{-mx}}{1-e^{-m}} - \frac{pe^{-px}}{1-e^{-p}} \right] \right\} \dots\dots\dots(2)$$

where

$$\eta = \frac{L_p}{L_p + L_2}, \quad m = \frac{R_2 T}{L_p + L_2},$$

$p = T/CR$ and $x = t/T$. When $m = p$ the second term is indefinite, but by series expansion of the exponentials it can be shown that the expression for i_2 becomes

$$i_2 = g_m V \cdot \eta \left\{ \frac{1}{m} \left(1 - \frac{me^{-mx}}{1-e^{-m}} \right) + \frac{m(1-a)e^{-mx}}{(1-e^{-m})^2} (x + e^{-m}[1-x]) \right\} \dots\dots\dots(3)$$

If we specify the departure of the waveform according to eqn. (2) above in terms of the slope non-linearity we obtain

$$\begin{aligned} &\text{slope non-linearity} \\ &= \frac{m - (1-a)(m+p)}{\frac{m}{1-e^{-m}} - \frac{(1-a)}{(m-p)} \left(\frac{m^2}{1-e^{-m}} - \frac{p^2}{1-e^{-p}} \right)}. \end{aligned} \dots\dots\dots(4)$$

By choosing

$$m = (1-a)(m+p)$$

i.e.

$$a = p/(p+m) \text{ or } p = am/(1-a) \dots\dots\dots(5)$$

the slope non-linearity becomes zero and the waveform has the same slope at the start and the finish of scan. This does not mean, of course, that the slope over the rest of the scan is constant and in general it is S-shaped. It is shown in Section 4 that this shape is desirable to compensate for distortion caused by the cathode-ray tube screen radius exceeding the deflection radius, and this choice of parameters to give equal initial and final slopes will now be assumed.

The non-linearity of this waveform may be expressed as the ratio of the difference between the maximum slope and the initial slope (or final slope, as these are equal) to the initial slope. Non-linearity according to this definition will be termed the "maximum" non-linearity.

It is shown in Appendix 2 that the maximum slope of eqn. (2) occurs when

$$\left(\frac{t}{T} \right)_{\max} = \frac{1}{m-p} \log_e \frac{(1-e^{-p})m}{(1-e^{-m})p} \dots\dots\dots(6)$$

and that the maximum non-linearity is given by

$$\frac{am e^{-m(t/T)_{\max}}}{(1-e^{-m}) \left[\frac{m}{1-e^{-m}} - \frac{(1-a)}{(m-p)} \left(\frac{m^2}{1-e^{-m}} - \frac{p^2}{1-e^{-p}} \right) \right] - 1} \dots\dots\dots(7)$$

Curves of $(t/T)_{\max}$ according to eqn. (6) are plotted in Fig. 10 with m as abscissa for various values of a . In Fig. 11 are shown similar curves for the maximum non-linearity. The curves $(t/T)_{\max}$ give some idea of the degree of asymmetry of the S-shaped deflection current. When the curve is symmetrical the point of maximum slope occurs at midscan, i.e. $(t/T)_{\max} = \frac{1}{2}$, and it will be seen that this can only be approached with small values of m and a .

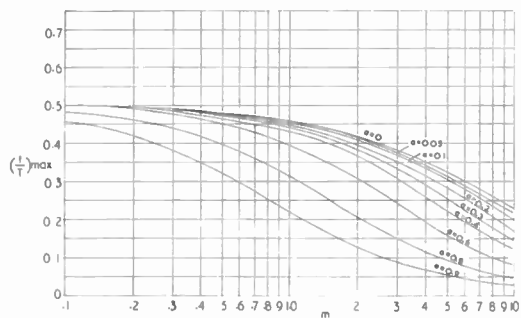


Fig. 10. Curves of eqn. (6), giving the point at which the maximum slope of the deflection current occurs as a function of a and m , when the shaping network time-constant satisfies eqn. (5).

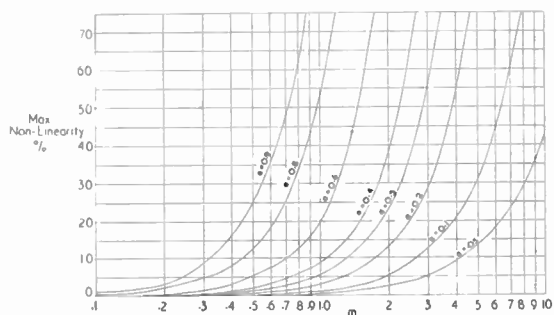


Fig. 11. Curves of eqn. 7, giving the maximum non-linearity as a function of a and m , when the shaping network time-constant satisfies eqn. (5).

An alternative shaping network, often more convenient in practice than that of Fig. 8, is shown in Fig. 12. The foregoing analysis also applies to this network when p and a are defined as shown in the figure.

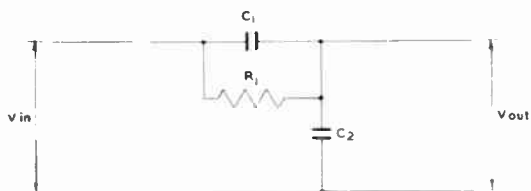


Fig. 12. Shaping network of different configuration to that of Fig. 8 but having an identical transfer characteristic. For this network a and p are given by $a = C_1/(C_1 + C_2)$ and $p = R_1(C_1 + C_2)$

3.3. Linearization by Negative Feedback

The theory of negative feedback amplifiers has received considerable attention over the last few decades and extensive literature is available. The well-known benefits resulting from the application of negative feedback to an amplifier are particularly advantageous in the field timebase amplifier and this has led to widespread use of this method for linearization in recent years. However, much that has been written on negative feedback amplifiers is of general nature and largely concerned with sinusoidal waveforms; many of the design procedures are, therefore, not directly applicable to timebase design. It is the purpose in this sub-section to examine theoretically such negative feedback systems as are commonly used in field timebase amplifiers.

The basic principle behind all the methods used is to feedback to the input an opposing voltage proportional to the deflection current. If the loop gain is sufficiently high the deflection current becomes proportional to the input voltage, so that a linear input sawtooth produces a linear deflection current. As it is impossible to achieve an infinite loop gain, any practical circuit must fall short of this ideal and there will be some residual non-linearity. It can be shown that the effect of feedback strictly proportional to deflection current is to reduce the gain and the effective value of m for the anode circuit by a factor r given by

$$r = 1 + (\text{mid-frequency loop gain})$$

and that the slope non-linearity of the deflection current produced by a linear sawtooth input is

$$100(1 - e^{-m/r})\%$$

(The curve of Fig. 24 applies directly to the evaluation of the non-linearity if m/r is substituted for $T/C'R'$).

A feedback voltage proportional to the deflection current may be produced in various ways. The simplest and most obvious of these is by inserting a resistor in series with the deflection coils, but this suffers from two disadvantages. The first is the reduction in the power efficiency of the output circuit, and it is necessary to use resistance values small compared with the deflection coil resistance. This leads to the second disadvantage of a low loop gain. An additional stage of amplification is usually

necessary if feedback is to be worthwhile and the system becomes uneconomical for a normal domestic receiver. Nevertheless, when the best performance is desired regardless of cost, it can be considered a good method, as it includes the whole output circuit within the feedback loop.

An improvement in loop gain could be obtained by using the voltage developed across the resistance of the deflector coils. Although this cannot be done directly, on account of the deflector coil resistive and inductive components being inseparable, it is possible to develop the desired voltage by means of the resistance-capacitance dual fed from the deflector coils. This arrangement is illustrated in Fig. 13, where the necessary relationships are also given. This method avoids wastage of power and will occasionally be satisfactory over a single stage with high resistance deflection coils. However, the tendency during the last few years towards exclusive use of low impedance coils (dictated mainly by production methods) has resulted in the loop gain being insufficient over a single stage and additional amplification is still necessary.

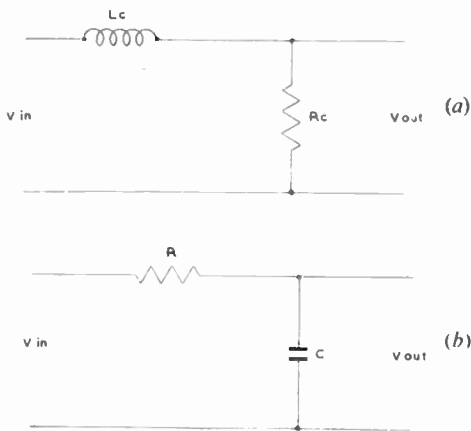


Fig. 13. (a) Equivalent circuit of the deflection coils and (b) its R-C equivalent, having identical transfer characteristic, when $RC = L_c/R_c$

To enable sufficient loop gain to be obtained over a single stage it is necessary to derive the feedback voltage from the primary of the output transformer. The R-C dual of the equivalent circuit for the transformer and deflector coils enables a voltage to be developed identical with that across the fictitious reflected secondary

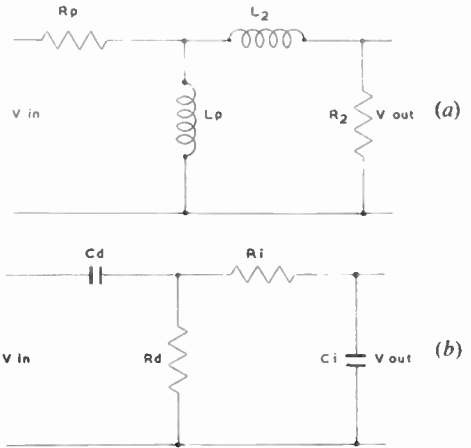


Fig. 14. (a) Equivalent circuit of the field output transformer and the field deflection coils, as in Fig. 3(b) and (b) its R-C equivalent, having identical transfer characteristic, when $C_i R_i = L_p R_p$, $C_d R_d = L_p/R_p$ and $C_i/C_d = R_p/R_2$.

circuit resistance (R_2 of Fig. 3(b)). This network is shown in Fig. 14(b) along with the necessary relationships between the constants of the anode circuit and the component values. These relationships are usually cited for design purposes, but it should be remembered that a linear deflection current is only obtained from a linear sawtooth when the gain is infinite. Although feeding back a voltage proportional to the deflection current, derived in one of the ways just described, will reduce the non-linearity of the deflection current due to the transformer shunt inductance, it is invariably the case that the degree of non-linearity is still intolerable because of insufficient loop gain. The non-linearity of the input sawtooth also contributes to the total non-linearity of the deflection current and the resulting effect is manifest as a gradual cramping towards the bottom of the picture.

To reduce the non-linearity without increasing the loop gain it is necessary to introduce some form of shaping network. This may be positioned so as to modify either the input, the grid or the feedback waveforms and thus provide the correct grid drive waveform from the approximately linear input and deflection current waveforms. These three possible circuit arrangements are shown diagrammatically in Fig. 15 where β represents the network used to develop a feedback voltage proportional to the deflection

current (and duplicating, as shown in the Figure, that section of the transformer-deflection coil equivalent circuit following the point from which the feedback is taken).

To simplify the expressions the feedback voltage, denoted by V_f , is assumed equal to zi_2R_2 , that is, a fraction, z , of the voltage developed across the hypothetical reflected deflector coil and transformer secondary resistance, R_2 (Fig. 3(b)).

The form taken by the shaping network in each of the three possibilities represented in Fig. 15 will now be considered and the capabilities of each system examined.

3.3.1. Shaping network modifying the input waveform (Fig. 15(a))

It has been stated in the preceding paragraphs that the effect of feedback directly proportional to the deflection current is to divide the gain and the effective value of m for the anode circuit by the factor r , which in the case of a single pentode stage is given by

$$r = 1 + z\eta R_2 g_m$$

where $\eta = L_p / (L_p + L_2)$.

From the point of view of linearity correction, therefore, the stage can be treated as if it were an amplifier without feedback having values of m and gain, $1/r$ th of the actual no-feedback values. The shaping network of Section 3.2 is therefore the appropriate choice for linearity correction and the analysis of that section applies directly.

The condition for zero slope non-linearity (i.e. equal initial and final slopes) is in this case

$$m/r = (1-a)(m/r+p); \quad a = p/(m/r+p)$$

or $p = am/r(1-a)$.

Thus the required value of p is likewise divided by the same factor r and the waveform of V_{in} is less curved than when feedback is absent. This is counterbalanced, however, by the necessity for its amplitude to be r times greater.

3.3.2. Shaping network modifying the grid input waveform (Fig. 15(b))

The shaping network is now positioned immediately before the grid of the valve and its input is made up of the difference between V_{in} and V_f , being approximately linear. The

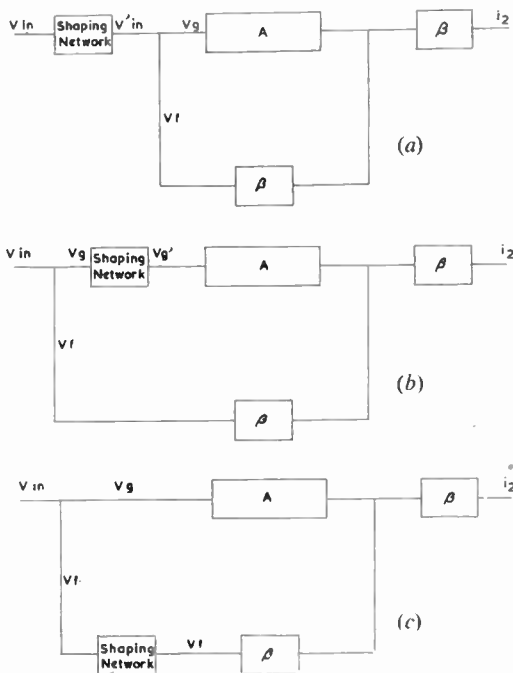


Fig. 15. (a) Block diagrammatic representation of a feedback amplifier with an appropriate β network providing a feedback voltage V_f proportional to the deflection current, and an auxiliary shaping network in the input path.
 (b) As at (a), but with the shaping network in the amplifier input circuit.
 (c) As at (a), but with the shaping network in the feedback path.

shaping network of Fig. 15 is again an appropriate choice to provide the necessary shape of grid input waveform.

It can be shown that the value of p for this network necessary for zero slope non-linearity of the deflection current waveform is $am/(1-ar)$. If $ar > 1$ the condition requires a negative value for p which is, of course, physically impossible.

The performance of this method of linearization is inferior to that next to be described and it will not therefore be considered in detail.

3.3.3. Shaping network modifying the feedback waveform (Fig. 15(c))

The shaping network is now positioned in the feedback circuit and it is assumed to be placed after the β circuit, modifying V_f to V'_f , as shown in Fig. 15 (c). It is further assumed that it does not load the β circuit and thereby affect

V_f directly. The requirements to be met by the shaping network can now be examined.

The shaping circuit must modify V_f to V_f' in such a way that when this is subtracted from V_{in} , V_o is of the correct parabolic shape.

Algebraically, we have

$$V_o = V_{in} - V_f'$$

i.e.

$$V_f' = V_{in} - V_o$$

Now V_{in} is assumed to be linear. Therefore V_o , being parabolic, must be proportional to the integral of V_{in} , i.e.

$$V_f' = V_{in} - A \int V_{in} \cdot dt \quad (A = \text{const.})$$

Furthermore, when V_o is parabolic V_f is also linear, so that we may write $V_f = BV_{in}$, where B is a constant, and the equation above becomes

$$\begin{aligned} V_f' &= V_f/B - (A/B) \cdot \int V_f \cdot dt \\ &= XV_f - Y \cdot \int V_f \cdot dt \end{aligned}$$

where X and Y are constants. The shaping network in the feedback line must therefore subtract the integral of the input voltage instead of add it as in the case of the non-feedback amplifier.

This can easily be done by altering the connections to the basic integrating network which is shown in Fig. 16. Referring to this figure, the output voltage V_o is approximately the integral of the input voltage V_{in} when T/CR is small. The voltage across R , V_r , will be, therefore

$$V_r = V_{in} - V_o = V_{in} - U \cdot \int V_{in} dt,$$

where U is a constant. To maintain the common earth point for the input and output terminals,

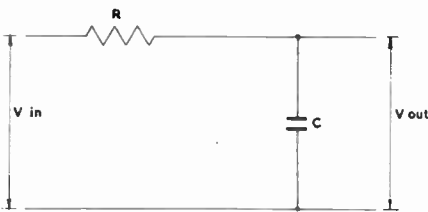


Fig. 16. The basic resistance-capacitance "integrator" shaping network. The output voltage is approximately the integral of the input waveform when T/CR is small.

the network is inverted, becoming as shown in Fig. 17. This is generally known as a "differentiator" network on account of its output being approximately the first derivative of the input voltage when T/CR is large. The term "subtractive integrator" would be more appropriate in the present application but the description "differentiator" is so well established that it will be adhered to.

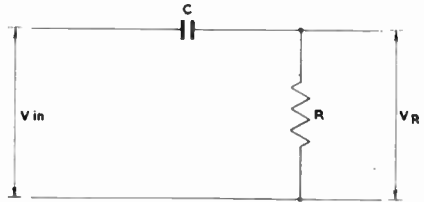


Fig. 17. Alteration of the output connections to integrator circuit of Fig. 16 produces the circuit shown, and from which the output is made up of the integral of the input waveform subtracted from the input waveform. When T/CR is large the output is approximately the first derivative of the input waveform. It is generally known as a "differentiator" network on account of this property.

It is shown in the Appendix 2 that when such a network is used for shaping, the reflected deflection current i_2 is given by

$$i_2 = g_m \cdot \hat{V} \eta \cdot \left\{ \frac{r}{m} - \frac{(\lambda_1 + p)e^{\lambda_1 x}}{(\lambda_1 - \lambda_2)(1 - e^{\lambda_1})} + \frac{(\lambda_2 + p)e^{\lambda_2 x}}{(\lambda_1 - \lambda_2)(1 - e^{\lambda_2})} \right\} \dots\dots\dots(8)$$

where λ_1 and λ_2 are the roots of the auxiliary equation

$$\lambda^2 + \left(\frac{m+p}{r} \right) \lambda + \frac{mp}{r} = 0.$$

The condition for equal initial and final slopes of i_2 is

$$p = m/(r-1) \dots\dots\dots(9)$$

the deflector coil current then being S-shaped. When the condition of eqn. (9) is satisfied the roots λ_1 and λ_2 are complex if $(r-1) > 1/3$. The expression for i_2 then assumes a sine and cosine form when expressed in real terms. In this case the time at which the maximum slope occurs is given by

$$\tan v \left(\frac{t}{T} \right)_{\max} = \frac{u \sin v - v \cos v + ve^{-u}}{v \sin v + u \cos v - ue^{-u}} \dots\dots\dots(10)$$

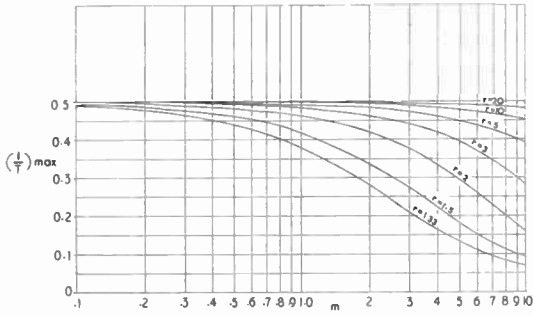


Fig. 18. Curves of eqn. (10) giving the point at which the maximum slope of the deflection current occurs, as a function of r and m , when the shaping network satisfies eqn. (9).

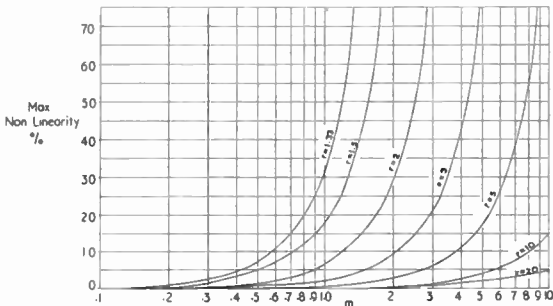


Fig. 19. Curves of eqn. (11) giving the maximum non-linearity of the deflection current as a function of r and m when the shaping network satisfies eqn. (9).

where u and v are the real and imaginary parts of the conjugate complex roots, λ_1 and λ_2 , i.e.

$$\lambda_1 = u + jv, \quad \lambda_2 = u - jv.$$

Also the expression for the maximum non-linearity is given by

$$\begin{aligned} \text{max. non-lin.} = & e^{u(t/T)_{\text{max}}} \left\{ \cos v \left(\frac{t}{T} \right)_{\text{max}} + \right. \\ & \left. + \left(\frac{e^{-u} - \cos v}{\sin v} \right) \sin v \left(\frac{t}{T} \right)_{\text{max}} \right\}. \end{aligned} \quad \dots\dots(11)$$

Curves of $(t/T)_{\text{max}}$ and the maximum non-linearity against m for various values of r according to these eqns. (10) and (11) are shown in Figs. 18 and 19 respectively.

The use of a separate network of the differentiator type in series with the feedback line for linearity correction is normal practice when feedback is taken from the secondary circuit

of the field output transformer, and the above theory enables the performance to be predicted. However, when the feedback is taken from the anode of the output valve it is found in practice that this extra network is usually unnecessary and acceptable results can be obtained by merely altering the constants of the β network of Fig. 14(b). It has often been pointed out in connection with this "dual" circuit that component values predicted by the design formulae usually quoted (and given in the figure) require adjustment in practice, and the discrepancy is often considerable. The preceding analysis has shown why this is so and also indicates how a more accurate design procedure can be derived.

If an additional differentiator section were to be used, then providing that the loading effects of succeeding networks can be ignored, it can be positioned to either precede or follow the network. If the extra differentiating section is inserted before the network the circuit of Fig. 20(a) is obtained. There are now two cascade differentiating sections, RC and $R_d C_d$, and it will usually be found that the calculated

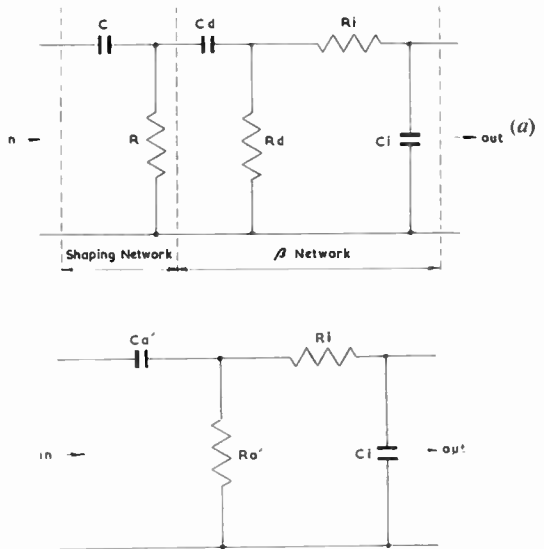


Fig. 20. (a) Complete form of the feedback network when the feedback is taken from the anode, comprising the networks of Figs. 14(b) and 17.

(b) Approximate equivalent to the complete network at (a), in which the two cascade differentiator sections have been replaced by a single section according to the relationship

$$C_d' R_d' = CR, \quad C_d R_d / (CR + C_d R_d)$$

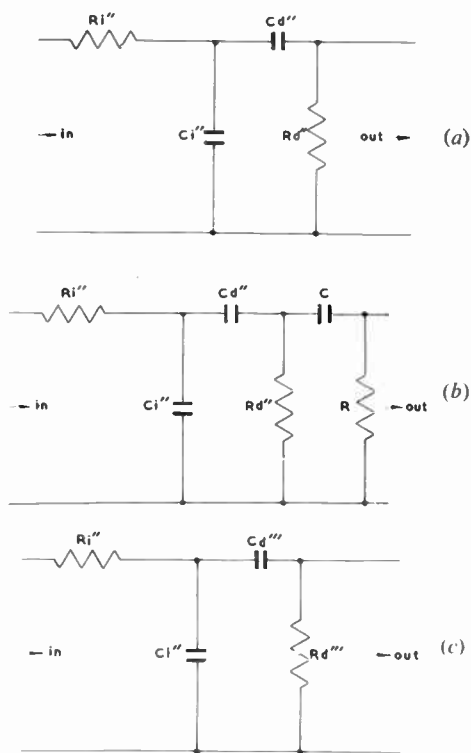


Fig. 21. (a) and (b) Alternative form for the network of Fig. 14(b), having an identical transfer characteristic when the components are related to those of Fig. 14(b) by

$C_d'' R_d'' = C_d R_d$, $C_i'' R_i'' = C_i R_i$ and $R_i''/R_d'' = C_i/C_d$
 (c) Approximate equivalent to the complete network of (b), in which the two cascade differentiating sections have been replaced by a single section having the relationships

$$C_d''' R_d''' = C_d'' R_d'' \cdot CR / (C_d'' R_d'' + CR)$$

time-constant of $R_d C_d$ is very much greater than that of RC . Under these conditions it can be shown that the combined effect of these two sections can be closely approximated by a single section having a time-constant equal to the two time-constants combined "in parallel," i.e. $T_1 T_2 / (T_1 + T_2)$. The complete network of Fig. 20(a) can therefore be approximated by the simpler network shown in Fig. 20(b), where the components are related to those of Fig. 20(a) as shown. It will be obvious that this simpler configuration will lead to somewhat increased non-linearity compared with the more complex circuit, the increase depending on the ratio of the time constants of the two differentiating sections of Fig. 20(a).

An alternative arrangement for the β network, occasionally more convenient in practice, is that of Fig. 21(a) which has a transfer characteristic identical with that of Fig. 20(a) when the components are related as shown. Using this form of the network we can position the shaping network following it to give the configuration of Fig. 21(b). The two cascade differentiating sections can then be combined as before to give the feedback network of Fig. 21(c).

The use of a feedback network which is the R-C complement of the equivalent anode load circuit to provide a feedback current is generally attributed to Blumlein⁶, and has been referred to by many writers (e.g. refs. 7, 8 and 9). This method of linearization has become very popular in recent years because it enables a useful feedback factor to be obtained over a single stage.

A practical problem with this type of feedback circuit is that of adding the feedback voltage to the input sawtooth. The simplest method is to use a resistive adder as shown in Fig. 22. This can often take the form of a potentiometer and thereby serve also as height control. The main disadvantage of this simple system is the attenuation of the input sawtooth. The feedback voltage is also attenuated, but this is not necessarily a disadvantage. It is shown in Section 4.1 that the non-linearity associated with the exponential input normally obtained from simple sawtooth generators leads to an optimum value for the gain reduction factor r . This optimum value is usually less than that obtained with 100 per cent feedback, and some attenuation in the feedback path is necessary if it is to be realized. The optimum value for r , r_{opt} , is

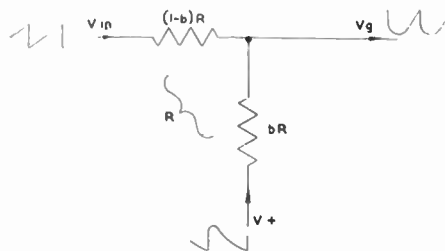


Fig. 22. Simple resistive adder for combining input sawtooth and feedback voltages.

dependent on the degree of attenuation of the input sawtooth, and to arrive at the exact values for r_{opt} and the tapping ratio involves a tedious process of successive approximation. However, it is rarely necessary to take this past the second stage of approximation to obtain satisfactory practical values, and the following procedure is usually satisfactory.

First, r_{opt} is obtained, as described in Section 4.1, assuming that the input sawtooth is not attenuated. Referring to Fig. 22, the grid input voltage is $bV_{in} - (1-b)V_f$, that is, the feedback voltage is attenuated by the factor $(1-b)$. The loop gain, if feedback is taken from the anode becomes $(1-b)g_m\eta R_2$ and

$$r = 1 + (1-b)g_m\eta R_2.$$

Now $g_m\eta R_2 (=G)$ is fixed and we obtain the value of b necessary to give the optimum value of r , r_{opt} , as

$$b = 1 - (r_{opt} - 1)/G. \quad \dots\dots(12)$$

This gives the first approximation for tapping ratio b of the resistive adder. To compensate for the attenuation of the input sawtooth its amplitude must be increased by the factor $1/b$ which will increase its slope non-linearity. If b approaches unity this increase can be ignored, but if b is much less than unity it will be possible to reduce the total non-linearity by altering the feedback factor r . To obtain the second approximation for b , r_{opt} is obtained as before using eqn. (17) but with the first term of this equation divided by the first value of b . This second value of r_{opt} is then to obtain the second value of b . If required, successive further approximations follow the same procedure.

An alternative to the resistive adder for combining feedback and input voltages is by using a "split" charging capacitor for the sawtooth generator, as shown in Fig. 23. The feedback voltage is developed across the bottom capacitor C_c' , and the sawtooth voltage across the top capacitor C_c . The bottom capacitor C_c' , forms with R_i the integrating section of the feedback network, the top capacitor often being considered as effectively in parallel with C_c' for the integrating process. This is, however, only strictly true when the loop gain is infinite, and analysis shows that when the loop gain is low the effect of R_c and C_c during scan on the

integrating action of C_c' and R_i is mainly dependent on the ratio R_c/R_i , their effect decreasing as this ratio increases. The converse effect of R_i and C_c' on the sawtooth generation process is to add to the sawtooth voltage developed across C_c , a sawtooth voltage approximately given by

$$\frac{V_s \cdot R_i}{R_c} (1 - e^{-t/R_i C_i});$$

which can again be reduced by a high value of R_c/R_i .

Difficulties arise during flyback when the discharging valve is connected across both capacitors, as shown in Fig. 23. The mechanism during flyback is mainly to re-distribute the charges on C_c and C_c' , instead of to discharge C_c . This greatly complicates analysis of the circuit and resort is invariably made to experiment for determination of the circuit values.

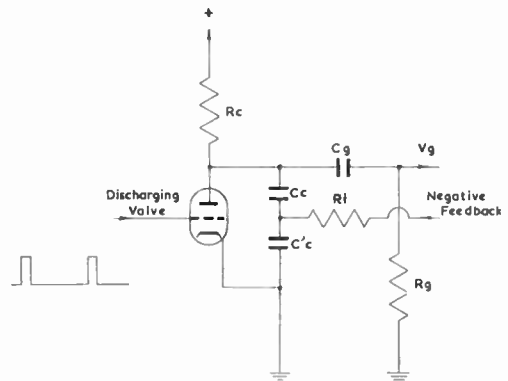


Fig. 23. Circuit showing the use of a "split" sawtooth generating capacitor for combining the feedback voltage with the generated sawtooth.

This method of combining the sawtooth and feedback voltages suffers from the disadvantage of being inherently less stable at low frequencies than the resistive adder. Its inferior stability arises because it possesses two more differentiator networks in the feedback loop than the resistive adder. One of these networks is necessary to provide a grid return for the valve and the other is formed by the components R_c and C_c . For this reason it is particularly important to investigate the stability of the feedback loop with this type of adder, and a Nyquist plot in the low frequency region is

desirable. An advantage of the capacitive adder is the low impedance of the combined output.

Many other feedback and combining circuit arrangements can be devised but for purposes of design they can be usually reduced to one of the cases discussed and treated accordingly.

3.4. Comparison of Linearization Methods

The preceding sections have shown that the two most important linearization methods are (i) that using the shaping network of Fig. 8 (or Fig. 12) in conjunction with a non-feedback amplifier and (ii) that using negative feedback proportional to the deflection current with an R-C differentiator network in the feedback path.

The performance of both these types is rather similar in that the deflection current can be given equal initial and final slopes when the linearizing network time-constant p , is chosen to satisfy either eqn. (5) or eqn. (9), as appropriate. The deflection current in this case is S-shaped and the point along the scan at which the maximum slope occurs is given by the curves of Figs. 10 and 18. The maximum non-linearity, defined by

$$\frac{\text{max. slope}}{\text{initial slope}} - 1$$

is given in Figs. 11 and 19. Before these curves can be compared directly it is necessary to relate the parameter a used in connection with method (i) to that r used in the analysis of method (ii). This can be done by reference to the overall gain of the amplifier and including the shaping network. The overall gain can be expressed in terms of the ratio of the peak-to-peak voltage across R_2 of Fig. 3(b) to the peak-to-peak input sawtooth, that is $i_{2(p-p)}R_2/\hat{V}$. We then obtain for the non-feedback amplifier (method (i))

$$i_{2(p-p)}R_2/\hat{V} = g_m \cdot \eta \cdot R_2 \cdot a \dots\dots\dots(13)$$

and for the feedback amplifier method (method (ii))

$$i_{2(p-p)}R_2/\hat{V} = g_m \cdot \eta \cdot R_2/r \dots\dots\dots(14)$$

when a single pentode stage is assumed. Provided that the anode load circuit and the valve are identical in each case the overall gain is proportional to a and $1/r$ respectively. Thus a feedback amplifier having a gain reduction factor r of, for example 3.0 (corresponding to loop gain of 2.0) has the same overall gain as a non-feedback amplifier using

a shaping network having $a=1/3$. It is interesting to note that the presence of the additional differentiating network in the feedback loop for linearization does not affect the overall gain of the amplifier as defined by eqn. (14).

Comparing now the curves of Figs. 11 and 19 we see that the feedback amplifier has substantially less non-linearity for equal values of a and $1/r$. Also, comparison of Figs. 10 and 18 reveals that the value of $(t/T)_{\text{max}}$ is much nearer to $\frac{1}{2}$ for the feedback amplifier, indicating better symmetry of the S-shaped deflection current. The superiority of the feedback amplifier is particularly marked for the higher values of r .

The feedback method also has the advantage of reducing

- (a) the influence of valve variability on performance,
- (b) the susceptibility to valve microphony,
- (c) the effect of hum generated within the feedback loop, and
- (d) the non-linearity due to the cathode bias and the grid coupling networks.

When feedback is taken from the anode some disadvantages are present and which are,

- (e) greater susceptibility to hum from the h.t. supply,
- (f) deflection current is dependent on the deflection coil resistance and, therefore, on their operating temperature,
- (g) the possibility of feeding line timebase pulses, picked up by the field deflection coils, back into the field sawtooth generator. This may impair the interlace.

Disadvantage (e) is most serious when it is necessary to operate the complete receiver from a mains supply unsynchronized to the transmitter. In such cases it is almost essential to include extra smoothing for the field timebase amplifier.

Due to the gradual reduction in cabinet size permitted by increased scanning angles, the temperature rise of the deflection coils is now often sufficient to cause a serious reduction in height during operation, and disadvantage (f) then assumes some importance. Compensation for this effect is possible by means of a

temperature-sensitive resistor. A popular method is to connect such an element in series with the deflection coils, and by the correct choice of initial resistance, material and mounting position the total resistance of the deflection circuit can be maintained substantially constant over the operating temperature range. However, some degradation in the power of efficiency of the output circuit is involved. An alternative method avoiding this defect and favoured some years ago, is to arrange for the input sawtooth drive to increase with temperature by using a temperature-sensitive resistor in the sawtooth input circuit.

4. Design Aspects

4.1. Non-linearity of the Input Sawtooth

The foregoing analysis has examined the performance of both feedback and non-feedback amplifiers on the basis of a linear input waveform and linear valve characteristics. In practice neither of these are strictly linear and their non-linearity can considerably modify the various effects previously discussed. First, consider the input wave.

and 12). It can be shown that the slope non-linearity is given by

$$100(1 - e^{-T/C'R'}) \text{ per cent}$$

where $R'C'$ is the time-constant of the charging resistor and capacitor. Furthermore, the peak-to-peak output voltage (assuming that the capacitor is completely discharged before the commencement of each charging period), expressed as a percentage of the steady applied potential, is also given by the same function. A curve of this is shown in Fig. 24. The slope non-linearity is thus directly related to the peak-to-peak output voltage (for a given supply potential) and any improvement in one aspect must be at the expense of the other.†

The non-linearity of the input sawtooth is a decisive factor in the overall non-linearity and it largely determines the choice of parameters for the linearization networks. In order to arrive at simple formulae for design purposes it will be assumed that the total non-linearity of the deflection current can be obtained by summing the individual contributions of the various sources of non-linearity.

The two main sources of non-linearity are,

- (a) the non-linearity of the input sawtooth and
- (b) the residual non-linearity of conventional shaping networks.

The non-linearity due to (a) can only be reduced at the expense of the peak-to-peak amplitude which will in turn demand more amplifier gain for a given output. Now the overall gain of a single pentode stage, in terms of the ratio of the peak-to-peak output to the peak-to-peak input is given by eqns. (13) and (14), and for given values of g_m , η and R_2 , can only be increased by either increasing a or reducing r for the relevant method of linearization. For a fixed value of m the curves of Figs. 11 and 19 show that this will increase the non-linearity of source (b). The converse also applies and it would be expected, in view of the shape of the curves that an optimum value of a or r will exist

† It is, of course, possible to incorporate an additional shaping network in the sawtooth generator itself and thereby secure an appreciable reduction in the non-linearity of the sawtooth output for a given peak-to-peak amplitude. This expedient is seldom used though, because it not only increases the circuit complexity, but also involves difficulties due to the loading effects of successive networks, which tends to reduce their effectiveness.

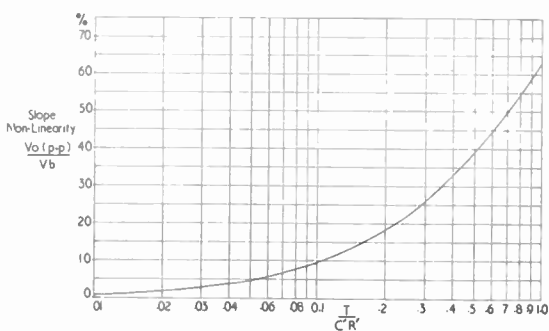


Fig. 24. Curve of the function $100(1 - e^{-T/C'R'})\%$, giving the slope non-linearity and the peak-to-peak output voltage as a fraction of the supply voltage for a simple resistance capacitance sawtooth generator of time constant $C'R'$.

As mentioned previously at the beginning of section 3, the input waveform is normally exponential, being obtained from the charging of a capacitor through a resistor with a steady applied potential. The slope of such a wave gradually decreases during the scan period and the non-linearity caused by this has been examined by many writers (e.g. refs. 10, 11,

giving the least total non-linearity of the deflection current, for a given value of basic gain ($g_m \cdot \eta \cdot R_2$), peak-to-peak output current and the supply voltage to the sawtooth charging network. The optimum value can be arrived at as follows, in the case of a feedback amplifier (the results apply equally well to the non-feedback amplifier if $1/a$ is substituted for r).

Rearranging eqn. (14)

$$\hat{V}/r = i_{2(p-p)}/g_m \cdot \eta = \text{a constant.} \dots\dots(15)$$

Now, as shown above, for a simple R-C sawtooth generator we may write

$$\text{slope non-linearity} = s = \hat{V}/V_s$$

where \hat{V} is the peak-to-peak sawtooth voltage developed and V_s the steady applied potential, so that eqn. (15) becomes after substituting for \hat{V}

$$s/r = i_{2(p-p)}/g_m \cdot \eta \cdot V_s = \text{constant} \dots\dots(16)$$

Furthermore, the residual non-linearity of the feedback amplifier is a function of m and r , but as m will be already fixed by the transformer and deflector coil design, it is, for the present purpose, a function of r only. We will accordingly express the residual non-linearity as $f(r)$. The total non-linearity is approximately, therefore,

$$\text{total non-linearity} = s + f(r).$$

Substituting for s from eqn. (16) we obtain

$$\text{total non-linearity} = \frac{i_{2(p-p)}}{g_m \cdot \eta \cdot V_s} \cdot r + f(r) \dots\dots(17)$$

The function $f(r)$ can be conveniently obtained from the curves of Fig. 19 for any particular value of m . The variation in the total non-linearity with r may be calculated from eqn. (17) and the optimum value for r deduced. Equation (15) may then be used to obtain the necessary peak-to-peak sawtooth input voltage.

4.2. The Effect of Valve Curvature

It is shown in Section 3.1 that the curvature of the valve characteristics contributes towards providing the correct anode current waveform.

This effect is beneficial in any amplifier regardless of the method used for linearization, and reduces the amount of shaping required; slightly modifying the theoretical values for the shaping network. However, in the case of a feedback amplifier some of its effect is lost because the feedback action tends to linearize the valve characteristic. This is advantageous in so far as it makes the assumption of a linear valve characteristic in the preceding theory more realistic.

4.3. Flat Face Distortion with Wide-angle Cathode-ray Tubes

It has been shown elsewhere¹³ that the deflection of the spot on a cathode-ray tube having a flat screen is not directly proportional to the deflection coil current. The resulting raster when the deflection current is linear exhibits progressive stretching towards the edges of the picture and the effect increases rapidly with the scanning angle. This non-linearity can be expressed in terms of the spot velocity produced by a linear deflection current as

$$\text{max. non-linearity} = \frac{\text{maximum velocity}}{\text{minimum velocity}} - 1.$$

The way in which this varies with the total deflection angle is given in Table 1.

Fortunately, the tube face is not quite flat and this reduces these figures somewhat. Also the deflection coils often compensate to some degree for the distortion, so that in practice the non-linearity is only about half that indicated in the table. The vertical deflection angles for the cathode-ray tubes in use at the present time are approximately

- 45° for a 70° diagonal angle,
- 62° for a 90° diagonal angle,
- 87° for a 110° diagonal angle.

It can be seen therefore that the effect is unlikely to be troublesome with a 70 deg tube but becomes increasingly important with 90 deg and 110 deg tubes. To counter this distortion

Table 1

Total deflection angle (degrees)	20	30	40	50	60	70	80	90	100
Max. non-linearity (%)	4.7	11	20	37	54	82.4	122	183	276

it is necessary for the deflection current to be S-shaped. The residual non-linearity of the two main linearizing methods has been shown to be of this form when the equal initial and final slope condition is satisfied. There is no guarantee that the precise shape of the curve is the same as that required, but, if the curve can be made reasonably symmetrical and has the necessary amount of non-linearity, it is to be expected that the discrepancy in shape will be a second-order effect, and can be ignored in an approximate treatment.

The performance of the two main linearizing methods discussed in Section 3.4. is given directly by the curves of Figs. 11 and 19 for the case of a linear sawtooth input, and from which we may estimate their potentialities in providing the necessary amount of non-linearity. Of equal importance is the symmetry of the deflection waveform and it is apparent that perfect symmetry only occurs as a limiting condition. For the purpose of comparing the amount and symmetry of the non-linearity using the curves it will be assumed that $m=2$ (i.e. the z.i.s. condition) for the anode circuit. Table 2 is then obtained.

It is clear from this Table that the non-linearity of the feedback amplifier is much less than that of the non-feedback type having an equivalent gain. In fact, alone it is insufficient to provide the required amount of non-linearity to compensate for the flat face distortion occurring with any diagonal deflection angle exceeding 70 deg, even with a feedback factor as low as 2. On the other hand, the non-feedback amplifier has inherently more dis-

tortion and would appear to be capable of providing sufficient correction alone for up to 90 deg tubes, although the symmetry becomes rather poor.

However, the non-linearity of the input sawtooth has been ignored and the time-constant of the sawtooth generator charging network can usually be chosen to supply the additional non-linearity that may be required with either method of linearization. It then becomes necessary to readjust the time-constant of the shaping network within the amplifier to restore the equal initial and final slope condition. This has the effect of moving the point of maximum slope slightly towards the end of scan, which is a desirable result, as the non-linearity of both types of amplifier otherwise occurs somewhat before halfway along the scan when the input sawtooth is linear. It is normally possible to introduce up to 50 per cent slope non-linearity in the input sawtooth before the asymmetry of the deflection current becomes serious. This corresponds to 100 per cent maximum non-linearity as defined above, and in conjunction with the residual non-linearity of the linearizing networks and that from other sources, should permit satisfactory correction for the flat face distortion of conventional cathode-ray tubes having diagonal deflection angles of up to, and somewhat beyond, 110 deg.

Should the linearity prove insufficient in a particular design it is possible to employ a non-linear resistor¹⁴. This also offers the advantage of rather more flexibility, although it does, of course, increase the circuit complexity.

Table 2

Non-feedback amplifier using the shaping network of Fig. 8. $m=2$

a	0.05	0.1	0.2	0.3	0.4	0.5
max. non-lin. %	2.5	5.2	13	23	38	60
$(t/T)_{min}$	0.425	0.41	0.40	0.38	0.37	0.34

Feedback amplifier using differentiator network for linearization. $m=2$

r	20	10	5	3.33	2.5	2.0
max. non-lin. %	0.5	0.5	3.0	8.0	17	29
$(t/T)_{min}$	0.497	0.492	0.482	0.466	0.44	0.42

5. Conclusion

An analysis has been made of conventional linearization methods which includes a quantitative treatment of their imperfections. In the case of those methods using some form of shaping network it has been shown that the deflection current becomes S-shaped under certain conditions, and the necessary relationships between the parameters has been derived.

The non-linearity of the sawtooth input to the amplifier is of exponential form when a simple sawtooth generator is used and the effect of this on the overall linearity has been considered. It has been shown that the presence of this non-linearity leads to an optimum value for the attenuation introduced by the linearization process and a design procedure to achieve the least possible overall non-linearity has been suggested.

The practicability of using the inherent non-linearity of the time base to correct for deflection distortion occurring with conventional wide-angle cathode-ray tubes has been considered, and it appears that this should be possible for total deflection angles of up to at least 110 deg.

6. Acknowledgments

The author wishes to express his thanks to Mr. D. W. Heightman and Mr. H. S. Wood for their interest and encouragement in the work on which this paper is based. The author's colleagues, Mr. D. B. Chapman and Mr. T. Bates, have rendered valuable assistance in discussing the theoretical aspects of the paper and providing experimental verification of the results. Finally, acknowledgment is due to the management of Messrs. Mains Radio Gramophones Limited, for permission to publish this paper and to Mrs. J. Taylor for helping in its preparation.

7. References

1. F. Kerkhof and W. Werner, "Television", p. 178, 1st English Edition Philips Technical Library (Cleaver Hume, London, 1952.)
2. W. T. Cocking, "Television Receiving Equipment", Appendix 5, 4th Edition (Iliffe, London, 1957).
3. E. T. Emms, "Theory and design of television frame output stages", *Electronic Engineering*, 24, pp. 96-101, March 1952.
4. K. Schlesinger, "Magnetic deflection of kinescopes", *Proc. Inst. Radio Engrs*, 35, p. 813, August 1947.
5. O. S. Puckle, "Time Bases", p. 122 et seq., 2nd Edition (Chapman & Hall, London, 1951).

6. A. D. Blumlein, British Patent No. 479113.
7. W. T. Cocking, "Negative feedback circuits" (editorial), *Wireless Engineer*, 28, p. 165, June 1951.
8. Puckle, *loc. cit.*, p. 137.
9. S. W. Amos and D. C. Birkinshaw, "Television Engineering—Vol. 4, General Circuit Techniques" p. 216, Appendix J (Iliffe, London, 1958).
10. Kerkhof and Werner, *loc. cit.*, p. 126.
11. S. W. Amos and D. C. Birkinshaw, "Television Engineering, Vol. 3, Waveform Generation", p. 172, Appendix C (Iliffe, London, 1957.)
12. B. Chance, and others, "Waveforms", p. 259 (McGraw-Hill, New York, 1949).
13. D. G. Fink, "Television Engineering Handbook", p. 6-3 (McGraw-Hill, New York, 1957).
14. B. G. Dammers, A. G. W. Uijtens, A. Boekhorst and H. Heyligers, "Improvements in television receivers—V. stabilization of the line and frame output circuits", *Electronic Applications Bulletin*, 18, No. 4, p. 140, 1957-58.

8. Appendix 1:

Limiting case for linearization by valve curvature alone with triode valve.

The condition for the grid voltage not to require a negative slope (i.e. having a minimum along the scan) will be when the load-line at start of scan has a common tangent with the valve $I_a - V_a$ characteristic.

The slope of the load line on the valve $I_a - V_a$ characteristic is

$$\frac{dV_a}{d(t/T)} / \frac{dI_a}{d(t/T)}$$

Now, referring to Fig. 3(b), $V_a = V_b - V_1$

Therefore,
$$\frac{dV_a}{dt} = -dV_1/dt$$

The equation to the anode current necessary to produce a linear deflection current, defined by $i_2 \left(2 \frac{t}{T} - 1 \right)$, when referred to the primary is,

$$I_a = i_2 \frac{R_2 T}{L_p} \left(\frac{t}{T} + \frac{L_p + L_2}{R_2 T} - \frac{1}{2} \right)^2 + I_m \dots \dots \dots (18)$$

where I_m is the minimum value of the anode current.

Also the equation for the primary voltage V_1 is

$$V_1 = R_p \cdot I_a + i_2 \cdot R_2 \left(2 \cdot \frac{t}{T} + 2 \cdot \frac{L_2}{R_2 T} - \right) \dots (19)$$

Differentiating these two equations and dividing we obtain

$$\frac{dV_1}{d(t/T)} \bigg/ \frac{dI_a}{d(t/T)} = R_p + T \frac{L_p}{\left(t/T + \frac{L_p + L_2}{R_2 T} - \frac{1}{2} \right)}$$

Putting $(t/T) = 0$ and $\frac{dV_1}{d(t/T)} = - \frac{dV_a}{d(t/T)}$

we finally obtain

$$\frac{\frac{dV_a}{d(t/T)}}{\frac{dI_a}{d(t/T)}}(0) = - \left[R_p + \frac{L_p}{T \left(\frac{L_p + L_2}{R_2 T} - \frac{1}{2} \right)} \right] \dots(21)$$

In this equation we have three cases:

- (i) when $\frac{L_p + L_2}{R_2 T} < \frac{1}{2}$, the second term is negative.
- (ii) when $\frac{L_p + L_2}{R_2 T} = \frac{1}{2}$, the second term is infinite and the loadline at the start of scan is parallel to the V_a axis, touching the line $I_a = I_m$

and

- (iii) when $\frac{L_p + L_2}{R_2 T} > \frac{1}{2}$, the second term is positive.

The second term will always exceed the first (R_p) so that the sign of eqn.(20) is determined by the second term.

Thus, for the preceding three cases at the start of scan,

- (i) $\frac{L_p + L_2}{R_2 T} < \frac{1}{2}$; $\frac{dV_a/d(t/T)}{dI_a/d(t/T)}(0)$ is positive and the load line curves back, presenting a negative resistance to the valve.
- (ii) $\frac{L_p + L_2}{R_2 T} = \frac{1}{2}$; $\frac{dV_a/d(t/T)}{dI_a/d(t/T)}(0)$ is infinite and the loadline is parallel to V_a axis.
- (iii) $\frac{L_p + L_2}{R_2 T} > \frac{1}{2}$; $\frac{dV_a/d(t/T)}{dI_a/d(t/T)}(0)$ is negative and the load line presents a positive resistance to the valve.

The required limiting condition for the grid voltage not to have a minimum along scan is when

$$- \left(R_p + \frac{L_p}{T \left(\frac{L_p + L_2}{R_2 T} - \frac{1}{2} \right)} \right) = R_a$$

or

$$\frac{L_p}{T \left(\frac{1}{2} - \frac{L_p + L_2}{R_2 T} \right)} = R_a + R_p \dots\dots\dots(22)$$

The factor $(L_p + L_2)/R_2 T$ when expressed in terms of the secondary circuit constants becomes $(L_s + L_c)/T(R_s + R_c)$, giving the limiting condition as

$$L_p = T(R_a + R_p) \left(\frac{1}{2} - \frac{L_s + L_c}{T(R_s + R_c)} \right) \dots(23)$$

9. Appendix 2:

Deflector coil waveform resulting from an input derived from the shaping network of Fig. 8.

Referring to Fig. 3(b), the relationship between I_a and i_2 is given by the differential equation.

$$L_p \cdot \frac{dI_a}{dt} = R_2 \cdot i_2 + (L_2 + L_p) \cdot \frac{di_2}{dt} \dots(34)$$

Changing the variable to t/T we have

$$L_p \cdot \frac{dI_a}{d(t/T)} = R_2 T \cdot i_2 + (L_2 + L_p) \cdot \frac{di_2}{d(t/T)}$$

Putting $t/T = x$, $R_2/T(L_2 + L_p) = m$ and $L_p/(L_2 + L_p) = \gamma$, the equation becomes

$$\frac{di_2}{dx} + m \cdot i_2 = \gamma \cdot \frac{dI_a}{dx} \dots\dots\dots(25)$$

We will assume that $I_a = g_m V_g$.

From eqn.(1) we have the expression for the input waveform as

$$\frac{V_o}{V} = (1-a) \cdot \frac{e^{-px}}{(1-e^{-p})} + x \frac{(1-a)}{p}$$

where $p = T/CR$

The differential equation (25) now becomes

$$\frac{di_2}{dx} + m \cdot i_2 = g_m \cdot \gamma \cdot V \left[\frac{(1-a)}{(1-e^{-p})} (-p) \cdot e^{-px} + 1 \right]$$

Using integrating factor e^{mx} we obtain

$$i_2 = g_m \cdot \gamma \cdot V \left[\frac{1}{m} - \frac{(1-a)}{(1-e^{-p})} \frac{pe^{-px}}{(m-p)} \right]$$

This solution is the particular integral; the complementary function is $i_2 = Ae^{-mx}$, giving the complete solution as

$$i_2 = g_m \cdot \tau_1 \cdot \hat{V} \left[\frac{1}{m} - \frac{(1-a)pe^{-px}}{(1-e^{-p})(m-p)} + B \cdot e^{-mx} \right]$$

Using the condition that $\int_0^1 i_2 dx = 0$, we obtain

$$B = \frac{m}{(1-e^{-m})} \left[\frac{(1-a)}{(m-p)} - \frac{1}{m} \right]$$

and the complete solution is then,

$$i_2 = g_m \cdot \tau_1 \cdot \hat{V} \left\{ \frac{1}{m} \left[1 - \frac{me^{-mx}}{1-e^{-m}} \right] + \frac{1-a}{m-p} \left[\frac{me^{-mx}}{1-e^{-m}} - \frac{pe^{-px}}{1-e^{-p}} \right] \right\} \dots\dots\dots(26)$$

When $m = p$, this becomes

$$i_2 = g_m \cdot \tau_1 \cdot \hat{V} \left\{ \frac{1}{m} \left[1 - \frac{me^{-mx}}{1-e^{-m}} \right] + \frac{m(1-a)e^{-mx}}{(1-e^{-m})^2} \cdot (x+e^{-m} \cdot [1-x]) \right\} \dots\dots\dots(27)$$

The slope of i_2 according to eqn.(26) is

$$\frac{di_2}{dx} = g_m \cdot \tau_1 \cdot \hat{V} \left[\frac{me^{-mx}}{1-e^{-m}} - \frac{(1-a)}{(m-p)} \left(\frac{m^2e^{-mx}}{1-e^{-m}} - \frac{p^2e^{-px}}{1-e^{-p}} \right) \right] \dots\dots\dots(28)$$

When $x = 0$, this becomes

$$\frac{di_2}{dx}(0) = g_m \cdot \tau_1 \cdot \hat{V} \left[\frac{m}{1-e^{-m}} - \frac{(1-a)}{(m-p)} \left(\frac{m^2}{1-e^{-m}} - \frac{p^2}{1-e^{-p}} \right) \right]$$

and when $x = 1$, it becomes

$$\frac{di_2}{dx}(1) = g_m \cdot \tau_1 \cdot \hat{V} \left[\frac{me^{-m}}{1-e^{-m}} - \frac{(1-a)}{(m-p)} \left(\frac{m^2e^{-m}}{1-e^{-m}} - \frac{p^2e^{-p}}{1-e^{-p}} \right) \right]$$

The difference in slope between $di_2/dx(0)$ and $di_2/dx(1)$ may be shown to be zero when

$$m = (1-a)(m+p)$$

i.e. when $a = \frac{p}{p+m}$ or $p = \frac{am}{(1-a)}$

The point of maximum slope of i_2 (eqn.26) is obtained by equating the second differential to zero.

Denoting the time at which the maximum slope occurs by x_{max} we obtain

$$e^{(m-p)x_{max}} = \left(\frac{1-e^{-p}}{1-e^{-m}} \right) \frac{m^2}{p^3} \cdot \left(\frac{p-am}{1-a} \right) \dots(29)$$

If the condition for zero slope non-linearity above is satisfied, then eqn.(29) yields

$$x_{max} = \left(\frac{t}{T} \right)_{max} = \frac{1}{(m-p)} \cdot \log_e \frac{(1-e^{-p})m}{(1-e^{-m})p}$$

Substituting this condition back in eqn.(28) gives the maximum slope as

$$\frac{di_2}{dx}(\max) = \frac{g_m \cdot \tau_1 \cdot \hat{V} \cdot ame^{-mx_{max}}}{1-e^{-m}} \dots(30)$$

and the initial and final slopes as

$$\frac{di_2}{dx}(0) = \frac{di_2}{dx}(1) = g_m \cdot \tau_1 \cdot \hat{V} \left[\frac{m}{1-e^{-m}} - \frac{(1-a)}{(m-p)} \left(\frac{m^2}{1-e^{-m}} - \frac{p^2}{1-e^{-p}} \right) \right]$$

The non-linearity expressed as the difference between the maximum and initial slopes relative to the initial slope, here termed the 'maximum non-linearity', is given by

max. non-linearity =

$$\frac{ame^{-mx_{max}}}{(1-e^{-m}) \left[\frac{m}{1-e^{-m}} - \frac{(1-a)}{(m-p)} \left(\frac{m^2}{1-e^{-m}} - \frac{p^2}{1-e^{-p}} \right) \right]} - 1$$

This equation does not readily lend itself for computation by slide rule, but it can be brought into the following form, which is more suitable for this purpose:

max. non-linearity

$$= \frac{(1-2a)(1-e^{-p})e^{-mx_{max}}}{a(e^{-p}-e^{-m})} - 1$$

10. Appendix 3:

Deflector coil waveform produced by a feedback amplifier incorporating a differentiator network in the feedback path.

Referring to Fig. 15(c) we have

$$V_g = V_{in} - V_f' \dots\dots\dots(31)$$

The differential equation for the β circuit is

$$\frac{di_2}{dx} + m \cdot i_2 = \tau_1 \cdot \frac{dI_a}{dx} \dots\dots\dots(32)$$

Substituting $i_2 = V_f/zR_2$, $I_a = g_m V_g$ and $g_m R_2 \eta = G$, and for V_g from (31) we have

$$\frac{dV_f}{dx} + mV_f = zG \left(\frac{dV_{in}}{dx} - \frac{dV_f'}{dx} \right) \dots\dots(33)$$

The differential equation for the shaping network of Fig. 17, is, using the notation of Figs. 15(c) and 17,

$$\frac{dV_f'}{dx} + pV_f' = \frac{dV_f}{dx} \dots\dots\dots(34)$$

Putting eqns.(33) and (34) into operational form and substituting $V_{in} = x \cdot \hat{V}$ we obtain

$$(D+m)V_f + z \cdot G \cdot D V_f' = z \cdot G \cdot \hat{V} \dots\dots\dots(35)$$

and

$$D V_f - (D+p)V_f' = 0 \dots\dots\dots(36)$$

Eliminating V_f' between these two equations yields

$$\left[D^2 + \left(\frac{p+m}{r} \right) \cdot D + \frac{pm}{r} \right] V_f = \frac{zpG\hat{V}}{r} \dots\dots\dots(37)$$

where $r = 1 + zG$.

The solution of this equation is

$$V_f = \frac{zG\hat{V}}{m} \left(1 + A e^{\lambda_1 x} + B e^{\lambda_2 x} \right) \dots\dots\dots(38)$$

where λ_1 and λ_2 are the roots of the auxiliary equation

$$\lambda^2 + \left(\frac{p+m}{r} \right) \lambda + \frac{pm}{r} = 0 \dots\dots\dots(39)$$

Similarly by eliminating V_f between eqns.(35) and (36) we obtain

$$\left[D^2 + \left(\frac{p+m}{r} \right) D + \frac{mp}{r} \right] V_f' = 0 \dots\dots\dots(40)$$

The solution of which is

$$V_f' = E \cdot e^{\lambda_1 x} + F e^{\lambda_2 x} \dots\dots\dots(41)$$

where λ_1 and λ_2 are again the roots of eqn.(39).

The constants E and F are related to A and B , substitution for V_f and V_f' in eqn.(36) yielding

$$E = \frac{zG\hat{V}}{m} \left(\frac{\lambda_1}{\lambda_1+p} \right) \cdot A \text{ and } F = \frac{zG\hat{V}}{m} \left(\frac{\lambda_2}{\lambda_2+p} \right) \cdot B$$

so that eqn.(41) becomes

$$V_f' = \frac{zG\hat{V}}{m} \left[A \left(\frac{\lambda_1}{\lambda_1+p} \right) \cdot e^{\lambda_1 x} + B \left(\frac{\lambda_2}{\lambda_2+p} \right) \cdot e^{\lambda_2 x} \right] \dots\dots\dots(42)$$

The constants A and B in the solutions for V_f and V_f' are determined from the known conditions within the network, which are:

that the charge upon C cannot change during flyback;

and: that the anode current during flyback divides between L_p and L_2 in inverse proportion to their inductances.

These two conditions can be expressed as

$$V_f'(1) - V_f'(0) = V_f(1) - V_f(0), \text{ and}$$

$$V_f(1) - V_f(0) = zG\hat{V} - zG[V_f'(1) - V_f'(0)]$$

From these two conditions we obtain

$$A = - \frac{m(\lambda_1+p)}{r(\lambda_1-\lambda_2)(1-e^{\lambda_1})};$$

$$B = \frac{m(\lambda_2+p)}{r(\lambda_1-\lambda_2)(1-e^{\lambda_2})}$$

$$V_f = \frac{zG\hat{V}}{m} \left[1 - \frac{m(\lambda_1+p)e^{\lambda_1 x}}{r(\lambda_1-\lambda_2)(1-e^{\lambda_1})} + \frac{m(\lambda_2+p)e^{\lambda_2 x}}{r(\lambda_1-\lambda_2)(1-e^{\lambda_2})} \right] \dots\dots\dots(43)$$

and

$$V_f' = zG\hat{V} \left[1 - \frac{\lambda_1 e^{\lambda_1 x}}{(\lambda_1-\lambda_2)(1-e^{\lambda_1})} - \frac{\lambda_2 e^{\lambda_2 x}}{(\lambda_1-\lambda_2)(1-e^{\lambda_2})} \right]$$

By differentiating eqn.(4) with respect to x and setting $[dV_f/dx](1) = [dV_f/dx](0)$ we obtain the condition for zero slope non-linearity as

$$p = \frac{m}{r-1} \dots\dots\dots(44)$$

This condition will be assumed to be satisfied in all the following treatment. The auxiliary equation (39) thus becomes

$$\lambda^2 + \left(\frac{m}{r-1} \right) \lambda + \frac{m^2}{r-1} = 0 \dots\dots\dots(45)$$

The roots λ_1 and λ_2 of this equation are

$$\lambda_1 ; \lambda_2 = -\frac{p}{2} \pm \frac{p}{2} \sqrt{\frac{4}{r} - 3} \dots\dots\dots(46)$$

From this it will be seen that the roots are complex if $r > 4/3$. This inequality is always satisfied in practice so that we shall express the roots as

$$\lambda_1 = u + jv \text{ and } \lambda_2 = u - jv \dots\dots\dots(47)$$

where from (46)

$$u = -\frac{p}{2} \quad \text{and} \quad v = \frac{p}{2} \sqrt{3 - \frac{4}{r}} \quad \dots(48)$$

both u and v being real.

The coefficients A and B now assume conjugate complex forms and the solution for V_f may be written as

$$V_f = \frac{zG\hat{V}}{m} \left\{ 1 + e^{ux} [P \cos vx + Q \sin vx] \right\} \dots(49)$$

where

$$P = -\frac{m}{rv} \left[\frac{v(1 - e^u \cos v) + e^u(u+p) \sin v}{(1 - e^u \cos v)^2 + e^{2u} \sin^2 v} \right]$$

$$Q = -\frac{m}{rv} \left[\frac{(u+p)(1 - e^u \cos v) - ve^u \sin v}{(1 - e^u \cos v)^2 + e^{2u} \sin^2 v} \right]$$

By setting the initial and final slopes equal we obtain

$$\frac{Qu - Pv}{Pu + Qv} = \frac{1 - e^u \cos v}{e^u \sin v} \quad \dots\dots\dots(50)$$

The point, $(t/T)_{\max}$, of maximum slope for V_f is found by equating the second differential of V_f to zero, when we obtain

$$\tan v \left(\frac{t}{T} \right)_{\max} = -\frac{u(Pu + Qv) + v(Qu - Pv)}{u(Qu - Pv) - v(Pu + Qv)} \quad \dots\dots\dots(51)$$

Using eqn.(50) to eliminate terms containing P and Q yields

$$\tan v \left(\frac{t}{T} \right)_{\max} = \frac{u \sin v - v \cos v + ve^{-u}}{v \sin v + u \cos v - ue^{-u}} \quad \dots(52)$$

The maximum slope $\frac{dV_f}{dx}(\max)$ is found to be

$$\frac{dV_f}{dx}(\max) = \frac{zG\hat{V}}{m} e^{u(t/T)_{\max}} \left\{ [Pu + Qv] \cos v(t/T)_{\max} + [Qu - Pv] \sin v(t/T)_{\max} \right\}$$

and the initial slope $\frac{dV_f}{dx}(0)$ (also equal to the final slope when eqn.(44) is satisfied),

$$\frac{dV_f}{dx}(0) = \frac{zG\hat{V}}{m} (Pu + Qv)$$

The maximum non-linearity is

$$\frac{\frac{dV_f}{dx}(\max) - \frac{dV_f}{dx}(0)}{\frac{dV_f}{dx}(0)} = \frac{\frac{dV_f}{dx}(\max)}{\frac{dV_f}{dx}(0)} - 1$$

which becomes, using the expressions above for $\frac{dV_f}{dx}(\max)$ and $\frac{dV_f}{dx}(0)$, and using eqn.(50)

$$\begin{aligned} \text{max. non-lin} &= e^{u(t/T)_{\max}} \left\{ \cos v \left(\frac{t}{T} \right)_{\max} + \left(\frac{e^{-u} - \cos v}{\sin v} \right) \sin v \left(\frac{t}{T} \right)_{\max} \right\} - 1 \quad \dots(53) \end{aligned}$$

When u and v are small we may use the first few terms of the series for sine, cosine, tangent and the exponential in expression (52) which, after neglecting the higher powers, becomes

$$\left(\frac{t}{T} \right)_{\max} = \frac{1}{3} \left(\frac{3-u}{2-u} \right) = \frac{1}{2} \left(\frac{1-u/3}{1-u/2} \right)$$

This shows that, as u tends to zero, $(t/T)_{\max}$ tends to $\frac{1}{2}$, and the waveform of V_f becomes symmetrical.

NEW BRITISH STANDARDS

The following is a selection of the new and revised British Standards on subjects of interest to members which have been issued during recent months. The Brit.I.R.E. has been represented on the Technical Committees concerned with preparation of those Standards marked with an asterisk(*). Copies of the Standards may be obtained from B.S.I., Sales Branch, 2 Park Street, London, W.1., at the prices indicated.

B.S. 397:1960. Primary cells and batteries. Price 15s.

The latest revision of B.S. 397: 1946, "Leclanché type primary cells and batteries," has been expanded to include also revisions of B.S. 966: 1951, "Batteries for valve-type hearing aids" and B.S. 1766: 1951, "Dry batteries for domestic radio receivers," which have now been withdrawn. The new standard differs from the previous editions in that it specifies discharge tests for hearing-aid batteries and introduces mercury cells. A change which will be noticed by almost all the users of batteries for cycles, pocket lamps, etc., is that the familiar numbering system by which the cells are identified has been changed to bring it into line with an internationally agreed system.

B.S. 397 deals with primary cells and batteries for general industrial and domestic applications. Performance tests, dimensions, nominal voltages and designations for dry batteries and cells are specified, together with requirements for wet cells. Also included in the 56 pp. illustrated publication are appendices giving guidance on the allocation of sockets for new designs of batteries (not yet standardized) and approximate British and American equivalents of cells and batteries which have been standardized internationally.

B.S. 448: 1959. Electronic-valve bases, caps and holders. Section B5B/F.* Price 2s.

This document specifies the dimensions of the B5B/F valve base and outline. It replaces Section B5B of B.S. 448: 1953.

B.S. 1568:1960. Magnetic tape sound recording and reproduction. Price 4s. 6d.

This 16-page publication incorporates two revised specifications: B.S. 1568, "Magnetic tape sound recording and reproduction," and B.S. 2478 (the standard for tapes and spools for commercial and domestic magnetic tape sound recording and reproduction—issued in 1954, and now withdrawn).

The new standard deals with the essential features of recording on magnetic tape coated on one side only. It also specifies features of the tape itself and of the associated recording and reproduction equipment which are necessary to ensure satisfactory interchangeability. It applies to single-track and two-track recordings, the latter being either single-channel or stereophonic.

The specification clauses deal with: dimensions of tape; tape-winding; identification of recorded side of tape and of recorded tapes; colour codes for leaders; tape speed; spools; position and dimensions of magnetic sound tracks; recording characteristic; tolerances on recorded levels; tolerances for reproducing equipment. There are four diagrams.

B.S. 2133A: 1960. Fixed ceramic-dielectric capacitors Grade 1 for use in telecommunication and allied electronic equipment. Grade 1: General requirements and tests.* Price 12s. 6d.

This new standard deals with capacitors which are suitable for use in tuned circuits or in any other application where low loss and stability of capacitance are essential. They are for radio-frequency currents not exceeding 1 ampere or a reactive power not exceeding 200 VAR and having a nominal temperature co-efficient not exceeding 1,500 parts per million. They are not intended for radio interference suppression nor for isolation purposes in telecommunication equipment. (Dealt with in B.S. 613 and B.S. 415.)

Part 1 includes a series of mechanical robustness and climatic and durability tests for the capacitors together with colour codes for indicating capacitance value, tolerance and temperature co-efficient. Part 2 of B.S. 2133A, comprising a list of standard sizes, ratings, etc., will be published in due course.

B.S. 3146: Part 1: 1959. Investment castings in metal. Part 1: Carbon and low alloy steels. Price 6s.

The facility with which complex shapes can be accurately produced without expensive or difficult machining is the reason for the rapid growth in popularity of investment casting. The first part of a new British Standard for investment castings in metal has now been produced to fulfil the needs of industry in this expanding field.

Castings made from carbon and low alloy steels are the subject of the first part; further parts to be published later will deal with higher alloy steels and special temperature steels. Castings of the type specified in this new publication are those whose manufacture involves the investment of an expendable pattern by refractory slurry; castings by the shell moulding process are thus excluded.

B.S. 3234: 1960. Polythene insulation and sheath of electric cables. Price 4s.

This new British Standard is the third in the series dealing with various kinds of insulation and sheath for electric cables (the other two were B.S. 2746, dealing with PVC, and B.S. 2899, dealing with rubber). Three main kinds of polythene compound are recognized, and these are sub-divided into ten types, distinguished by the presence or absence of polyisobutylene (or butyl rubber) and carbon black. Tests are specified for melt flow index, tensile stress and elongation at break, power factor and permittivity, carbon black content and dispersion, residual antioxidant, polyisobutylene or butyl rubber content, and colour stability. The requirements of the new standard relate to samples taken from the finished cable.

Video-Frequency Equipment for Television Centres of the Soviet Union†

by

B. A. BERLIN ‡

A paper presented on 1st July 1959 during the Institution's Convention in Cambridge.

Summary : Details are given of the present state of the television broadcasting network and the proposals for its extension over the next seven years. A brief classification of the equipment for television centres is given in accordance with its programme potentialities. A new television equipment designed for mass production is briefly described. Technical performances of television cameras are discussed and the reasons for certain principles adopted in their design are outlined.

1. The Present Equipment

The past five years have been marked by a rapid growth of the television broadcasting network in the U.S.S.R. Whereas in 1953 there were only three television centres in the Soviet Union (in Moscow, Leningrad and Kiev) their number had increased to sixty by the end of 1958.

equipment rooms (depending on the number of channels). Fig. 1 shows part of the video equipment at a typical television operating centre having eight camera channels.

Two camera channels with super-iconoscope television cameras are used for motion-picture transmission as well as for the transmission of captions and slides (stationary pictures) from a

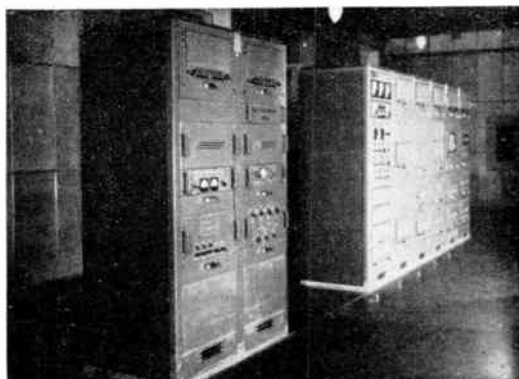
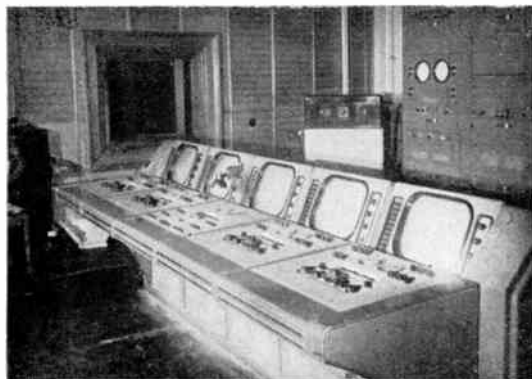


Fig. 1. Equipment room of a television operating centre. The equipment shown is now in operation at the majority of television centres of the Soviet Union.

All these centres (except those in Moscow and Leningrad) have standard equipment comprising two to eight camera channels with one or two

slide projector. The other channels with similar cameras are used for transmissions from one or two studios depending on the number of available channels and studio dimensions.

† Manuscript received 1st July, 1959 (Paper No. 557.)

‡ State Committee for Radio Electronics, Moscow. U.D.C. No. 621.397.712(47)

Telefilm projectors with pulse brightening during the frame fly-back time are used for motion-picture projection.

Most of the programme centres are provided with mobile transmitter units for outside broadcasts. These units are equipped with television camera tubes of the image orthicon type, one of which is shown in Fig. 2.



Fig. 2. An image orthicon camera for outside broadcasts. The controls placed below in the rear part of the camera serve for lifting and lowering the mount (when the camera is installed on a special mount) and for optical focusing. The position of controls facilitates the operator's work during panning shots.

2. New Construction Techniques

The network of existing programme television centres constitutes the basis for the further extension of television over the vast territory of the Soviet Union. New transmitting equipment has now been manufactured which is being installed at all newly-built television centres as well as at centres which are being reconstructed and extended.

The distinguishing feature of this new equipment is a new basic construction which provides a technological versatility and cheapness in mass production. It also incorporates a number of circuit improvements which tend to raise the quality of transmitted images and to widen the programme potentialities. The basic elements of this construction are an assembly rack or container shown in Fig. 3 and a light metal cast

carcase of the unit shown in Fig. 4. The inter-unit wiring is built into the carcase and terminating plugs or sockets are provided. The necessary electrical units are installed in the rack and connected by means of flexible connectors. A typical unit is shown in Fig. 5.

The new construction enables the television centres of our cities to be supplied with equipment for different numbers of camera channels (from two to eighteen channels) depending on the local requirements. The number of theatres and other places of entertainment in every city is such that local programmes differing in composition are possible. These considerations were taken into account in designing the equipment.

3. Extending the Network of Television Centres

The equipment supplied to television centres may be classified according to its programme potentialities.

A multi-programme television centre may be defined as one that is equipped for simultaneous transmission of two or more programmes, one

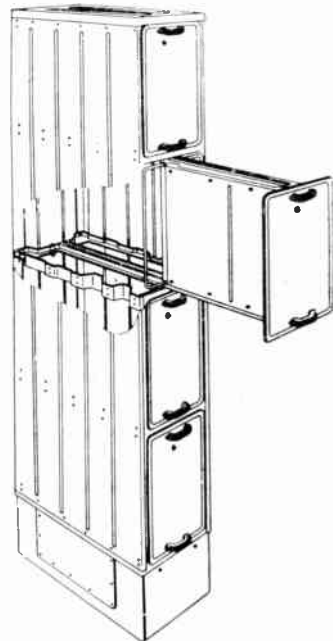


Fig. 3. Basic construction of an assembly rack with one unit withdrawn.

of which is a colour television programme from a studio, as well as for the recording of programmes by means of filming from a kinescope screen. Such centres have several studios and film projection rooms, a network of permanent outside broadcast points located in theatres or at stadiums, and a group of mobile camera channels and radio link equipment.

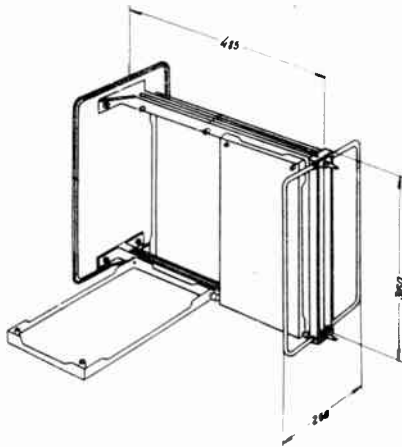


Fig. 4. Light metal cast carcase of a typical unit. Dimensions are in millimetres.

There is an inter-city (trunk) transmission equipment room at a multi-programme television centre in which demodulation and preliminary switching of signals coming from microwave radio links and cable communication links is accomplished. If necessary, the number of such communication links may amount to eighteen.

Multi-programme television centres are designed for such cities as Moscow and Leningrad and for certain capitals of the Union republics.

As follows from its name, a single programme television centre ensures the transmission of no more than one programme. Provision is also made at single programme television centres for switching in film equipment, for the transmission of outside broadcasts, etc.

Finally, there are relay (repeating) television stations designed for the re-transmission of programmes coming from a microwave radio link or a cable link. The equipment of a

repeating station is arranged to be suitable for the inclusion of news from a local studio or a programme of telecasts from an outside broadcast unit.

Over the next seven years a hundred television operating centres will be built in the Soviet Union. These will be mainly repeating centres, since all the capitals of the Union republics as well as the majority of large cities of the country already have their own television operating centres. During the same period many existing operating centres will be reconstructed to enable them to handle more ambitious programmes.

4. Studio Centre Equipment

New television transmitting equipment which has been produced by the industry since 1958 is suitable for simultaneously handling signals coming from a studio, from an outside broadcast unit, or from an inter-city transmission equipment room. This is provided for both by the switching system and by means of a new synchronizing generator designed for operation in a centralized synchronization system.

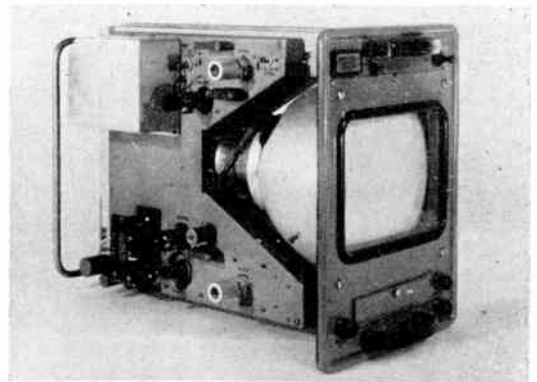


Fig. 5. Display monitor unit.

A general idea of the new equipment may be obtained from Fig. 6 and Fig. 7 which show respectively the equipment room and motion-picture projection room of a four channel television centre. In designing the equipment, special attention has been paid to the provision of accommodation and facilities for the work of

the programme and technical personnel of the television operating centre. This was achieved by reducing to a minimum the number of units in the director's and sound mixer's control board as can be seen from Fig. 8. The director's board is located in a separate room adjacent to the studio and contains all necessary switching controls. No valves are used in the control and

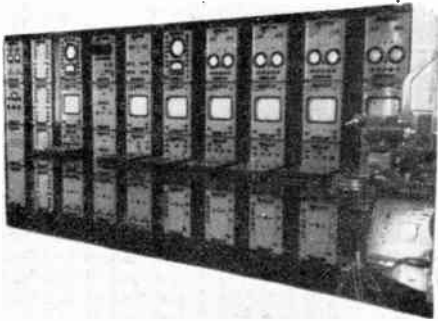


Fig. 6. General view of a four-channel television centre equipment room with new equipment.

signalling devices and the switched signals as such do not enter the director's compartment. The transmitted programme and video-frequency signals are viewed on the display monitors.

An additional feature of the new equipment is its versatility of application. Based on the units previously developed for the so-called small television centre for four camera channels, a whole complex of equipment for different applications has been created. These basic units constitute in fact as much as forty per cent of the total equipment for colour television

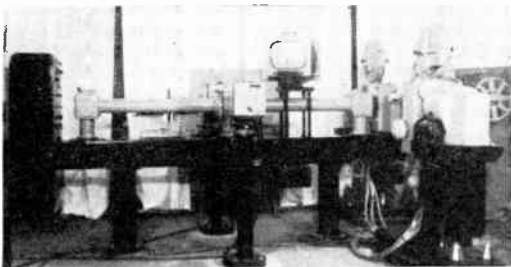


Fig. 7. Film projection room of a four-channel television centre.

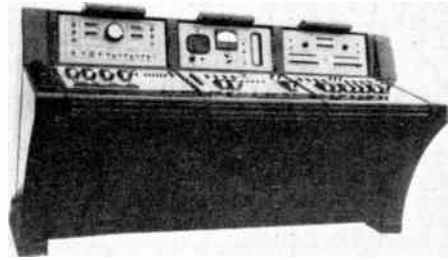


Fig. 8. Director's and sound mixers' control board.

centres and about ninety per cent of the complete equipment for outside broadcast units. An outside broadcast vehicle fitted with the new equipment is shown in Fig. 9. The same units are used in fixed radio links employed for communication between the studio and the transmitter, and in test and measuring devices designed for the manufacturers of colour and monochrome television receivers, etc.

Because of the versatility of the new equipment the camera channel rack can be used with any of the new cameras irrespective of whether they employ a super-iconoscope, an image orthicon or a vidicon tube. No modifications are needed and the same control knobs may be used for remote control of the camera tube operating conditions.

5. Camera Techniques

New television cameras using super-iconoscopes with an additional photo-cathode and studio or outside broadcast image orthicons have the same standard construction but different circuits for the units peculiar to the different types of camera tubes. Figure 10 illustrates a new image orthicon television camera designed for use in outside broadcasts and in studios. The cameras are equipped with the objectives specially designed for use in television which have focal lengths ranging from 29 mm to 1000 mm (relative apertures 2.8 to 8 respectively). In designing these objectives special attention has been paid to lens power and resolving power over the entire image field. These objectives have a resolving power of at least forty lines per mm in the centre of the image field and eighteen to twenty lines per mm at the edges.



Fig. 9. Outside broadcast vehicle fitted with new equipment.

To obtain effective optical focusing of the image under the conditions of rapid changes of the distance of the object, it was found necessary to retain the identical number of revolutions of focusing control when objectives with different focal lengths are set in the operating position on the turret. Moreover, it is desirable to have the optical image on the television camera tube photo-cathode kept in focus with the objectives with different focal lengths, that is, to have automatic focus adjustment. In the cameras which were formerly produced for studios, this problem was solved by a system of mechanical pushers and eccentrics. However, owing to the increasing number of objectives included in the complete television camera set and the great range of focal lengths, an electro-mechanical drive with a selsyn follow-up system is used for optical focusing in new cameras. In these focusing is effected by rotating a potentiometer control brought out to the side wall of the camera casing.

The cameras also have additional controls for camera mount adjustment and for optical focusing adjustment; these controls may be used at the operator's will when the cameras are installed on portable or automotive camera mounts. Additional controls are placed on the bottom and on the rear end of the camera. Thus a better manoeuvrability of mounted television cameras may be obtained. To save time in replacing an operating objective and to reduce camera weight a manual drive for the objective replacing gear is provided.

The adjustment of camera illuminating conditions is accomplished remotely from the

camera channel control board. This is achieved by means of a disc placed between the photo-cathode and the objective which enables a continuous variation of the light transmission coefficient. This method has an advantage over the previously used method of diaphragming the objective in which the operator could not stress the most important detail in a transmitted field (image) by means of defocusing the background.

To provide high quality checking of the transmitted image a video-signal from the i.f. amplifier output is applied to the camera viewfinders. For example, the operator may observe the mixer output signal on the camera viewfinder when transmissions are made with mixing video signals from two or more sources and use is made of the electric effect unit. This is necessary to enable the operator to secure and maintain the correct matching of mixed images.

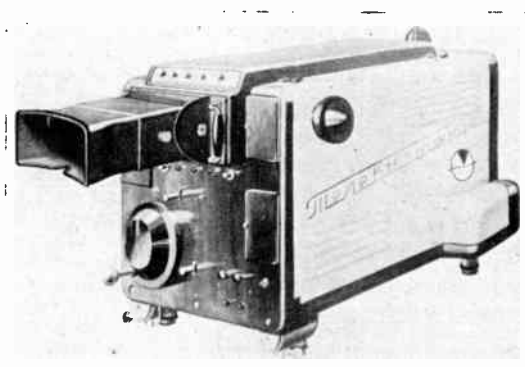


Fig. 10. A new image orthicon camera designed for use in outside broadcasts and studios. A super-icoscope camera with additional photo-cathode designed for transmissions from studios is produced in the same constructional form.

An electronic scaling device is used in the image orthicon camera which allows the operator to make instant changes in the transmitted image scale in proportion of 1.4:1 and 1.8:1 by pressing a button. The scaling is effected by changing the image transition ratio from the photo-cathode to the image orthicon target, i.e. by switching in an additional coil and corresponding change of voltages on the camera tube electrodes.

A vidicon camera unit is used for the transmission of motion pictures and stationary pictures from a slide projector. This camera unit is shown in Fig. 11. Film projection is made by means of a film projector with forty per cent illumination.

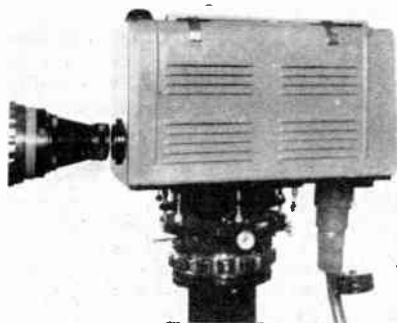


Fig. 11. A vidicon camera for motion-picture transmission.

The following equipment is installed in the film projection room: two 35-mm film projectors (as a minimum), one 16-mm film projector, a slide projector and two vidicon cameras. The transmission of full-length films is accomplished by means of one camera and the transition from one part of the film to another is effected by automatic switching in an optical switch which provides the image projection from any of the above sources to any of the two cameras.

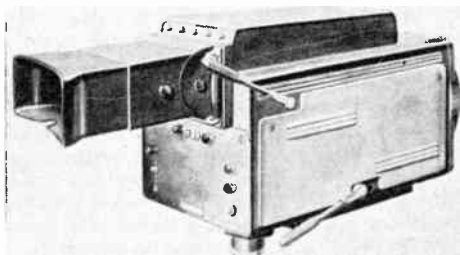


Fig. 12. A vidicon camera with view-finder and turret designed for use in small studios.

A modification of a vidicon camera with electronic view-finder and a turret having a set of objectives is also produced, shown in Fig. 12, which is suitable for use in small studios.

The camera may be removed from the rest of the equipment to a distance of up to 700 metres. Therefore, an adjustable pulse-delay circuit for timing the pulses entering the camera unit as well as mixing the line synchronizing-pulses with the signal applied to the camera view-finder from the equipment room are provided in the camera channel for compensating signal time delays in the connecting cable. Furthermore, compensation for fall in amplitude of the higher frequency signal components and for voltage drop in the camera supply cable is provided in the camera and the camera channel.

Among other features of the electric circuits is the application of adjustable aperture correction for the compensation of phase distortion. Moreover, an adjustable gamma correction is introduced which is used mainly during motion-picture transmissions and studio transmissions made with image orthicon cameras. A complex anti-noise correction is employed in studio super-iconoscope cameras. All these innovations have contributed to the improvement of the transmitted picture quality.

6. Conclusions

In addition to the considerably extended programme potentialities, the greater conveniences in service, and the improvement of the transmitted picture quality as compared to the equipment produced previously, the cost of the new equipment has been reduced by a factor of 1.5 and the required space by as much as forty per cent in the case, for instance, of television centres for four camera channels. This is because the construction and circuitry of this equipment is designed with a view to its application in television centres of all classes, in checking and measuring sets and in other television devices. Greater possibilities for mass production were thus achieved since the way was open to a wide application of casting in which special production instruments and tools were justified.

The Application of Phase-Locking Techniques to the Design of Apparatus for Measuring Complex Transfer Functions †

by

G. THIRUP ‡

Summary : The theory of phase-lock synchronization is given briefly. Two devices for measuring complex voltage ratios are described. In the first, which has a frequency range 1-110 Mc/s, the voltage ratio to be measured is converted to a constant intermediate frequency of 450 kc/s. The frequency difference between the signal generator and the local oscillator is kept constant by coupling the tuning shafts mechanically and by a phase-lock synchronizing device; special means for extending the pull-in range, making use of a coarse and fine electronic adjustment, are described. The second instrument has a frequency range of 30-700 Mc/s, and here the local and signal generators are free-running and are separately tuned manually. A double frequency conversion system is used. The frequency of the second local oscillator, by means of a phase-lock device, is kept 450 kc/s below the frequency difference of the signal and first local oscillator. A description is also given of how the complex measuring results can be displayed on a cathode-ray tube.

1. Introduction

By means of phase-lock synchronization it is possible to lock the frequency of an oscillator to the sum of a number of frequencies. This principle is used in communications technique for keeping a transmitter frequency equal to the sum of a number of crystal-controlled frequencies and a low continuously variable frequency.

In the present paper arrangements will be considered where the emphasis is not so much on the accuracy of the frequency itself as on the difference between the frequencies of two voltages. One of the voltages is used as a measuring voltage, the other as a local oscillator voltage. In this way the intermediate frequency is always the same, so that a highly selective i.f. amplifier, the noise figure of which is low, can be used. With this system it is possible to carry out measurements with extremely low voltages. Such a device, having a frequency range of 20-1040 kc/s and an intermediate frequency of 3 kc/s, has been described by Kersten¹. In section three we shall consider an instrument using the same principle for the range 1-110 Mc/s and having an intermediate frequency of 450 kc/s. This instrument has special means for varying

the frequency over a wide range if the synchronization is lost.

In section four we consider another instrument, where the difference between the frequencies of the two oscillators is not kept constant, but the intermediate frequency follows, by means of a double frequency conversion system, the difference of the frequencies of the two oscillators. One i.f. lies between 10.6-10.8 Mc/s while the second i.f. is 450 kc/s. The second local oscillator frequency, lying between 10.15 and 10.35 Mc/s, is kept to its correct value by means of phase-lock synchronization. The two high frequency oscillators, which may have frequencies from 30 Mc/s up to several hundred Mc/s, are not synchronized. They are tuned by hand, and as soon as their frequency difference approaches 10.7 Mc/s, the phase-lock synchronization of the 10.25 Mc/s oscillator comes into action and its frequency follows the frequency difference of the high frequency oscillators, provided this remains within certain limits.

2. Theory of Phase-lock Synchronization

2.1. The Holding Range

Figure 1 shows a block diagram of a simple phase-lock system. The oscillator A is the synchronizing oscillator and is considered as a local oscillator supplying voltage to the mixing circuit M. The oscillator B is to be synchronized. A part of its voltage is applied as a signal voltage to the mixing circuit M. In the case of synchro-

† Manuscript received 25th May 1959. (Paper No. 558.)

‡ Formerly with Philips Research Laboratories, Eindhoven, Netherlands; now with Thomas B. Thrige, Odense, Denmark.

U.D.C. No. 621.373.42:621.317.77

nization, the two oscillator frequencies are equal, and we get a d.c. output current which is applied via the filter F to an electronic tuning device of the oscillator B. The d.c. output current i is given by

$$i = SV \cos \varphi \quad \dots\dots(1)$$

where S is the conversion transconductance of the mixer M, V is the voltage from oscillator B and φ is the phase difference between the voltages of the two oscillators. The filter F is

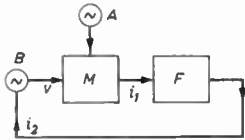


Fig. 1.
Simple phase-lock system.
A: synchronizing oscillator. B: synchronized oscillator. M: mixing circuit. F: filter.

assumed to have no attenuation at d.c. The current i has changed the oscillator frequency by $\beta = \alpha i$, where α is a proportionality factor depending on the electronic tuning device of the oscillator B. We then obtain

$$\beta = \alpha SV \cos \varphi \quad \dots\dots(2)$$

from which it will be seen that β reaches its maximum value β_0 and minimum value $-\beta_0$ at $\varphi = 0$ and π respectively. Synchronization can thus only be achieved in a range of $2\beta_0$. This range, called the holding range, can be increased by increasing one or more of the factors α , S or V . It is, however, not possible to increase β_0 beyond certain limits, because the filter F introduces a shift of phase in the closed loop B, M and F of Fig. 1 and tends to make the system unstable.

2.2. Stability in the Holding Range

We can examine the stability of the phase-regulating loop B, M and F of Fig. 1, as has been done by Salmet². Suppose that the system is synchronized and then opened between M and F, and assume that a d.c. current from an external source is applied to the filter in order to keep the frequency of the oscillator B at its proper value. Furthermore a small current of complex amplitude i_1 and angular frequency ω is applied to the filter. The filter output current has the complex amplitude $i_2 = F(j\omega) i_1$ where $F(j\omega)$ is the filter transfer junction. The angular frequency of the oscillator is then $p = p_0 + \alpha |i_2| \cos(\omega t + \psi)$ where $\psi = \arg i_2$ and p_0 is the

angular frequency for $i_2 = 0$. The high frequency voltage then becomes

$$V \cos \left[\int (p_0 + \alpha |i_2| \cos(\omega t + \psi)) dt \right] \\ = V \cos \left[p_0 t + \frac{\alpha |i_2|}{\omega} \sin(\omega t + \psi) \right]$$

which for small values of $\alpha |i_2| / \omega$ gives

$$V \left[\cos p_0 t - \frac{\alpha |i_2|}{\omega} \sin p_0 t \sin(\omega t + \psi) \right] \quad \dots\dots(3)$$

This voltage is mixed in M which gives an output current component of angular frequency ω and complex amplitude

$$\frac{VS\alpha}{j\omega} i_2 \sin \varphi = \frac{\beta_0 i_2}{j\omega} \sin \varphi \\ = \frac{\beta_0 F(j\omega) i_1}{j\omega} \sin \varphi.$$

We originally introduced a current having the complex amplitude i_1 into the system, so the loop return ratio T then becomes for $\varphi = 90^\circ$

$$T = - \frac{\beta_0 F(j\omega)}{j\omega}$$

If the function T encircles the point $-1 + j0$ of the T -plane in counterclockwise direction when ω moves from $-\infty$ to $+\infty$, then the system is unstable. If $F(j\omega)$ contains at least one pole, which is always the case in practice, an increase of $SV\alpha = \beta_0$ will make the curve cross the critical point. We are thus not able to increase infinitely the holding range of the synchronization without making the system unstable.

2.3. The Pull-in Range

The range within which the oscillators can be brought into synchronization, called the pull-in range, is much more difficult to calculate than the holding range. For the case of an RC-filter, an analysis has been carried out by Jelonek, Celinski and Syski³. It is difficult to say anything about the pull-in range in the case of a general filter function, but below we will derive one necessary condition for pulling-in.

Let the synchronizing oscillator have the frequency p_1 and the oscillator which is to be synchronized the frequency p_0 , the difference being $\omega = p_0 - p_1$. Synchronization can then be assumed to take place in the following way:

The oscillator to be synchronized is frequency modulated with the frequency ω , giving sidebands of the frequencies $p_0 \pm \omega$. As p_0 and p_1 are brought nearer to each other, the $p_1 = p_0 - \omega$ component will increase in amplitude, and at a certain value the oscillator jumps into synchronization. It is evident that if ω is so high that it is beyond the cut-off frequency of the low-pass filter, we will not get any frequency modulation and thus no synchronization.

It is possible to study this problem in more detail. Let the alternating voltage at the output of the filter be $i_2 \cos \omega t$. A phase-modulated h.f. voltage is then excited and is, for small phase deviations, given by expression (3). This voltage is mixed in M with the local oscillator voltage from A having the frequency $p_1 = p_0 - \omega$ and the phase φ . We get an additional d.c. current from the mixing circuit given by

$$i_{dc} = \frac{SV\alpha i_2}{\omega} \cos \varphi \dots\dots\dots(5)$$

and a component of frequency ω

$$i_1 = VS \cos (\omega t + \varphi).$$

This current is sent through the filter giving an amplitude attenuation with a factor $|F|$ and phase shift $-\psi$; the output current of the filter is then $|F| VS \cos (\omega t + \varphi - \psi)$, which must be equal to the a.c. current i_2 we originally introduced into the circuit, thus $\varphi = \psi$ and $i_2 = FVS$. Introducing these conditions into eqn. (5) we obtain

$$i_{dc} = \frac{(SV)^2 |F| \alpha}{2\omega} \cos \psi = \frac{|F| \beta_0^2}{2\alpha\omega} \cos \psi.$$

We see that when ψ exceeds 90 deg, the sign of i_{dc} changes and the frequency is pushed away from synchronization. The pull-in range must thus always be less than twice the frequency at which the filter has a phase shift of 90 deg.

2.4. Locking at the Difference between Two Frequencies

Up till now we have only considered simple phase-lock systems as shown in Fig. 1. If we want to lock the oscillator frequency to the difference of two frequencies, a circuit as shown in Fig. 2 can be used. In the mixing circuit M the voltages from the two oscillators A and B are mixed giving an output of the difference frequency $f_A - f_B$. This output is filtered in F_1 and then mixed in M_1 with a voltage from

oscillator C having a frequency f_c . The output of M_1 is filtered in F; in the case of synchronization this output is a direct current which

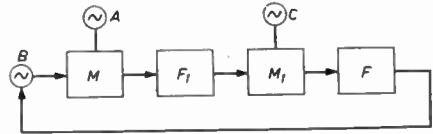


Fig. 2. Phase-lock system which synchronizes the frequency of the oscillator B to the sum of the frequencies of the oscillators A and C. M and M_1 : mixing circuits. F_1 and F: filters.

keeps the frequency of oscillator B at its right value and we have $f_B = f_A - f_C$. The difference between the frequencies of the oscillators A and B are thus kept constant, and we will make use of this property in the apparatus to be described in sections 3 and 4. The investigations of this system can be carried out as in the case of Fig. 1, the only difference being that the filter function of F_1 must now also be taken into account.

3. An Instrument for Complex Measurements in the Range 1-110 Mc/s

3.1. Principle of the Instrument

The principle explained above has been used in the instrument shown in block diagram form in Fig. 3. This instrument is intended for measuring the complex transmission function of

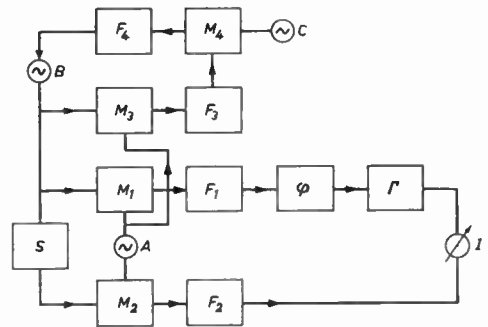


Fig. 3. Block diagram of a device for measuring complex voltage ratios in the frequency range 1-110 Mc/s of the circuit S. B: signal generator. M_1 and M_2 : mixing circuits driven by the local oscillator A. F_1 and F_2 : filters. φ : adjustable phase-shifter. Γ : adjustable attenuator. I: selective zero indicator. The frequency of B is kept equal to the sum of the frequencies of oscillators A and C by means of a synchronizing loop similar to Fig. 2, and consisting of a mixing circuit M_3 , a filter F_3 , a mixing circuit M_4 and a filter F_4 .

the circuit S, which is excited by the oscillator B, having the frequency f_B . The input and output voltages of S are applied to the two identical mixing circuits M_1 and M_2 , which are excited by the common local oscillator A having the frequency f_A . The output components having the frequency $f_A - f_B$ are filtered out in the identical filters F_1 and F_2 . We now make use of the fact that the complex ratio of two components having the frequency $f_A - f_B$ is the same as the complex ratio of the h.f. input voltages of M_1 and M_2 . The two i.f. voltages are made equal by adjusting the phase-shifter φ and the attenuator Γ , the readings of which give the phase and attenuation of the circuit S. The equality of the two i.f. voltages is indicated by the selective zero indicator I.

The frequency difference $f_A - f_B$ must be within narrow limits, because the phase-shifter is accurate only in a small frequency range, and in order to take advantage of a selective zero indicator tuned to a fixed frequency. The frequency difference is kept constant by means of a phase-lock synchronizing loop similar to that of Fig. 2. In Fig. 3 the synchronizing loop is formed by the mixing circuit M_3 , the filter F_3 , the mixing circuit M_4 and the filter F_4 the output of which controls the frequency of the oscillator B. The oscillator C oscillates on the frequency to which the selective indicator I is tuned.

3.2. Construction of the Oscillators

In the actual instrument the oscillators A and B cover the frequency range 1-110 Mc/s in six ranges. The intermediate frequency is 450 kc/s. The oscillator A is a balanced oscillator using a 2×150 pF tuning capacitor. The oscillator B is made in the same way, but its inductances are wound on ferrite cores which can be more or less saturated by a magnetizing coil excited by the output from the filter F_4 . The two tuning capacitors are mechanically coupled. The 2×6 inductances of the oscillators are mounted in two television channel selectors, where one coil occupies the place of two television circuits. The construction of such a coil is shown in Fig. 4 where W_1 is the magnetizing winding wound on a ferroxcube 3A⁴ core F_1 . The high frequency winding W_2 is wound on a plate F_2 of magnetic material. The kind of material and

the number of turns for the various frequency ranges are given in Table 1. In order to improve the stability of the phase-synchronizing loop an inductance of 5 mH in series with a resistance of 1500Ω have been inserted in parallel to the magnetizing coil.

3.3. Influence of Parasitic Couplings

Parasitic couplings inside the apparatus will cause erroneous measuring results and must therefore be reduced to a sufficiently low level. The parasitic couplings may be due to the following four causes: (a) direct coupling between the oscillators A and B, (b) coupling via the common local oscillator A, (c) coupling via the circuit S caused by voltage components excited by the mixing circuits M_1 and M_2 , and (d) coupling by modulation of the voltage of oscillator B caused by an alternating voltage component penetrating the filter F_4 . The coupling mentioned in point (a) can be avoided by a proper screening of the oscillators; the

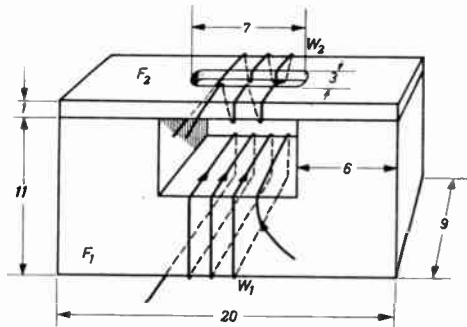


Fig. 4. Coil for the electronic tuning of oscillators. W_1 is the magnetizing winding wound on a Ferroxcube 3A core F_1 . The oscillator coil W_2 is wound on a plate F_2 of magnetic material. Number of turns and data regarding the material are given in Table 1.

Table 1
Data for the oscillator coils.

Frequency range Mc/s	Number of turns of magnetizing coil	Material of oscillator coil	Number of turns of the oscillator coil
0.9—2.2	2500	ferroxcube 4A ⁴	2×150
2.1—6.0	1200	ferroxcube 4C ⁴	2×45
5.8—13.5	1200	ferroxcube 4C ⁴	2×17
12.5—27	2500	ferroxpiana ⁹	2×17
24.5—53	2500	ferroxpiana ⁹	2×6
49—110	3000	ferroxpiana ⁹	2×3

coupling mentioned in (b) can be prevented by introducing buffer stages between A and M_1 and M_2 ; and that of point (c) by introducing buffer stages between S and M_1 and M_2 . The coupling referred to in point (d) is closely related to the phase-lock synchronization. At the output of F_4 we have a.c. components of the frequencies $nf_c = n(f_A - f_B)$. These components modulate the voltage of oscillator B in frequency and the oscillator voltage contains components having the frequencies f_B , $f_B + (f_A - f_B)$, $f_B + 2(f_A - f_B)$. These compounds are mixed in M_1 and M_2 . The f_B -component causes the right i.f. component, the $[f_B + (f_A - f_B)]$ -component a d.c. component, and the $[f_B + 2(f_A - f_B)]$ -component a spurious i.f. component. The last component will thus falsify the measurements. This spurious component can be suppressed by sufficient attenuation of the filter F_4 at twice the correct i.f. Mixing products of other frequencies than 450 kc/s in the output of M_1 and M_2 will not influence the measurements because a selective zero indicator is used.

3.4. Coarse Frequency Adjustment

The oscillators A and B can only be pulled into synchronization if the difference between their free-running frequencies is lower than half the pull-in range. It will thus be an advantage to have a broad pull-in range, because the accuracy of the free-running frequency difference then does not need to be so high. A broad pull-in range requires a broad holding range, which again requires a high value of the factor αSV of eqn. (2). This factor cannot be increased indefinitely without disturbing the stability of the phase-lock loop. These difficulties can be overcome by increasing the pull-in range artificially, which can be achieved in the following way: As soon as the synchronization is broken, a device is started, which applies an extra current to the frequency regulating device of the oscillator B. This current makes the frequency of B vary over a range which is several times the normal pull-in range. At a certain value of the current the system jumps into synchronization. The additional current is by some means kept at the value which caused the synchronization and provides for a coarse adjustment of the frequency of B, while the normal synchronizing loop takes over the fine adjustment.

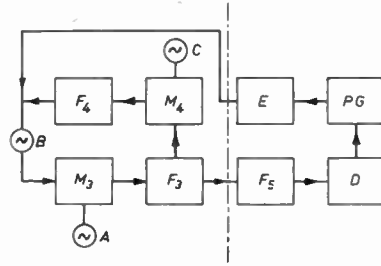


Fig. 5. Searching device for increasing the pull-in range of a phase-lock system. The part to the side of the broken line is the same as in Fig. 3. F_5 : selective amplifier. D: rectifier. PG: pulse generator. E: pulse counting device.

A detailed description of the coarse adjustment system will now be given. A block diagram is shown in Fig. 5. The part of the diagram to the right of the broken line is the coarse frequency adjustment system, while the part to the left is the real synchronizing circuit and is taken from Fig. 3. When the circuit is synchronized, the filter F_3 supplies a 450-kc/s voltage to the selective amplifier F_5 tuned to 450 kc/s. The output of F_5 is converted in the detector D into a negative d.c. voltage which prevents the pulse generator PG from generating pulses. As soon as the synchronization is broken, the output frequency from M_3 differs from 450 kc/s and is not passed by the amplifier F_5 , the d.c. voltage from D disappears and the pulse generator makes pulses at a rate of 50 pulses per second and with a pulse-width of 2 millise. These pulses are counted in a single decade counter valve $E1T^5$ and cause a current to flow through the tuning device of oscillator B as shown in Fig. 6. Before the synchronization was broken the current was i_a , the breaking of the synchronization makes the current decrease stepwise till the oscillator is synchronized, the pulse-generator stops and the counter valve current remains at its new level. If the current should be increased instead of being

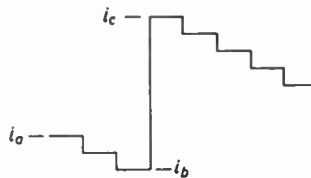


Fig. 6. Coarse-adjustment current in the frequency regulating device.

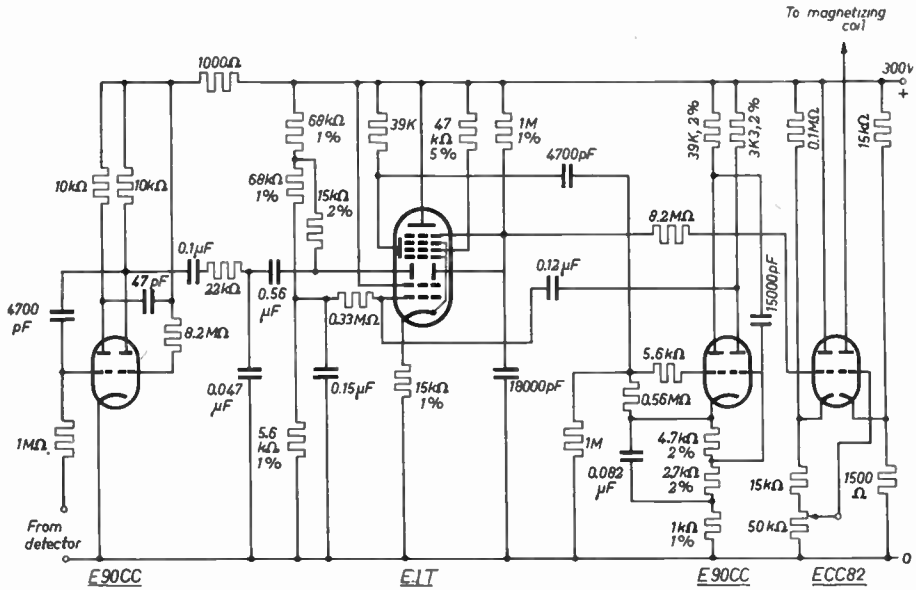


Fig. 7. Detailed diagram of the pulse generator and counting device of Fig. 5.

Note.—The resistor symbols in this diagram follow Continental practice; they do not have the British Standard significance of non-inductive properties.

decreased, the counter valve counts to its bottom level i_b , jumps then to i_c and counts till synchronization is achieved. It is, however, a necessary condition that the pull-in range of the synchronizing system be broader than the frequency jump caused by a counter valve current-step. The total pull-in range when using a coarse and a fine adjustment is then determined by the difference between the top and bottom current shown in Fig. 6. The whole synchronizing process is carried out in a fraction of a second. Figure 7 shows a detailed diagram of the pulse counting circuit. The valve E90CC at the left generates pulses and starts as soon as the d.c. voltage from the detector disappears. The pulses are counted in the counter valve E1T and the E90CC at the right provides for resetting of the counter valve when it has reached its minimum current. The valve ECC82 is used as a cathode follower and d.c. amplifier. By means of the 50-kΩ potentiometer the quiescent current through the magnetizing coil can be adjusted.

3.5. Comparison with an Older Instrument

The rest of the instrument is very similar to an instrument described previously⁶, in which

the two voltages of constant frequency difference were excited by mixing a voltage having a variable frequency in the range 200-300 Mc/s with two voltages having frequencies of about 200 Mc/s and differing by the required amount. The advantage of the present instrument over this other one is its much simpler construction, as the highest frequency occurring in the new instrument is only about 100 Mc/s while in the previous one it was about three times higher. A further advantage is that the noise level in the new instrument is lower. In the old instrument the voltage acting as a local oscillator had first to be amplified and the amplifier introduced noise into the signal channel because balanced mixing circuits were not used. The new instrument, though not using balanced mixing circuits, has less noise because no amplifier is used for the local oscillator voltage.

4. Instrument for Complex Measurements or Display at Higher Frequencies

4.1. Introduction

The apparatus described in the preceding section has an upper frequency limit of 110 Mc/s and for practical reasons the frequency range could not be extended much be-

yond this limit. The same principle could, of course, be used at higher frequencies, but several practical difficulties would have to be expected. So it was decided to change the principle and not to synchronize the two oscillators A and B of Fig. 3 at a constant frequency difference, but to keep them free-running. By means of a double frequency conversion system in the i.f. part, the tuning of the i.f. system follows the frequency difference of the oscillators A and B. This principle has the advantages that commercially available high-frequency generators can be used and that the frequency regulating takes place at a rather low frequency. The upper frequency limit is then determined mainly by the performance of the high frequency mixing circuits and the frequency of the available generators.

4.2. Principle of the Measuring Instrument

The instrument, a block diagram of which is shown in Fig. 8, works in the following manner.

The generator B supplies a voltage to the circuit S to be measured. In this set-up the frequency of this voltage may be between 30 and 700 Mc/s. The input and output voltages of the fourpole S are applied to two identical mixing circuits M_1 and M_2 , which are driven by a common local oscillator A. This local oscillator has a frequency which is 10.6-10.8 Mc/s lower than the frequency of B, so that we get two intermediate frequency outputs having a frequency between 10.6 and 10.8 Mc/s, which are amplified in two identical, selective i.f. amplifiers F_1 and F_2 . The complex ratio of the output voltages of the amplifiers is the same as the complex ratio of the two h.f. input voltages. This ratio can be measured by adjusting the adjustable phase-shifter φ and attenuator Γ of Fig. 8 till the i.f. voltages cancel each other.

The performance of the phase shifter and attenuator depends on the value of the intermediate frequency, but within the range of 10.6-10.8 Mc/s we may assume that the performance is independent of the frequency. The compensation of the two i.f. voltages is indicated by a zero indicator. If this indicator had a bandwidth of 10.6-10.8 Mc/s we would get too much noise. We can get a narrow bandwidth by using a phase-lock device which always keeps a narrow band zero indicator tuned to the proper frequency. This indicator consists of a mixing cir-

cuit M_3 excited by the local oscillator C and a selective amplifier F_5 . The frequency of C, by means of the mixing circuit M_3 , filter F_3 , mixing circuit M_4 and filter F_4 , is synchronized at a frequency which is 450 kc/s lower than the i.f. frequency. The mixer M_3 gets its synchronizing voltage before compensation takes place, otherwise the synchronization would disappear when compensation was obtained.

The output of the amplifier F_5 can be mixed with a beat oscillator giving a beat of 1 kc/s, which again can be amplified in a selective amplifier having a bandwidth of 50 c/s. We

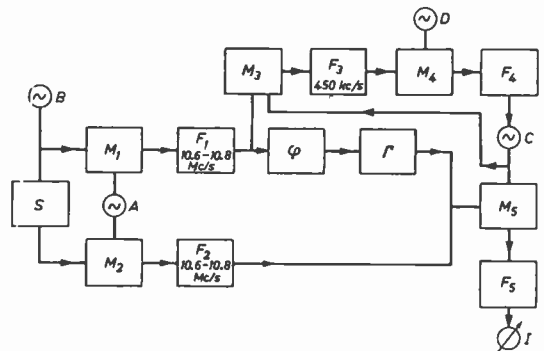


Fig. 8. Block diagram of an apparatus for measuring complex voltage ratios of the circuit S at frequencies of 30-700 Mc/s. B: signal generator. M_1 and M_2 : mixing circuits. A: local oscillator. F_1 and F_2 : selective amplifiers. M_3 : mixing circuit driven by the local oscillator C. F_5 : selective i.f. amplifier. I: zero indicator. The loop, consisting of mixing circuit M_3 , filter F_3 , mixing circuit M_4 and filter F_4 , keeps the frequency of C at such a value that the output frequency of M_3 is always that of the oscillator D.

are thus able to measure at frequencies up to 700 Mc/s with a bandwidth of 50 c/s, which gives a low noise level. A 50- μ V high frequency voltage at the input of the mixing circuits M_1 and M_2 is sufficient for a good adjustment of φ and Γ .

In the apparatus described, the facility of one-knob tuning is not provided, as in the instrument described in Section 3. The oscillator B is first set to the measuring frequency, then A is tuned to a frequency which is about 10.7 Mc/s lower. The generator C then jumps into synchronization and the output voltage of mixer M_5 then has the precise frequency 450 kc/s.

4.3. Parasitic Effects

Because of the high frequencies used, the mixing circuits M_1 and M_2 of Fig. 8 are equipped with germanium diodes. The mixing circuits are thus not unidirectional as in the case of mixing valves, and there are some parasitic couplings between the two signal channels. The parasitic coupling has two causes, namely coupling via the common local oscillator A, and coupling by various mixing products via the measured object S.

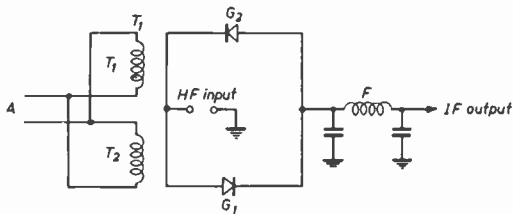


Fig. 9. Diagram of a balanced mixing circuit. A: local oscillator input. T_1 and T_2 : toroidal current transformers. G_1 and G_2 : diodes 1N21D. F: intermediate frequency output circuit.

The coupling via the local oscillator can be diminished by using balanced mixing circuits. Figure 9 shows a diagram of one of the mixing circuits. The local oscillator voltage enters at A. The diodes G_1 and G_2 are excited via the toroidal transformers T_1 and T_2 , each having six primary turns and a single secondary turn. The circuit F_1 consisting of two capacitances and an inductance, is tuned to 10.7 Mc/s. The coupling between the two channels via the common local oscillator can be kept below -40 db, at some frequencies even below -70 db.

The coupling between the two channels caused by various mixing products takes place at the frequencies $q+np$ where q is the signal frequency, p the local oscillator frequency and n an integer. This coupling can be diminished by inserting attenuators between the circuit to be measured and the mixing circuit. Let the attenuator have an attenuation factor of γ and let the voltage at the circuit to be measured be V_1 , then the voltage at the mixing circuit is γV_1 . The voltage of an excited higher order mixing product is $\delta\gamma V_1$, where δ depends on the mixing circuit and the order of the mixing product. This higher order mixing product causes a volt-

age of $\gamma^2\delta V_1$ at the circuit to be measured, while in the case without attenuators we had δV_1 , so we get an improvement of γ^2 . Experience has shown that by inserting 12 db attenuation the effect of the mixing products becomes sufficiently low.

It is required that the 10.7 Mc/s twin amplifiers of Fig. 8 have equal transmission functions in the range 10.6-10.8 Mc/s. This can be achieved by stabilizing the d.c. supply voltage, and the effect of filament voltage variations is diminished by stabilizing the anode current with a 1000- Ω cathode resistor and by giving the grid a positive voltage with respect to the chassis. The anode impedances consist of tuned circuits, the coils of which are wound with constantan wire in order to reduce the temperature effects.

When tuning the oscillators A and B it may happen that their frequency difference becomes 9.8 Mc/s instead of 10.7 Mc/s, because 9.8 Mc/s will also give 450 kc/s with a local oscillator frequency of 10.25 Mc/s. This can be avoided by always moving the dials of one of the generators A or B towards the frequency of the other, then the first response will be the correct one.

It is also possible to obtain lock-in of the oscillator C at 10.25 Mc/s when the frequency of B is 10.7 Mc/s higher than the frequency of A. In this case all the measuring results will turn out as complex conjugate of what they should be. One can always be sure of measuring the correct value by first tuning the oscillator B to the measuring frequency and then setting A to a frequency which is more than 10.7 Mc/s below the frequency of B. When increasing the frequency of A, the first lock-in of C is the right one.

4.4. Display Unit

Both the apparatus which have been described make use of a compensating method, which requires adjustments of a phase and an amplitude dial. It would save work if we could avoid the compensation and get the results displayed directly on the screen of a cathode-ray tube. Such devices, working at much lower frequencies, are known^{7,8}. A description will now be given of how, instead of adjusting φ and Γ of Fig. 8, a complex quantity can be made visible as a bright spot on a screen.

The block diagram of the apparatus is shown in Fig. 10. The first part is the same as in the case of Fig. 8. The two identical 10.7 Mc/s amplifiers F_1 and F_2 are followed by the two mixing circuits M_3 and M_4 excited by the local oscillator C. The signals are transposed to 450 kc/s and filtered in the two selective amplifiers F_3 and F_4 . The frequency of the local oscillator C is kept to its right value by the synchronizing loop $M_3 - F_3 - M_7 - F_7$. The output voltages from F_3 and F_4 are again mixed in the mixing circuits M_5 and M_6 with a voltage from the generator E, having a frequency of 445 kc/s. The signals are thus transposed to 5 kc/s and are filtered in filters F_5 and F_6 . The 5-kc/s output voltages of F_5 and F_6 have the

generator B to the input terminals of M_1 and M_2 . The dot must then appear at the point $1 + j0$ on the complex plane.

The display unit has means for adjusting the phase and amplitude till the dot appears at $1 + j0$ if this is not already the case. If the high frequency is changed, the dot will only remain at $1 + j0$ if the voltage delivered by the generator B and the magnitude of the transconductance of M_2 are independent of the frequency and if M_1 and M_2 have equal phase-shifts. Experience has shown that for a carefully designed circuit the phase deviation will not exceed ± 3 deg.

Generally the amplitude deviation will be

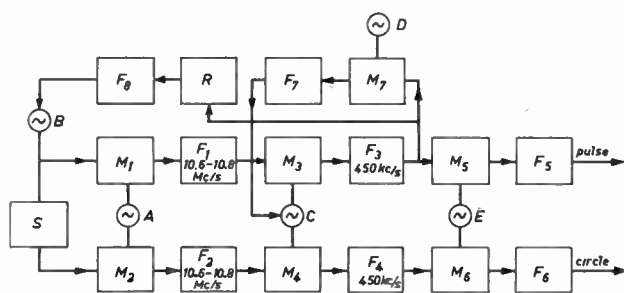


Fig. 10. Block diagram of an apparatus for displaying the complex voltage ratio of the circuit S on a cathode-ray tube.

B: signal generator. A: local oscillator. M_1 and M_2 : mixing circuits. F_1 and F_2 : selective amplifiers. M_3 and M_4 : mixing circuits excited by the local oscillator C. F_3 and F_4 : selective amplifiers. M_5 and M_6 : mixing circuits driven by the local oscillator E. F_5 and F_6 : filters. The frequency of C is kept to its right value by the output of F_7 , which obtains its input from the mixing circuit M_7 driven by the local oscillator D. R is a rectifier and F_8 a d.c. amplifier, the output of which regulates the amplitude of B.

same complex ratio as the high frequency voltages at the circuit S, provided that the two channels, each consisting of three mixing circuits and three filters, are identical. The two 5-kc/s voltages are then used for displaying the complex voltage ratio on a television screen in the manner described by Van Schagen⁸. The 5-kc/s signal having its origin in the output voltage of the circuit S is used for writing a circle on the tube, the radius of the circle being proportional to the high frequency output voltage of S. The circle is suppressed, and it is rendered visible only for a short time in each 5 kc/s period by a pulse derived from the 5 kc/s voltage having its origin in the high frequency input voltage of S. The dot on the screen then shows the complex voltage ratio of the circuit S.

The fulfilment of the condition that the two channels of Fig. 10 must be equal, is easily checked by applying a common voltage from the

same complex ratio as the high frequency voltages at the circuit S, provided that the two channels, each consisting of three mixing circuits and three filters, are identical. The two 5-kc/s voltages are then used for displaying the complex voltage ratio on a television screen in the manner described by Van Schagen⁸. The 5-kc/s signal having its origin in the output voltage of the circuit S is used for writing a circle on the tube, the radius of the circle being proportional to the high frequency output voltage of S. The circle is suppressed, and it is rendered visible only for a short time in each 5 kc/s period by a pulse derived from the 5 kc/s voltage having its origin in the high frequency input voltage of S. The dot on the screen then shows the complex voltage ratio of the circuit S.

too high, but by means of a regulating circuit the influence can be reduced. This regulating circuit works in the following way: The output from F_3 of Fig. 10 is amplified and rectified in the device R, the output of which is compared with a constant d.c. voltage. The difference between the two d.c. voltages is amplified in a d.c. amplifier, the output of which is used as anode voltage for the generator B. If the amplitude of the transfer conductance of the two mixing circuits M_1 and M_2 depends in the same way on the frequency the regulating circuit will take care that the dot remains at $1 + j0$ when the frequency is changed. Experience has shown that it is possible to keep the variations of the dot within ± 5 per cent., while without a regulating circuit the ratio of maximum and minimum amplitudes would be about three.

A device similar to that described above can also be applied to the circuit of Fig. 3. In this

case we can take advantage of single knob tuning of the signal and local oscillator frequencies.

5. Other Applications of the Equipments

The instruments described in Sections 3 and 4 are designed for measuring complex voltage ratios, but they are also well suited as generators and zero-indicators for h.f. bridges. The generator B is used for exciting the bridge. The zero indicator terminal of the bridge is connected, for example to M_2 , and part of the voltage of generator B is applied to M_1 . The latter voltage provides for the right frequency difference between oscillators A and B. We thus have the advantage of using a narrow band zero indicator which is always tuned to the right frequency. When using the instrument described in Section 3 we further have the advantage of single knob tuning of both oscillators.

6. Acknowledgment

The author is indebted to Mr. J. W. Houben for carrying out most of the experimental work with the two instruments described.

7. References

1. R. Kersten, "Verfahren zur Ableitung der Überlagerungs-frequenz eines Empfängers aus der Messfrequenz eines Senders," *Frequenz*, **11**, pp. 370-379, 1957 and **12**, pp. 15-25, 1958.
2. G. Salmel, "An analysis of pulse synchronized oscillators," *Proc. Inst. Radio Engrs*, **44**, pp. 1582-1594, 1956.
3. Z. Jelonek, O. Celinski and R. Syski, "Pulling effect in synchronized systems," *Proc. Instn Elect. Engrs*, **101**, Part IV, pp. 108-117, 1954.
4. J. J. Went and E. W. Gorter, "The magnetic and electrical properties of ferroxcube materials," *Philips Tech. Rev.*, **13**, pp. 181-193, 1952.
5. A. J. W. M. van Overbeek, J. L. H. Jonker and K. Rodenhuis, "A decade counter tube for high counting rates," *Philips Tech. Rev.*, **14**, pp. 313-326, 1953.
6. G. Thirup, "An instrument for measuring complex voltage ratios in the frequency range 1-100 Mc/s," *Philips Tech. Rev.*, **14**, pp. 102-114, 1952.
7. E. C. Pyatt, "Equipment for continuous vectorial display of alternating voltages in the frequency range 5 kc/s to 3 Mc/s," *J. Brit.I.R.E.*, **16**, pp. 563-569, 1956.
8. M. J. van Schagen, "Apparatus for displaying of complex diagrams at varying frequencies," *Philips Tech. Rev.*, **18**, pp. 380-383, 1957.
9. A. L. Stuijts and H. P. J. Wijn, "Crystal-oriented ferroxcube materials," *Philips Tech. Rev.*, **19**, pp. 209-217, 1958.

News from the Sections . . .

Karachi Section

The Annual Dinner of the Section was held on 31st March at the Beach Luxury Hotel, Karachi, when the Section Officers entertained as chief guest, Dr. Salimuzzaman Siddiqui, director of Pakistan Council of Scientific and Industrial Research. Other guests included Mr. S. M. Hussain, member of the Federal Public Service Commission, Al Haj Abdul Hamid, chief engineer, Posts and Telegraphs, Dr. M. R. Chowdhury, director of the Pakistan Standards Institution, Mr. M. A. Satter, principal of Karachi Polytechnic and Mr. A. F. C. Gibson.

In his speech Dr. Siddiqui paid tribute to the work of the Institution in broadening human knowledge and establishing international co-operation. He regarded the local meetings as being a particularly valuable source of information on the latest advances and developments in the fields of radio and electronics.

M. A.

West Midlands Section

The second Birmingham meeting of the Section was held at the Matthew Boulton Technical College on March 8th; a paper on "Transistor Power Amplifiers" was read by Mr. F. Butler, O.B.E., B.Sc. (Member).

As a preliminary to the paper, a short film on the manufacture of transistors was shown. Mr. Butler then reviewed the standard forms of transistor circuitry, explaining their characteristics as applied to the low-power stages of audio amplifiers. This theme was further extended to a number of more complex circuits, some novel and recently developed from their counterparts in thermionic circuitry. These included the "super-alpha pair," various forms of the cascode amplifier and some direct-coupled high linearity phase-splitters, together with various feedback arrangements of conventional design and methods of obtaining high input impedance. The importance of stabilizing the d.c. operating conditions of a transistor was stressed and several schemes to achieve this stability were explained.

Next, the speaker dealt with driver circuits and power output stages. The basic principles of Class B operation were explained, considera-

tion being given to the linearity problems presented by currently available power transistors. The importance of good heat sink design and factors affecting choice of operating conditions were discussed, and several complete power amplifier circuits involving these design points were presented.

Finally, Mr. Butler compared the performance of transistor audio amplifiers with thermionic circuitry of equivalent power rating, and drew the conclusion that for circuits of up to four watts output, transistor equipment was competitive with the best high-fidelity thermionic equipment, providing that all due attention was given to its design.

F. D.

South Midlands Section

At the Section's Malvern meeting on March 29th, Mr. M. W. Gough, M.A., had an audience of 40 to hear his paper "Microwave Propagation—some characteristics and curiosities."

Considering post-war developments, Mr. Gough gave a wide survey of microwave systems and their problems, beginning with the influence of ground reflections on line-of-sight paths. The effect of polarization was then discussed and it was shown that at the angles considered, vertical polarization has a poor reflection co-efficient which causes less signal variation.

Gain-height was then considered and it was shown how heavy losses can occur on point-to-point links if the height/frequency relationship is not correct. One interesting possibility was the use of radio mirrors and Mr. Gough pointed out that although they were expensive to install they were cheap to maintain. The surface smoothness of the mirrors was considered and then symmetrical and unsymmetrical systems were illustrated. As an example, a link in Northern Italy was described which provides 120 circuits using two-mirror systems along with active repeaters.

Mr. Gough's next subject was the troposphere. He dealt with inversion layers and total internal reflection and showed the effects of nocturnal layering on a link in the Persian Gulf area. The last topic was microwave diversity systems.

P. W. G.

of current interest . . .

Mr. P. C. Saggar

The Honorary Local Secretary of the Bombay Section of the Institution, Mr. Prem Chand Saggar (Associate Member) is at present on visit to the United Kingdom. Mr. Saggar who is senior lecturer in radio and electronics at St. Xavier's Technical Institute, is visiting various manufacturing organizations over the next two or three months.

1960 Battery Symposium

Following the success of the 1958 Battery Symposium held at the Signals Research and Development Establishment, Christchurch, the Inter-Departmental Committee on Batteries has undertaken to sponsor a similar Symposium at two-yearly intervals. Arrangements are now in hand to hold the second Symposium at The Pavilion, Bournemouth, on 18th, 19th and 20th October, 1960.

It is expected that 25 papers will be presented covering a wide field of subjects concerned with research, development and application of battery systems. Further information may be obtained from Mr. F. C. Wells, S.R.D.E., Somerford, Christchurch, Hants.

Radio Communication using "Passive" Satellites

Two teen-age amateur radio operators—one a freshman at the Massachusetts Institute of Technology, the other still at school in Maryland—have reported what was probably the world's first successful two-way radio communication with the aid of artificial satellites. During the early morning hours of February 6th, 1960, coded signals were sent and received over a distance of 200 miles between New York City and Bethesda, Md. At the time of their contact, America's *Explorer VII* satellite and Russia's *Sputnik III* were in low orbit and passed almost simultaneously off the Atlantic coast about 150 miles east of Atlantic City, N.J.

Although the exact nature of the aid furnished by the satellites must be determined by further experiments, the report leaves little doubt that radio contact was made possible by the nearby passage of either one or both "passive" satellites. In the opinion of Dr. Jerome B.

Wiesner, Director of the M.I.T. Research Laboratory of Electronics, the two-way communication probably involved only one satellite, or its ionized trail. Two possible methods have been set forth by the M.I.T. student to explain his achievement. One is known as "CW reflection" or the "Kraus effect" whereby the wake of ionization from the satellite provides an ionospheric scatter source; the other is re-radiation of signals from the antennas of passing satellites due to the closeness of radio frequencies used. Contact was made on 21·011 Mc/s and both sets were operating at about 300 watts power with no directional antennas.

British Scientific Instruments Exhibition in Russia

As a result of the report of the recent delegation of the Scientific Instrument Manufacturers' Association of Great Britain, which went to Moscow at the beginning of November, an exhibition of British scientific instruments will be held in Moscow from the 16th to 26th June, 1960. This exhibition will be the first to be put on in Russia by a British organization of manufacturers in a specialized field.

The Autonomics Division of N.P.L.

The name of the Control Mechanisms and Electronics Division of the National Physical Laboratory has been changed to the "Autonomics Division." The word "Autonomics," meaning "self-governing," is considered to be particularly apt as a description of the new types of device that the Division aims to develop.

The Division has carried out much work in the field of automatic control and in pioneering digital computers, but now that industry has adopted these techniques, research has moved forward into new fields. By working closely with biologists in studying the methods which living physical systems use to achieve control, the Division hopes to discover underlying principles on which machines which can improve their own performance can be built. The autonomic devices of the future will be self-governing machines which discover for themselves how to recognize, how to translate and how to control.

Radio Engineering Overseas . . .

The following abstracts are taken from European and Commonwealth journals received in the Library of the Institution. Members who wish to borrow any of these journals should apply to the Librarian, stating full bibliographical details, i.e. title, author, journal and date, of the paper required. All papers are in the language of the country of origin of the journal unless otherwise stated. The Institution regrets that translations cannot be supplied.

HEAT SENSITIVE RESISTORS

Refractory heat sensitive resistors which permit the measurement and control of temperatures up to 1100°C have up to now found only limited use because of their relatively high price. A new type of "wide diffusion" refractory heat sensitive resistor has been developed and produced in quantity in France, and is claimed to have many applications, particularly in the field of control. A recent paper describes the resistors and suggests applications in the fields of thermometry and temperature control, relay timing and alarm equipment.

"Refractory heat sensitive resistances." J. Vergnolle and J. Tsoca. *L'Onde Electrique*, 40, pp. 252-4, March, 1960.

WAVEGUIDE SWITCHES

The construction and electrical performance of two broadband Ku-band waveguide switches are described in a paper from the National Research Council of Canada. They are operated by rotary solenoids and are suitable for low power applications as disconnecting devices. Both switches have a minimum attenuation of 40 db and a maximum insertion loss of 0.5 db. The v.s.w.r. is less than 1.2 across the band. Details are given for casting associated lossy material.

"Broadband isolation switches operate in Ku-band waveguides." A. Staniforth and K. Steele. *Canadian Electronics Engineering*, 4, pp. 35-38, January 1960.

RING MODULATORS

A new quasi-linear method for explaining the design of ring modulators has been derived experimentally in a recent German paper. The design of the differential transformer and the diode ring circuit (including linearization) and the choice of the carrier level (modulation depth) takes into consideration conversion loss, matching (complex load impedances, loss due to reflections) and harmonic distortion. The matching ratios are shown in a geometrical matching plane from which the transformation ratios of the differential transformers can be derived. The complex load impedance for both sides are taken into consideration in an equivalent circuit.

"The performance and the design of ring modulators." H. Bley. *Nachrichtentechnische Zeitschrift*, 13, pp. 129-36, 196-201, March and April 1960.

CIRCUITS FOR PHOTO-MULTIPLIERS

Circuits for the operation of a photo-multiplier to be used in investigations of upper atmosphere phenomena are described in a paper presented at the 1959 Australian I.R.E. Convention. The paper gives details of a high-voltage regulated power supply, a chopping oscillator and a narrow bandwidth tuned amplifier, all of which make use of transistors and semi-conductor diodes. The equipment which is designed for operation in the field or the laboratory, has low power consumption and stable characteristics. It is claimed to work satisfactorily in normal ambient temperatures.

"Transistor circuitry for a very sensitive photo-multiplier." J. R. Groves. *Proceedings of the Institution of Radio Engineers, Australia*, 21, pp. 142-7, March 1960.

CERAMIC VALVES

The development of electronic tubes displays a certain fundamental and permanent character—improvement in mechanical stability and in the ratio of power to volume, and an increase in the perveance per unit area of the cathode. A study of this development by a French engineer permits limits to be set to the use of traditional dielectrics in the manufacture of tubes, namely, the various types of glass, and shows the necessity on more and more occasions of replacing it by one of the new substances. Ceramics is a wide category from which a choice may be made and the most favourable of these substances is briefly described.

"The application of ceramics to electronic transmitting valves." G. Gallet. *Onde Electrique*, 40, pp. 201-206, February 1960.

SPIRAL ANTENNA

A spiral antenna is a radiator consisting of one or two spiral conductors and a reflector, and a device of this type was described in a paper read at the 1959 I.R.E. Canadian Convention in Toronto. The aerial is broad-band and circularly polarized, but because of its relatively low efficiency it is most satisfactory as a receiving aerial. It has been found that its usefulness for this application can be increased by the addition of a resistive termination.

"Resistive termination improves spiral antenna characteristics." F. V. Cairns. *Canadian Electronics Engineering*, 4, pp. 32-6, 40, January 1960.

WIDE-BAND PARABOLOID AERIALS

A paraboloid reflector can be illuminated by a helical radiator in such a way that a high gain is produced for circular polarization. However, helical radiators are not point radiators, their apparent phase centre, which should lie in the focal point of the paraboloid in order to produce a maximum gain, moves in position depending on frequency. An optimum mean distance between the vertex of the paraboloid and the helix can be found which produces reasonable gain figures and reasonable radiation patterns over a relatively large frequency band of up to approx. 1.6:1. A circularly bent, compact coaxial line with a tape-like inner conductor is used in a recent German development for matching the input impedance of the helix with the characteristic impedance of the feeder. It is shown that a paraboloid reflector with a diameter of 2 metres can produce gain figures of 19.5 db at 610 Mc/s, 22 db at 800 Mc/s and 23.5 db at 960 Mc/s. For a 3-m reflector the gain figures at these frequencies are respectively 21 db, 25.5 db and 27 db. All gain figures are based on a circularly polarized isotropic radiator. The axis ratio of the polarization ellipse is reduced from 6 db at 610 Mc/s to 2.3 db at 700 Mc/s and remains below this value at frequencies up to 960 Mc/s. The reflection coefficient remains below 15 per cent. over the whole frequency range from 610 to 960 Mc/s.

“Wide-band paraboloid antennas using helices as radiators for decimetric waves.” R. Hertz. *Nachrichtentechnische Zeitschrift*, 13, pp. 109-14, March 1960.

PUSH-PULL AUDIO AMPLIFIER

A new type of power output stage is described in a paper read at last year’s Australian I.R.E. Convention in which the normal limitations of conventional push-pull amplifiers are absent. The circuit is of the single-ended push-pull class with no output transformer, and the valves are connected in series for d.c. The improved behaviour is due to the system of driving one of the output valves with a signal derived from the departure of the output waveform from the undistorted input. Extremely low harmonic distortion (0.02 per cent. total) is obtained in class AB operation right up to the point of clipping, without the use of overall feedback and the output impedance is less than 0.01 of the load impedance, which is not critical. Very wide frequency response is also claimed.

“A low distortion single-ended push-pull audio amplifier.” C. T. Murray. *Proceedings of the Institution of Radio Engineers, Australia*, 21, pp. 134-7, March 1960.

TRANSISTORIZED FACSIMILE RECEPTION

A recent paper by an engineer with the National Research Council of Canada describes an experimental all-electronic slow scan facsimile system. After first deriving the relationship between bandwidth frame rate and resolution in an image transmission system, a system is described in which a frame with a resolution of approximately 100 by 100 elements is transmitted in 3.5 sec using a bandwidth of 2 kc/s. The transmitted signal is proportional to reflected rather than to transmitted light, so that it is not necessary to make photographic slides of the subject.

“A narrow band image transmission system with transistorized receiver.” J. S. Riordan. *Transactions of the Engineering Institute of Canada*, 3, pp. 113-8, December 1959.

AN AUSTRALIAN ANALOGUE COMPUTER

The University of New South Wales has recently developed an electronic analogue computer, UTAC, for university and industrial research. The first section of the computer has been in continuous use for over three years and it is intended to construct the second complete section which will essentially be identical with that already produced. There are at present 24 amplifiers in the computer and flexibility of operation is achieved by allowing any amplifier to perform any operation, either linear or non-linear. Plug-in computing components are widely used and a method of amplifier control is employed which allows all normal modes of operation while using only one relay per amplifier. Flexibility is enhanced by allowing a timing unit or variables in the computation to operate the control relays. A simple system of overall calibration making use of comparative measurements of voltage and time allows individual computing units to be calibrated to an accuracy of 0.1 per cent. A brief description is also given of a new type of generator for producing voltages which are arbitrary functions of time.

“The analogue computer UTAC.” C. P. Gilbert, R. M. Duffy and T. Glucharoff. *Journal of the Institution of Engineers Australia*, 32, pp. 11-7, January-February 1960.

JAPANESE ELECTRONIC COMPUTERS

The November 1959 issue of *The Journal of the Institute of Electrical Communication Engineers of Japan* is almost entirely devoted to descriptions of complete computers and circuits and the techniques associated with them; these include a numerically controlled milling machine. Members of the Brit.I.R.E. may obtain abstracts of the papers in English from the Librarian.